Transdermal Drug Delivery Adhesives with Foam Morphology

by

Diana Kate Lushington

A thesis submitted to the Graduate Faculty of
Auburn University
in partial fulfillment of the
requirements for the Degree of
Master of Science

Auburn, Alabama
December 12, 2011

Keywords: bandage adhesive, foam adhesive, pressure sensitive adhesive, transdermal drug delivery

Approved by

Gisela Buschle-Diller, Chair, Professor of Polymer and Fiber Engineering
Royall Broughton Jr., Professor Emeritus of Polymer and Fiber Engineering
Xinyu Zhang, Associate Professor of Polymer and Fiber Engineering

Abstract

Polyacrylate-based adhesives are common in commercial bandages for blister prevention and wound healing. In this research, pressure sensitive polyacrylate adhesive foams have been investigated that could potentially be used in transdermal drug delivery. A variety of foaming methods were investigated, such as high speed mixing, adding blowing agents, freeze drying, heating, and bulk polymerization of a reactive exothermic monomer. The products were characterized with FT-IR, tack, and peel resistance testing. A common drug was incorporated into the foams and its stability and release probability assessed. It was found that the drug impacted the viscosity and foam formation ability of the adhesive. Color changes were observed that suggested (partial) decomposition of the drug. Since the polymerization mechanism was free-radical addition, radical terminators (in particular chain transfer agents) were utilized in an effort to preserve the drug. The final drug loaded product was tested in a release trial to make a preliminary determination on the overall adhesive system's suitability. Finally, peel tests were conducted of the drug loaded samples and compared to those of commercial acrylate adhesives.

Acknowledgments

The author would like to express her sincere gratitude to her project advisor, Dr. Buschle-Diller, and to her committee members, Dr. Royall Broughton, Jr. and Dr. Xinyu Zhang, for their invaluable assistance and advice on this project. She would like to thank the Polymer and Fiber Engineering Department at Auburn University which was extremely helpful for the completion of this project and who provided financial support for this research. As well, she offers many thanks to Dr. Dosier, Biological Sciences Department Head, and Mr. Schreiber, a PhD candidate, for inspiring her current research topic and for the abundant financial support required for her adhesive testing working at ITV Denkendorf in Denkendorf, Germany. Additional thanks are in order to Dr. Thomas and Dr. Buschle-Diller for acting as liaisons between ITV Denkdendorf and Auburn University which allowed her the opportunity to conduct an adhesive research project there. She appreciates the generous time that Dr. Farag donated to develop a new standardized tack testing method for this project. Special thanks are also given to Vladimir, Idris, Hasan, and David for their help and encouragement. Finally, the author offers her deepest thanks to God, her parents, and Christoph for providing her with support and encouragement throughout the process.

Table of Contents

Abstract ii

Acknowledgments iii

List of Tables viii

List of Figures ix

1 Introduction 1

2 Literature Review 3

2.1 Purpose of bandages, construction, important properties and issues 3

2.2 Bandage adhesives 4

2.2.1 Pressure sensitive adhesives 4

2.2.2 Transdermal acrylate adhesives 5

2.3 Potential use for foam adhesives in blister bandage technology 6

2.3.1 The blistering process 6

2.3.2 Relationship between skin moisture and blisters 7

2.3.3 Impact of sweat on blister formation 8

2.3.4 Current blister bandage technology 8

2.4 Incorporation of anesthetics into bandages 9

2.4.1 Partition constant 10

2.4.2 Benzocaine 11

2.4.3 Polymer-drug interaction 11

2.4.4 Impact of radicals on the polymer-drug system 12
2.5 Adhesive formation 12
2.5.1 Adhesives in form of films 13
2.5.2 Adhesive sprays 13
2.5.3 Adhesives in foam form 13
2.6 Foams 14
2.6.1 Foam formation and stabilization 14
2.6.2 Stabilization by use of surfactants 14
2.7 Characterization of bandages and adhesives 14
2.7.1 Peel test 15
2.7.2 Evaluation of adhesive tack 15
2.7.3 Viscosity and MW of adhesive 16
2.7.4 Drug release from bandage adhesive 17
3 Experimental Procedures 18
3.1 Materials 18
3.2 Synthesis of adhesives 19
3.2.1 Adhesive monomers 19
3.2.2 Adhesive trials 19
3.3 Adhesive foam preparation 21
3.4 Synthesis of adhesive with incorporated benzocaine 22
3.5 Radical termination 23
3.6 Characterization of products 23
3.6.1 Chemical structure 23

3.6.2 Viscosity 24
3.6.3 Molecular weight distribution 24
3.6.4 Adhesive tack and pressure sensitivity 24
3.6.5 Foam porosity 25
3.6.6 Drug release trials 26
3.6.7 Peel test 26
4 Results and Discusion 28
4.1 Commercial bandages 28
4.1.1 Peel testing of commercial bandages and adhesives 28
4.1.2 Tack testing of commercial bandages and adhesives 30
4.2 Synthesis of alternative adhesive morphology 32
4.2.1 Adhesive composition 32
4.2.2 Further characterization of the model formulation, AI1_S3 34
4.3 Reactivity ratio studies on AI1_S3 38
4.3.1 Characterizing the adhesive copolymer structure using reactivity ratios 38
4.3.2 Reaction combinations from reactivity ratio studies 41
4.3.3 Hypothesis on adhesive copolymer structures 55
4.4 Tack and viscosity of adhesives 58
4.5 Adhesive foams 61
4.6 Incorporation of a drug for pain relief in adhesives 66
4.6.1 Adhesive with incorporated drug 66
4.6.2 Radical termination prior to benzocaine loading 68
4.6.3 Benzocaine release trial from loaded adhesive 68

4.7 Adhesive pressure sensitivity and peel test comparison 71

5 Conclusions 74

6 Recommendations for Future Work 76

References 77

Appendix 80

List of Tables

Table 1 Relationship between the partition coefficient, K_{ow}, and drug delivery method [31] 10

Table 2 Summary of adhesive reactant formulations 20

Table 3 Solutions for benzocaine solubility testing in IPA and MA mixtures 22

Table 4 Tack testing tension results of commercial acrylate bandages 30

Table 5 Monomer *Q* and *e* values [59-61] and the reactivity ratios of the monomer combinations 40

Table 6 Theoretical copolymer structure based on reactivity ratios 40

Table 7 Reaction times and qualitative observations of the reactivity ratio study products 42

Table 8 Tack and viscosity measurements of polymer samples without drug loading 60

Table 9 Pressure sensitivity data from applied compressive forces of 0.1 - 20N; SD is standard deviation, BSC denotes benzocaine loaded adhesives, AA refers to ascorbic acid loaded adhesives, surf indicates Alconox surfactant addition, and decomp BZC refers to a sample with decomposed BZC in it. 71

List of Figures

Figure 1 Schematic adapted from a patented adhesive bandage with foam backing [26] showingthe profile of the bandage (top) and the top view of the bandage showing the foam structure (bottom) 9

Figure 2 Blister bandage schematic adapted from a patent [27] 9

Figure 3 Benzocaine chemical structure [34] 11

Figure 4 Ascorbic acid ($AscH_2$ on left) donates two hydrogen and one electron for quenching chain radicals and forms ($Asc^{\bullet-}$ on right) a more stable tricarbonyl ascorbate radical [37] 12

Figure 5 Tacky polymer structure with many short side chains between entanglement points 16

Figure 6 Chemical structures of IOA, HEA, and VA monomers 19

Figure 7 Schematic of tack and pressure sensitivity test conditions. 25

Figure 8 Schematic of alternative testing methods: a) steel plates overlapping 25 mm with bandage spanned across the two plates, b) steel plates folded on top of one another, c) peel testing within the clamps of the Zwick machine, d) peel testing of the bandage between the two clamped steel plates. 27

Figure 9 Peel test data from commercial acrylate bandages 29

Figure 10 Schematic of PSA wetting skin. Mechanical adhesion (a) could originate at the interfaces from interlocking connections between the pores and adhesive. Specific adhesion (b) is shown in the form of hydrogen bonds between the PSA and skin. 31

Figure 11 FT-IR spectra of A0_P, AI1_P, and AI1_S3 products 34

Figure 12 Water on the surface of AI1_S3 (a); contact angle of water on AI1_S3 (b) 34

Figure 13 H-NMR of IOA-HEA-VA polymer in deuterated chloroform 36

Figure 14 DSC graph of AI1_S3 polymer 37

Figure 15 TGA graph of sample AI1_S3 38

Figure 16 FT-IR spectra of homopolymerization experiments AI1_RR3 to AI1_RR5.....44

Figure 17 FT-IR spectra for AI1_RR6-AI1_RR9 dried product 45

Figure 18 FT-IR spectra from dried products from AI1_RR10 and AI1_RR11 46

Figure 19 FT-IR spectra from dried products of AI1_RR13-AI1_RR15 47

Figure 20 FT-IR spectrum from dried product of AI1_RR16-AI1_RR20 49

Figure 21 FT-IR spectra of IOA solution polymerized products from reactivity ratio studies 50

Figure 22 FT-IR spectra of IOA bulk polymerized products and two reference peaks (AI1_RR7 and AI1_RR14). 51

Figure 23 FT-IR spectra of all HEA samples from the reactivity ratio studies 52

Figure 24 FT-IR spectra of VA samples from reactivity ratio studies 54

Figure 25 DSC runs of high viscosity liquids: poly(HEA) (a); poly(VA) (b); poly(IOA) (c).....57

Figure 26 Relationship between tack and MW_e 59

Figure 27 Foam cell size comparison 62

Figure 28 Phase diagram (adapted from [62]) showing liquid to gas phase change due to low pressure and temperature.....63

Figure 29 Surfactant additives for foam stabilization 64

Figure 30 Micrographs of bulk polymerized foams a) AI1_RR16, b) AI1_RR19, and c) AI1_RR20 at 10X magnification showing closed cell foam formation occurred 65

Figure 31 a) AI1_BC_RT3 UV-Vis spectra in 40% PPG/PBS after 8 min at 500 rpm of: control, ascorbic acid (AA) loaded, and ascorbic acid and benzocaine (BZC AA) loaded; b) UV-Vis absorbance spectra of the benzocaine and ascorbic AA loaded adhesive (BZC AA) from 0 min to 15 min after high speed mixing 70

Figure 32 Adhesive pressure sensitivity 72

Figure 33 Peel test results of AI1_S3, AI1_S3 foam, and benzocaine and ascorbic acid loaded AI1_BE_RT3 foam 73

Figure 34 FTIR spectra of RR3 (AI1_RR3) to RR5 (AI1_RR5) 80

Figure 35 FTIR spectra of RR6 (AI1_RR6) to RR9 (AI1_RR9) 81

Figure 36 FTIR spectra of RR10 (AI1_RR10) to RR11 (AI1_RR11) 82

Figure 37 FTIR spectra of RR13 (AI1_RR13) to RR15 (AI1_RR15) 83

Figure 38 FTIR spectra of RR16 (AI1_RR16) to RR20 (AI1_RR20) 84

1 INTRODUCTION

Bandages are an essential medical textile used to promote the wound healing process. Bandages provide protection from the external environment and manage wound fluids to promote proper healing and faster healing times. Since bandages are so useful, a variety of architectures and adhesives have been developed to accommodate a multitude of injuries, as well as the various locations on which wounds can occur.

With the advent of pressure sensitive adhesives (PSAs) in the 1850s [1], many kinds of PSA formulations and structures have been used to enhance bandage performance. The development of moisture permeable PSAs improved wound and skin ventilation to reduce microorganism growth. As well, the creation of transdermal PSAs for delivering drugs in a controlled manner greatly impacted patient care and treatment compliance. Many technological advancements have been reported in this field; however, there still exists the need for further adhesive improvement and for an accurate, reported mechanical characterization of these adhesives.

This project focuses on characterizing the peel properties of commercially available bandages and the formation of a foam adhesive which could be used for transdermal drug delivery. As of yet, there have been no reported peel values for commercially available medical tapes, so the first portion of this project focuses on finding a common range of values from these bandage adhesives. The second portion of the project is delegated to creating a foam adhesive, which could potentially be used for transdermal delivery. Currently, all foam-incorporated bandages

have a two-part system comprised of an adhesive medium and a separate carrier medium containing the foam. Synthesizing a foam-adhesive and characterizing peel from commercially available bandages are the dual goals of this project.

2 LITERATURE REVIEW

2.1 Purpose of bandages, construction, important properties and issues

Bandages play a multifaceted role in wound healing. A bandage must protect the wound from contamination and shield it from external forces, as well as, allow proper moisture ventilation and manage any exudate from the wound. The importance of the bandage's roles changes depending upon the wound type. Therefore the bandage must be designed to well accommodate the needs of the wound.

There are a variety of bandage architectures presently available [2-5]; therefore, only a basic construction of a bandage will be provided here. A basic bandage consists of some type of carrier medium, an adhesive, and a release liner. The carrier medium is typically a moisture permeable fabric or plastic on which an adhesive will stick, and the release liner is usually a plastic liner which allows for easy release of the adhesive without removing it from the carrier medium. [1]

The carrier medium can be multilayered and designed to be impenetrable to microorganisms, provide abrasion resistance, contain a hydrogel or a moisture wicking pad/foam, or it can even contain a drug delivering reservoir. Several common carrier materials currently in use are polytetrafluoroethylene (PTFE) for low friction coefficient films, lycra or stretch nylon for a thin stretch fabric layer, polyethylene terephthalate for woven fabric and closed cell foam backings. [2, 3, 6]

The adhesive media currently used in bandage technology is a pressure sensitive adhesive liquid film. Pressure sensitive adhesive media found in commercial bandage products include: natural and synthetic rubber resins, polyacrylates, silicones, polyisobutylenes, hydrogels, and polyurethanes. [7, 8]

2.2 Bandage adhesives

2.2.1 Pressure sensitive adhesives

Pressure sensitive adhesives (PSAs) are adherent liquids utilized in most adhesive bandages for their skin-friendly properties, ease of removal, and excellent adhesion with minimal force application. PSAs are capable of quickly wetting and adhering to a surface with minimal applied force.[9] There are three types which are pertinent to discuss with respect to this project: solventless PSAs, moisture vapor permeable PSAs, and transdermal drug delivering PSAs.

Solventless PSAs are quite popular due to their environmentally friendly manufacturing methods. Several of these PSA types include hot melt PSAs, radiation curable PSAs, and water-born PSAs. Hot melt PSAs, although environmentally friendly, either require the use of ultraviolet (UV) photoinitiation or the application of a molten adhesive. Neither of these application methods is ideal for consumer convenience. Radiation curable PSAs require UV and electron beam radiation for adhesive curing; however, the scission products created from photoinitation can physiologically react. Water-born PSAs are produced from an acrylic ester based polymerizable surfactant which adheres well to both dry and sweaty skin. Of the solventless PSAs, water-born PSAs possess faster coating speeds; however, they exhibit weaker barrier properties, have higher tack variability, and adhere to dirt more readily than the solvent formulated PSAs.[10-12] Due to lower adhesive performance, the solventless PSAs are less

favored over their solvent-based counterparts. More research is needed in this area to develop solventless PSAs that can better compete with other PSAs in the market.

Moisture vapor permeable PSAs provide better skin treatment than PSAs that are less vapor permeable. Moisture buildup under the adhesive can cause lesions on the skin, so proper moisture vapor permeation of the PSAs is required for extended use bandages. Moisture vapor permeable PSAs are typically acrylic copolymers with non-bound hydrophilic groups which facilitate moisture transport through the adhesive.[10] Several documented methods of improving vapor permeation are through blending in alginates into the adhesive or through the use of adhesive gels based on an acrylate or polyurethane, both of which adhere well even to sweaty skin. [10]

PSAs have also been utilized for transdermal drug delivery systems (TDDSs) through the incorporation of an adhesive drug carrier. TDDS PSAs contain a drug dispersed or dissolved in an adhesive matrix. Common adhesive compounds used for these kinds of delivery systems are acrylates, silicones, and polyisobutylenes. [13] Acrylates are the most popular TDDS adhesive because they can be tailored to accommodate a wider variety of drugs. [13]

2.2.2 Transdermal acrylate adhesives

Acrylate PSAs are amorphous and produced by free radical initiated polymerizations. They can be synthesized in an organic solvent or through aqueous emulsion. [7] A variety of monomers can be used for polymerization to obtain certain chain pendant groups which provide the adhesive with desirable chemical and physical properties. [7, 13] A unique quality of acrylate PSAs in comparison to the other PSAs is their inherent tackiness; this avoids using tackifier additives which can alter other properties such as peel resistance, sheer resistance, and ageing resistance. [1]

Molecular weight (MW) of the adhesive and its side chains are of particular importance to the adhesive's physical properties and the amount of irritation the user experiences. A study [13] found that the adhesive's MW was linked to how well the adhesive performed on the skin, in terms of how much adhesive residue remained, how much the skin lifted upon removal, and the degree of irritation felt from removal of the adhesive. MW limiting agents are sometimes required for the polymerization process. Carefully controlling the polymerization reaction time is also important in influencing the adhesive's MW.

Most transdermal delivering bandages have a drug reservoir or have a drug loaded in an adhesive film, and typically the diffusion rates are controlled. As of yet, there are no reported transdermal drug delivering bandages with drug loaded foam adhesives.

2.3 Potential use for foam adhesives in blister bandage technology

Foam carrier mediums are currently used in bandages to provide relief from normal and frictional forces; however, these mediums are separate from the adhesive. Foam bandages could potentially be used for pain relief from many afflictions such as Shingles, corns, and blisters. Blisters and blister bandages in particular will be further discussed herein.

2.3.1 The blistering process

According to a popular blister bandage manufacturer [14], there are five possible stages in the blistering process. The first stage of blister formation is rubbing of the skin by frictional forces which disrupt the surrounding tissues. This causes a water-filled blister to form – stage two. Next the blister burst open in stage three, and the wound is exposed; at this point, the skin may begin flaking off or even bleeding. Stage three is the most painful portion of the blister development because fresh skin and nerve endings are exposed to the outside environment.

Scabbing of the wound area occurs in stage four which can still be discomforting because nerve endings are still exposed, and the final stage of the process is the healing of the scab. [14]

A variety of commercial products are available for blister prevention, but after a blister is formed, a blister bandage is needed to promote adequate wound healing, prevent the introduction of additional moisture or bacteria from outside the wound, and allow for proper ventilation. Blister bandages can also be used for preventative measures, but a majority of bandage consumers do not take action until stage three of the blistering process. [14] Despite this fact, transdermal anesthetics have not yet been investigated for incorporation into blister bandage adhesives.

2.3.2 Relationship between skin moisture and blisters

A study [15] examining the effect of skin moisture on its coefficient of friction found a linear increase in skin friction when exposed to moisture. It is proposed that moisture acts as a keratin plasticizer in the stratum corneum by rehydration of the dead stratum corneum which allows for bending and stretching. The thickness of the foot sole's stratum corneum is only 0.5 to 1 mm thick.[16] Since the stratum corneum is adhered to the epidermal layers, it wrinkles to accommodate the rehydrated, swollen cells.[15] Wrinkling of the feet's skin, yields an uneven distribution of an applied force which can escalate the creation of a friction blister.

Since moisture promotes the blistering process, the water balance from the skin must be taken into consideration for adhesives used in blister bandages. Water loss from the skin occurs from perspiration or evaporation. Average water loss through the skin by diffusion is between 300 and 400 mL/day. [17] Sweat loss from skin can range from 100 mL/day for normal activities to 2 L/day from high impact exercise or extreme heat. [17] Evaporation from the skin is predominately controlled by cholesterol and lipids that compose the skin's lipid bilayers.

These bilayers also serve as hydrophobic barriers to prevent water-soluble substances (including hydrophilic drugs) from penetrating the skin. [16]

2.3.3 Impact of sweat on blister formation

Blister formation can occur on many different areas of the body, in particular on hands and feet. Hence, sweat production in these areas is of importance and can alter adhesive properties. Since blister formation typically does not occur in a densely populated hair follicle area, sweat production affecting an adhesive would come from eccrine sweat glands and ducts. [18]

Sweat is composed of water, Na^+, K^+, Ca^{2+}, Mg^{2+}, Cl^-, bicarbonate, lactate, ammonia, and urea. [19-22] Sweat pH has been found by several studies [22-24] to be dependent upon the area of sweat production, as well as dependent upon the dryness of the skin. Foot sweet was found to have a pH of 5.21 ± 0.72; whereas, hand sweat had a pH of 5.61 ± 0.83. [23] Skin inflammation has been shown to decrease skin pH. [24] As skin pH changes, cell membrane ionic gradients dissipate yielding cellular necrosis which further increases the likelihood of blister formation. [25] Since the body continually excretes water vapor and sweat, an adhesive being utilized for blister protection will need to accommodate these physiological features.

2.3.4 Current blister bandage technology

Patented bandages [26, 27] indicate two specific architectures some of which include foam. Figure 1 shows a schematic of a bandage adhesive commonly used in standard bandages with an absorbent pad; this contains both a foam and a PSA. The foam consists of a polyethylene (PE) cast film ranging 3 to 4 mm in height with predominantly closed foam cells. Figure 2 shows a bandage specifically designed for blisters. The suggested foam height in this case is 6 mm with tapered edges. The outer edges of the bandage contain a PSA layer, while the center contains the

foam. Thus far, no patented blister bandage or reported adhesive is comprised of a joint PSA-foam structure.

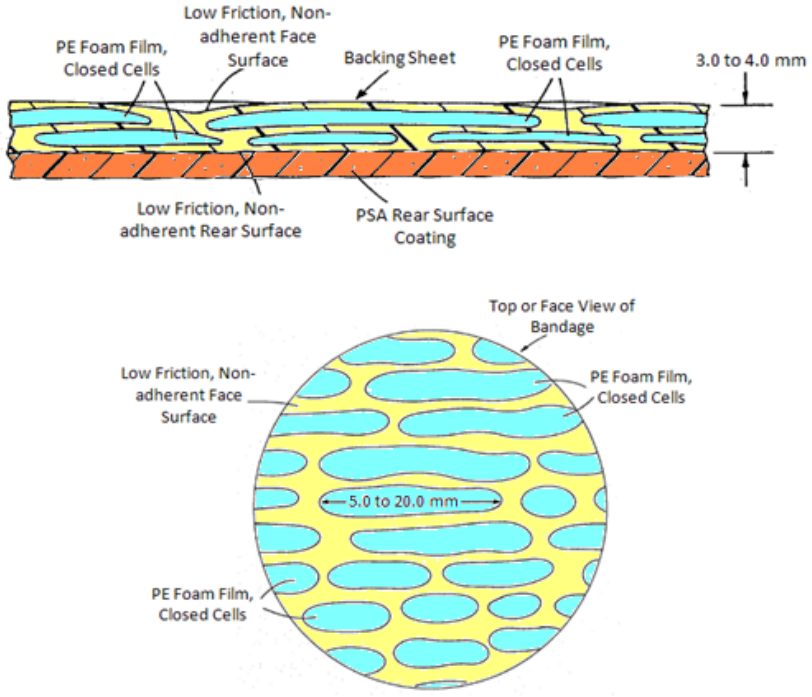

Figure 1 Schematic adapted from a patented adhesive bandage with foam backing [26] showing the profile of the bandage (top) and the top view of the bandage showing the foam structure (bottom)

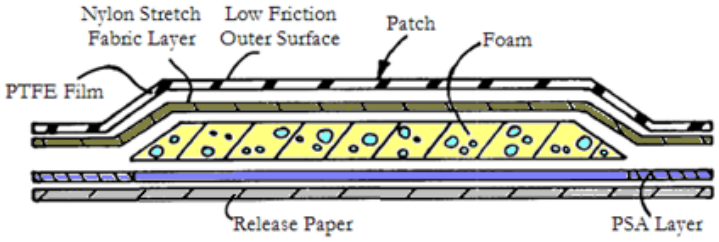

Figure 2 Blister bandage schematic adapted from a patent [27]

2.4 Incorporation of anesthetics into bandages

Transdermal drug delivering system (TDDS) bandages generally have three kinds of constructions. Bandages can have a drug reservoir which allows drug diffusion through a rate-

controlling membrane and an adhesive, or they can also be matrix systems with or without a rate-controlling membrane. [28, 29] There are many challenges that TDDS matrix systems face, such as drug delivery as a controlled means instead of simply through a 'burst' effect. As well, the drug could potentially interact with the matrix system and not diffuse or become inactive.

2.4.1 Partition constant

In order for a drug to be considered with a particular delivery method, its partition constant must first be assessed. A partition constant is a measure of an organic compound's miscibility or distribution between a hydrophilic and a lipophilic layer.[30] The partition constant K_{ow} can be measured from the compound's concentration in water versus octanol or water versus oil and is defined as,

$$K_{ow} = \frac{C_{\text{octanol}}}{C_{water}} \qquad 0 < K_{ow} < 4$$

where C_{octanol} and C_{water} are the molar concentrations of octanol and water, respectively. In pharmaceutical applications, the partition constant can be utilized to determine in which portion of the body a drug will best absorb. Table 1 is adapted from [31] which shows how the partition coefficient can be used to indicate the most efficient delivery mechanism.

Table 1 Relationship between the partition coefficient, K_{ow}, and drug delivery method [31]

Partition coefficient	Mechanism of delivery
Low K_{ow} (hydrophilic)	Injection
Medium K_{ow}	Oral
High K_{ow} (≥ 1, lipophilic)	Skin patch/ointment

2.4.2 Benzocaine

Benzocaine is a common anesthetic found in many over-the-counter products. It is commonly incorporated into dental anesthetic gels, sore throat sprays, and topical creams for relieving sunburn and hemorrhoid pain and acts a numbing agent that blocks the body's nerve signals wherever it is applied. In large amounts, benzocaine can be fatal; an overdose of benzocaine is reported to cause arrhythmias, seizures, comas, and slower brain activity. [32] Benzocaine has been studied for use in transdermal anesthetic delivery indicating that its partition coefficient is lipophilic enough for TDDSs. [33] It is soluble in methanol, diethyl ether, and slightly soluble in cold water. [32] Its chemical structure is shown in Figure 3.

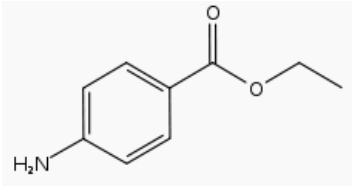

Figure 3 Benzocaine chemical structure [34]

Benzoyl peroxide was noted as having decreased anesthetic effects of benzocaine in a clinical study [34]. The study found from a skin prick test that a 75% increase in patient pain resulted when 5% benzoyl peroxide and 6% benzocaine cream were used versus the 6% benzocaine cream alone. This was reported as a result of benzocaine breakdown by benzoyl peroxide radicals or radicals formed from reacting with benzoyl peroxide. [34]

2.4.3 Polymer-drug interaction

In order for a drug to be loaded into a polymer matrix it must either be dispersed or dissolved within the adhesive. After loading, it must be possible to release the drug via a mechanism such as diffusion or matrix erosion. The polymer matrix must be inert in order for the drug to be released properly. However, the drug might also be entrapped in the polymer matrix and, due to

secondary molecular forces and the hydrophobicity/hydrophillicity of both mediums, diffusion might be prevented.[35] To ensure that the drug is being released from the polymer matrix, release studies must be performed specific to each system.

2.4.4 Impact of radicals on the polymer-drug system

Radicals can impact the polymer-drug system in a detrimental way by causing a chemical change of the drug or even its decomposition. As mentioned in 2.4.2, benzocaine has been reported to be sensitive to decomposition by radicals in the system. [34] Ascorbic acid, also known as vitamin C, is an oxygen free radical scavenger [36] and could be useful as a nontoxic compound for radical termination. Ascorbic acid has two hydroxyl groups which are hydrogen donating and one of which is electron donating, as shown in Figure 5. This tricarbonyl ascorbate radical is more stable than the free radicals it terminates, as the radical can be resonance stabilized between 3 carboxyl groups. [37] Its characteristic UV spectroscopy peaks are at the 265 nm wavelength for pH 5 and greater and at 245 nm for pH 3.2. [36]

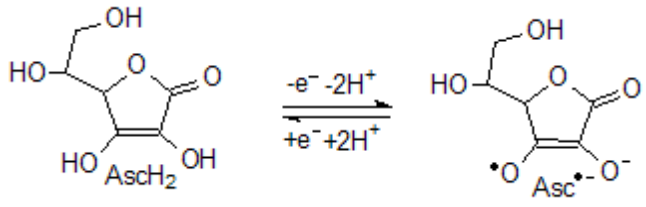

Figure 4 Ascorbic acid ($AscH_2$ on left) donates two hydrogen and one electron for quenching chain radicals and forms ($Asc^{\bullet -}$ on right) a more stable tricarbonyl ascorbate radical [37]

2.5 Adhesive formation

Depending upon their final applications, adhesives can take different forms. Adhesives can be cast into films, foams, and even sprayed onto substrates. Formation of these adhesives may require additives or special processing methods.

2.5.1 Adhesives in form of films

Adhesive films are utilized in labels, tapes, and protective films. Bandage adhesives which incorporate an adhesive film medium are classified as medical tapes. Adhesives tape films typically have coating weight values on the range of 25-40 g/m^2, and the suggested coating weight for medical tapes is 34-68 g/m^2. [1] In film form, the adhesive obtains a higher contact area with respect to sprayed on adhesives. Films can be obtained from the liquid adhesive in solution or from hot melt adhesives. The PSA can be extruded through a die or forced through a knife by hand which have a particular film height.

2.5.2 Adhesive sprays

Adhesive sprays can be applied in aerosol form or from a hot melt adhesive by using pneumatic pressure. These sprays typically provide a thinner layer of adhesive and often lack a full or continuous layer of adhesive coverage.

2.5.3 Adhesives in foam form

Adhesive foams have been used for conformable mounting tapes [1], safeguarding security materials [38], and biomedical implants [39]. An interesting application is a foam-like pressure sensitive tape which was imbedded with glass microbubble fillers. [1] For these glass microbubble filled tapes, the thickness of the pressure-sensitive layer needed to exceed three times the average diameter of the microbubbles to prevent breaking. [1] Many recently developed bandage adhesives have shown to provide the best properties with the addition of a foam carrier. [26, 27] Currently, no PSA foams have been reported for use in bandages.

2.6 Foams

2.6.1 Foam formation and stabilization

Foam formation as a result of freeze-drying has been reported for titanium foam [40], nanoporous cellulose foam [41], and even macroscopic solid foam from carbon nanotubes [42]. Foam formation has also been reported from boiling off a liquid [43] and from high-speed mixing [44]. In addition, both foam formation and stabilization can be achieved through the use of blowing agents [45-47]. All methods appeared suitable for their respective applications; however, the freeze drying and heating method seemed to provide the most stable and long lasting foam results.

2.6.2 Stabilization by use of surfactants

Surfactants were found to act as foam stabilizers by decreasing the liquid-gas contact angle. [48] A research study [49] showed that a non-ionic surfactant increased foam stability of $C_{12}EO_3$ (tri(oxyethylene) dodecyl ether) up to 10% surfactant concentration, after which point the surfactant affected solution viscosity and decreased foam stability. Contrary to this result, another study [48] found that at high surfactant concentrations about the critical micelle concentration level, stabilization of films and foams can occur via stratification, a micellar layering mechanism. Additionally, this study [48] reported that bubble size determines the rising velocity of the bubble; the bigger the bubble, the higher the velocity with which it will rise. As a result, bubble size and hence bubble velocity will impact the final formed foam structure.

2.7 Characterization of bandages and adhesives

Physical characterization of a PSA commonly consists of peel, tack, and sheer resistance. The definition of ‘adequate’ peel, tack, and sheer resistance is relative to the end application of

the PSA. In drug incorporated PSAs, the drug release from the TDDS must be characterized as well.

2.7.1 Peel test

Peel is defined as the strength of the adhesive joint. This is tested by debonding of the adhesive using a stress direction other than that of the laminate. The laminate is the product formed by joining two or more materials together. There are three means of peel testing: T testing, 90°, and 180° testing. [1, 50] These tests measure the strength required to debond the laminate. Once a peeling front is created, a machine measures the force required to propagate the tear along the peeling front.

2.7.2 Evaluation of adhesive tack

Tack is the adhesive's ability to bond instantaneously to a substrate. Adhesive tack is due to short macromolecular chain diffusion from the adhesive to the adherend substrate over a short contact time. [1] As previously mentioned, lower MW chains can achieve faster surface wetting, so it is critical for an adhesive polymer backbone to have the appropriate molecular weight distribution and/or to have side chains to provide this surface wetting capability. Increased side chains produce more entanglement points. Acrylic adhesives are reported as inherently tacky due to their high molecular weight between entanglements (MW_e). [1] Figure 4 is a pictorial representation of a tacky polymer structure with many side chains between entanglements.

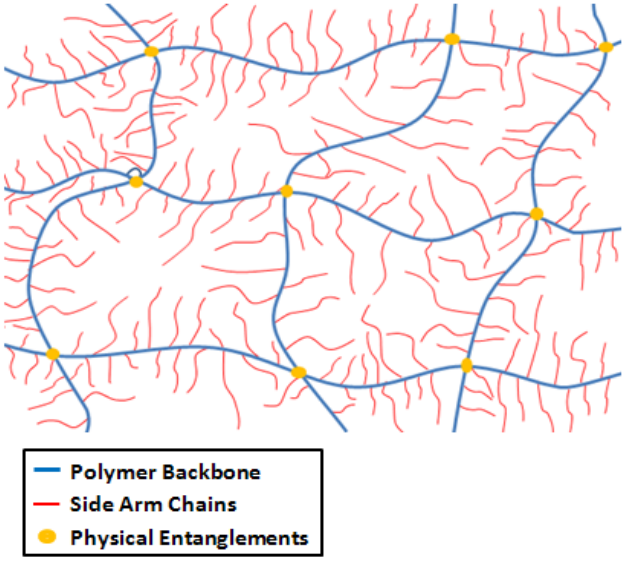

Figure 5 Tacky polymer structure with many short side chains between entanglement points

2.7.3 Viscosity and MW of adhesive

The viscous and elastic nature of PSAs allows them to quickly flow, dissipating an applied force, and to obtain contact with a surface; as well, it allows them to resist flow once an applied force is removed. [51] This dichotomous behavior of PSAs is due to their viscoelasticity. Viscoelastic behavior of PSAs is affected by the MW, molecular weight distribution (MWD), chain shape (i.e. branching, conformation, and crosslinking), and chain structure (i.e. level of hydrocarbon saturation, polarity of functional groups, and frequency of repeated groups). [1, 7, 52] Adhesives with low MW fractions achieve faster polymer relaxation times which allows quick wetting of a large surface area. [1] On the other hand, a critical MW (MW_c) must be reached for chain entanglement to take place; MW_c is the threshold value of MW required for chain entanglement to occur. If the propagating chains' MW does not achieve MW_c, the adhesive's dynamic storage modulus will not have a rubbery elastic plateau which is a critical material property requirement for pressure-sensitive debonding. [1] Therefore, a polydisperse

polymer mixture is necessary for the desired viscoelasticity in a PSA; it must both wet a surface well and also properly function as pressure sensitive products.

2.7.4 Drug release from bandage adhesive

The drug release profile from the adhesive is of utmost importance in a TDDS. If the drug remains contained within the adhesive or immediately diffuses from the adhesive exhibiting a burst effect, then the TDDS is useless. Drug release generally is regulated by diffusion and/or erosion of the polymer matrix. [53] Drug release from the adhesive can be either diffusion controlled or swelling controlled. [54] Erosion of a high viscosity liquid polymer matrix is more difficult to detect, while drug release from diffusion might be tracked with UV-Vis spectroscopy or similar methods.

3 EXPERIMENTAL PROCEDURES

3.1 Materials

The following materials for experimentation were purchased from Alfa Aesar®: vinyl acetate (VA), 99% stabilized with 8-12ppm hydroquinone; 2-hydroxyethyl acrylate (HEA), stabilized; benzoyl peroxide (BP), wet with 25% water; 1,2-Propanediol or propylene glycol (PPG), ACS grade, 99.5%; isopropyl tetradecanoate, 98%. HPLC grade chloroform was purchased from EMD Chemicals Inc. Ethyl acetate (EA), AR* ACS grade, 99.5% (by GC) was obtained from Mallinckrodt® Chemicals. Benzocaine (B) was acquired from TCI® America. Isooctyl acrylate (IOA) and 2,2'-azobisisobutyronitrile (AIBN) were purchased from Sigma Aldrich®. Agros Organics supplied 2,2,5,5-tetramethyl-imidazolidin-4-one (TMIO), 98% and 2,2,6,6-tetramethyl-4-piperidinol (TEMPOH), 99%. Sodium phosphate monobasic laboratory grade, potassium chloride, and ACS grade L-ascorbic acid were purchased from Fisher Scientific®. USP grade sodium chloride was purchased from BDH®. ACS grade isopropanol; Alconox* detergent powder and ACS grade methanol were supplied from VWR.

The following commercial bandages were used for testing: Gothaplast® Gotha flex transparent, BSN Medical GmbH Leukosilk® and 3M™ Micropore® fleece bandage which have hypoallergenic polyacrylate adhesives; Durapore™ Askina® Silk and Mölnlycke™ Mepore® dressing which have polyacrylate adhesives as well.

3.2 Synthesis of adhesives

3.2.1 Adhesive monomers

An IOA/HEA/VA copolymer filled with methyl methacrylate macromers previously published [55] for transdermal acrylate adhesives was modified and utilized for this experimentation. Methyl methacrylate macromers were not included in the adhesive formulation. The monomer structures used for polyacrylate formation are shown below in Figure 6. Any listed percentages are based on weight ratios (w/w) unless otherwise stated, and the reactants are listed in sequential order as they were added to the adhesive solutions.

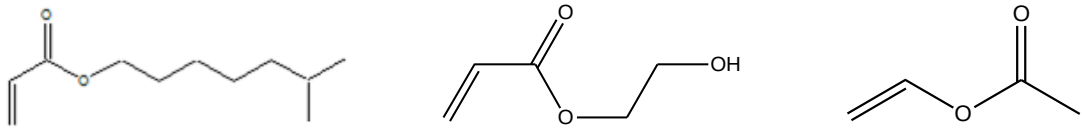

Figure 6 Chemical structures of IOA, HEA, and VA monomers

3.2.2 Adhesive trials

A summary of experiments is shown in Table 2. The original patented formulation has been given the sample code AI1_P. The processing method for all samples was identical. All adhesive mixes were N_2 purged and heated in an oil bath at 55 ± 2°C with stirring for 7 h. After synthesis, solvent evaporation in a hood was conducted before adhesive mechanical testing. A control batch (A0_S1) was created based on the AI1_P formulation without any added initiator.

Sample code abbreviations in Table 2 indicate what kind of initiator (if any) was used, for what purpose the adhesives were adapted from the patent recipe, if a drug was incorporated, and if any post-polymerization treatments were conducted. A0 signifies an adhesive formulation without an initiator. AI is an adhesive formulation incorporating a BP initiator (AI1) or an AIBN initiator (AI2). P denotes the patent formula. Modifications from the patent recipe have codes with an S. RR is used for experiments pertaining to the reactivity ratio study. Adhesives which

were further tailored in preparation for the drug incorporation are labeled with D. Adhesives incorporating benzocaine at the beginning or the end of the reaction are labeled as BC or BE, respectively. RT stands for the adhesive formulations customized for the radical termination study.

Table 2 Summary of adhesive reactant formulations

Sample ID	BP (g)	EA (mL)	IPA (mL)	IOA (mL)	HEA (mL)	VA (mL)	MA (mL)	BZC (g)	AIBN (g)	
AI1_P	0.10	3.8	0.1	1.6	0.5	0.5	0	0	0	*
A0_S1	0	3.8	0.1	1.6	0.5	0.5	0	0	0	
A0_S2	0	0	0	0	5	0	0	0	0	
AI1_S1	0.07	3.8	0.1	1.6	0.5	0.5	0	0	0	
AI1_S2	0.10	3.8	0.2	1.6	0.5	0.5	0	0	0	
AI1_S3	0.10	3.8	0.4	1.6	0.5	0.5	0	0	0	**
AI1_S4	0.07	3.8	0.4	1.6	0.5	0.5	0	0	0	
AI1_RR1	0.10	3.8	0	0	0	0	0	0	0	
AI1_RR2	0.10	3.8	0.4	0	0	0	0	0	0	
AI1_RR3	0.10	3.8	0	0	0	0.5	0	0	0	
AI1_RR4	0.10	3.8	0	0	0.5	0	0	0	0	
AI1_RR5	0.10	3.8	0	1.6	0	0	0	0	0	
AI1_RR6	0.10	3.8	0	1.6	0	0.5	0	0	0	
AI1_RR7	0.10	3.8	0	1.6	0.5	0	0	0	0	
AI1_RR8	0.10	3.8	0	0	0.5	0.5	0	0	0	
AI1_RR9	0.10	3.8	0	1.6	0.5	0.5	0	0	0	
AI1_RR10	0.10	3.8	0.4	1.6	0	0	0	0	0	
AI1_RR11	0.10	3.8	0.4	0	0.5	0	0	0	0	
AI1_RR12	0.10	3.8	0.4	0	0	0.5	0	0	0	
AI1_RR13	0.10	3.8	0.4	1.6	0.5	0	0	0	0	
AI1_RR14	0.10	3.8	0.4	1.6	0	0.5	0	0	0	
AI1_RR15	0.10	3.8	0.4	0	0.5	0.5	0	0	0	
AI1_RR16	0.10	0	0	5	0	0	0	0	0	
AI1_RR17	0.10	0	0	0	5	0	0	0	0	

AI1_RR18	0.10	0	0	0	0	5	0	0	0
AI1_RR19	0.10	0	0	1.6	0.5	0.5	0	0	0
AI1_RR20	0.10	0	0	1.6	0	0	0	0	0
AI1_D1	0.10	3.8	0	1.6	0.5	0.5	0.4	0	0
AI1_D2	0.10	3.8	0	1.6	0.5	0.5	0.6	0	0
AI1_D3	0.10	3.8	0.2	1.6	0.5	0.5	0.2	0	0
AI1_D4	0.10	3.8	0.1	1.6	0.5	0.5	0.3	0	0
AI1_D4_BC	0.10	3.8	0.1	1.6	0.5	0.5	0.3	0.1	0
AI2_D4_BC	0	3.8	0.1	1.6	0.5	0.5	0.3	0.1	0.1
AI1_BC1	0.10	5	0	0	0	0	0	0	0
AI1_BC2	0.10	0	5	0	0	0	0	0	0
AI1_BC3	0.10	0	0	5	0	0	0	0	0
AI1_BC4	0.10	0	0	0	5	0	0	0	0
AI1_BC5	0.10	0	0	0	0	5	0	0	0
AI1_BC6	0.10	0	0	0	0	0	5	0	0
AI1_BE_RT1	0.10	3.8	0.8	1.6	0.5	0.5	0	0	0
AI1_BE_RT2	0.10	3.8	2.4	1.6	0.5	0.5	0	0	0
AI1_BE_RT3	0.10	3.8	1.3	1.6	0.5	0.5	0	0	0

* Patented formulation

** Formulation adapted from AI1_P which is the basis for the following reactions

3.3 Adhesive foam preparation

Solution AI1_S3 was used for foam creation with blowing agents, freeze drying, high speed mixing, and the application of heat. Solutions AI1_RR19 and AI1_RR20 produced foam as a reaction product without requiring any further processing. For foam formation with the help of a blowing agent, the solution AI1_S3 was poured into a petri dish and air was blown into the liquid using a disposable pipette to create foam. Freeze drying of the sample was performed with a Labconco® Freeze Dryer 8. Solvent removal via freeze drying to produce foam involved pre-cooling the solution at 0°C for 12 h. After cooling, the film was removed and the contents were freeze dried for 4 h, until the foam remained stable. Heat application for foam formation was

carried out at 55°C. For high speed mixing for foam formation a HighSpeed™ DAC 150 FVZ-K mixer was used at 1100, 2400, 3000 and 3500 rpms for 30 s, 1, 2 and 3 min time spans.

Two surfactants were added to the adhesive solution prior to foam formation for freeze-drying. The surfactant used was Alconox®, a pure powder detergent. Ratios of 0.25%, 1% and 3% w/w of the detergent were added to the adhesive solution and mixed prior to freezing and freeze-drying. Isopropyl tetradecanoate, was added at 0.25% in a similar manner.

3.4 Synthesis of adhesive with incorporated benzocaine

Since benzocaine is reported as being soluble in methanol, its solubility was tested in various mixtures of isopropanol (IPA) and methanol (MA). Table 3 identifies the different solution concentrations tested for use in the adhesive compound. The mixture abbreviations in Table 3 indicate that benzocaine (B) was in the alcohol solution and in which alcohol(s), where isopropanol is I, methanol is M, and a mixture of both is IM. All solutions were mixed with a vortex mixer for 2 min.

Table 3 Solutions for benzocaine solubility testing in IPA and MA mixtures

Mixture	Benzocaine (%)	IPA (%)	MA (%)
BM1	20	0	80
BI1	20	80	0
BIM1	20	32	48
BIM2	20	40	40
BIM3	20	60	20

Several batches of adhesive were made using different amounts of IPA and MA (AI1_D1 to AI1_D4) in preparation for benzocaine addition. Adhesives with different initiators were prepared with a benzocaine loaded alcohol solution in AI1_D4_BC and AI2_D4_BC. Following these reactions, individual compounds with initiator were reacted with benzocaine (AI1_BC1 to

AI1_BC6); these vials were mixed for 2 min. Viscosity was measured and color was visually analyzed 24 h after assimilation at ambient temperature and again compared after 12 h of heating. A control solution of 4 mL methanol and 2% benzocaine was created. Additional mixtures of AI1_BC1 to AI1_BC6 were made without initiator and were not reacted for comparison.

A batch of AI1_S3 was polymerized for 7 h and then 2% benzocaine was added with N_2 purging. The sample was placed into a 55 ± 2°C oil bath for 4 h. Finally, the adhesive was visually compared with the AI1_S3 formulation.

3.5 Radical termination

Several chemicals were added to remove radicals from the adhesive solution prior to benzocaine incorporation. Isopropanol, chloroform, TMIO, and TEMPOH were added in 2:1 weight ratios to the benzocaine and stirred for 2 h prior to benzocaine incorporation. Ascorbic acid was added in a 1:1 weight ratio and stirred for 2 h prior to benzocaine addition. In order to observe the effect of the solid radical terminators (TMIO, TEMPOH, and ascorbic acid) on the adhesives, new adhesive formulations were created (AI1_BE_RT1 to AI1-BE_RT3).

3.6 Characterization of products

3.6.1 Chemical structure

Fourier Transform Infrared (FT-IR) and proton nuclear magnetic resonance (^{1}H NMR) were conducted on selected samples to evaluate their chemical structure. FT-IR analysis was performed on all samples in solution and dried using the Smart Orbit setting of a ThermoFischer

Scientific® Nicolet 6700 FT-IR. FT-IR analysis of each adhesive ingredient, benzocaine, and the benzocaine incorporated samples were also conducted.

^{1}H NMR was conducted using a Bruker Ascend 400 Hz NMR machine with Topspin 2.1 analysis software. Deuterated chloroform was utilized as the solvent. The three monomers (IOA, HEA, and VA), a pure adhesive sample, and an adhesive sample loaded with benzocaine were analyzed.

3.6.2 Viscosity

Rheological analysis was performed using a TA Instruments® ARG2 parallel plate viscometer following ASTM standard D2556 – 93a on dried adhesive samples. The samples were dried on a glass pane covered with Teflon tape in an oven at 55°C for 4 h, then left in air at 23°C for over 16 h. Selected adhesives in solution were also tested.

3.6.3 Molecular weight distribution

The adhesive's MW and MW distribution can be found using gel permeation chromatography (GPC). The test was conducted with tetrahydrofuran solvent in a Viscotek® 270 GPC system.

3.6.4 Adhesive tack and pressure sensitivity

Tack is the measurement of an adhesive's instantaneous bonding strength to an adherend. To determine pressure sensitivity of an adhesive, the adhesive's bond strength is measured with respect to changes in applied pressure. Testing of the adhesive tack and pressure sensitivity was conducted on the INSTRON® 5565 using the basic principles of the ASTM standard D 2979 – 01 for tack. Adhesives were cast on a 0.05 mm polypropylene film backing, heated to 50°C for 11 h for solvent evaporation, and then cooled for over 16 h at room temperature prior to testing.

Tack was measured by applying 0.1 N from a 1 cm diameter steel probe for 0.1 s, and pressure sensitivity was determined by comparing adhesive bond strengths for the application of 1 N, 2 N, 4 N, 8 N, and 20 N from the same probe for 5 s. The cyclic loading program was used to accomplish this testing procedure, and a 5 kg annular weight which has a slightly larger diameter than the moving probe was used to stabilize the adhesive site to which the probe would be adhering. A schematic of the test conditions is shown in Figure 7. The program parameters were as follows: testing speed of the probe was 0.83 mm/s until the required force loading (0.1 N, 1 N, 2 N, 4 N, 8 N, or 20 N) was achieved, this loading was maintained for the required time (0.1 s or 5 s), and a removal speed was 20 mm/s used.

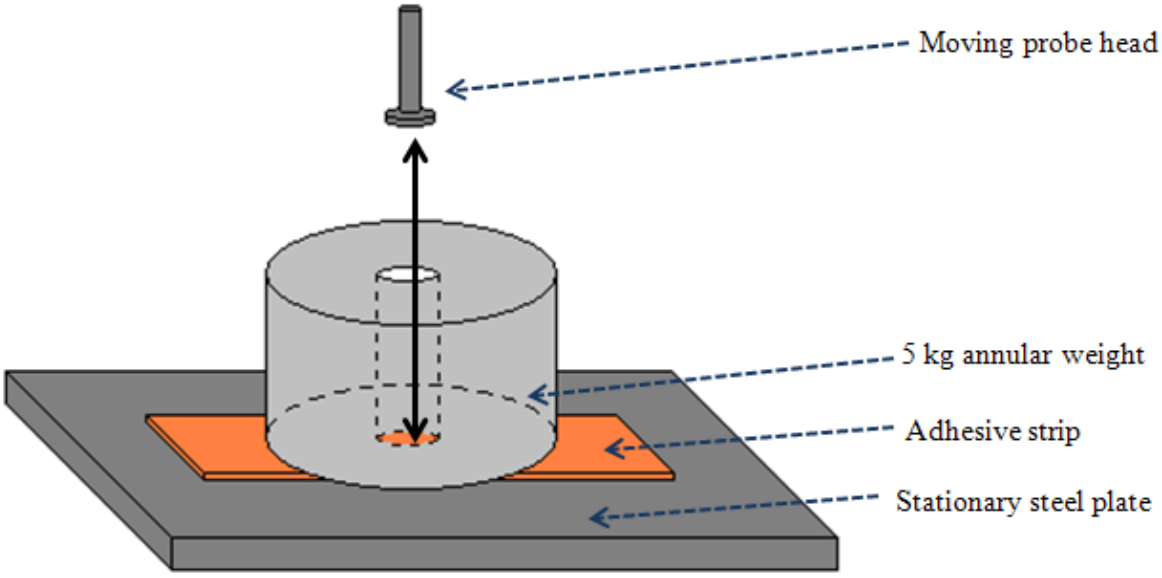

Figure 7 Schematic of tack and pressure sensitivity test conditions.

3.6.5 Foam porosity

The adhesive's foam porosity was characterized using an Olympus BH-2 microscope at 4X magnification. Ten drops of adhesive were freeze dried directly on a microscopy slide. Images of the foams were taken using a camera attached to the microscope.

3.6.6 Drug release trials

Drug release trials were conducted, according to [33], using 40% w/w propylene glycol in phosphate buffered saline solution and using UV-Vis spectroscopy to detect drug diffusion from the adhesive to the solution. For a control sample, an adhesive without an incorporated drug was used to compare with the drug loaded adhesives. The studies were conducted using a Shimadzu® UV-2450 UV-Vis Spectrophotometer at 500 rpm for various time intervals.

3.6.7 Peel test

Self-adhesive tapes from a variety of commercial bandages were peel tested using the standard DIN EN 1939, *Self-adhesive tapes – Determination of peel adhesion properties.* Protocol 8 from the standard was followed for measuring the tapes' adhesive relative strengths in the 180° peel test. Steel test plates 50 x 125 x 1.1 mm with a steel grade of 1.4301, 2R surface quality, and 50 nm surface roughness were utilized for peel testing. Seven commercial bandage tapes were investigated: Gothaplast® Gotha flex, BSN Medical GmbH Leukosilk®, 3M™ Micropore® fleece bandage, Durapore™ Askina® Silk, and Mölnlycke™ Mepore® dressing. With the exception of Mepore® which had a sample width of 20 mm, all samples had a 25 mm width.

Twenty-four hours prior to testing, the steel test plates were cleaned and left to dry under a fume hood in a 19 ± 1°C environment. The aforementioned bandages were kept at 23 ± 1°C for 2.5 h before testing. Specimens were prepared by adhering 125 mm of the 300 mm tape sample to the steel plate, pressing the sample twice in both lengthwise directions with the 2 kg standard FINAT roller, and then, pulling back the unadhered sample to remove 25 mm from the steel plate end for testing. All specimens were prepared in accordance with DIN EN 1939 standards – testing was conducted within 5 min after preparation.

A Zwick/Roell tensile testing machine was used for experimentation following Standard DIN EN 1939 testing regulations. A clamp span length of 170 mm was used with a peel speed of 5 mm/s with an initial force of 0.2 N. Bandage peel test data was measured from 0 to 80 mm length relative to the clamp distance. Data between 25 and 75 mm were analysed to avoid any erroneous readings from slack in the bandage between the test plate and clamp span. Sand paper was placed around the samples of Leukosilk®, Micropore®, Askina® Silk, and Mepore®.

An alternative testing method was devised to minimize sample elongation. Mepore® was adhered to two overlapping steel plates. The plates overlapped by 25 mm in the lengthwise direction, and the 300 mm bandage samples spanned both plates with excess sample adhering to the back of one plate. The two adhered steel plates were then placed on top of one another and one end of each plate was adjoined inside the clamps and tested from a clamp length of 114 mm. Figure 8 shows the schematics of these tests.

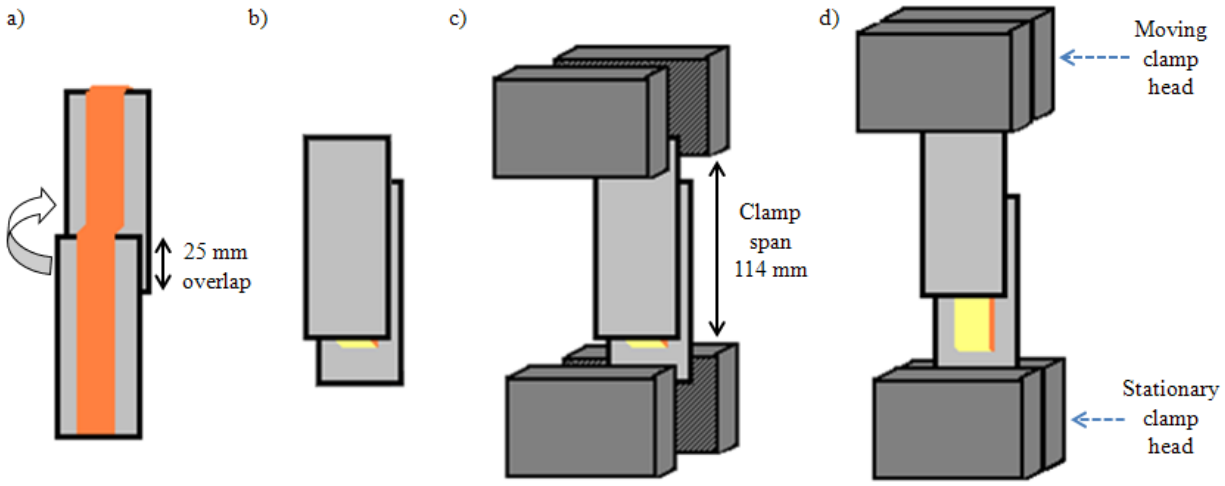

Figure 8 Schematic of alternative testing methods: a) steel plates overlapping 25 mm with bandage spanned across the two plates, b) steel plates folded on top of one another, c) peel testing within the clamps of the Zwick machine, d) peel testing of the bandage between the two clamped steel plates.

4 RESULTS AND DISCUSSION

4.1 Commercial bandages

Commercial polyacrylate based adhesive bandage tapes were selected for peel and tack testing as these results have not yet been reported. The exact chemical compositions and synthesis methods of the polyacrylate adhesives are proprietary information; thus, very few details relative to the polymer system and kind of drug incorporated were disclosed. Regardless, mechanical testing of these bandage adhesives provided a necessary benchmark for this project's experimental samples. All of these adhesives were of slab geometry and contained no transdermal drug additives.

4.1.1 Peel testing of commercial bandages and adhesives

Peel testing results from the commercial acrylate bandage tapes can be found in Figure 9. The values vary greatly within a range of 3 - 13 N. The hypoallergenic formulation from Gothaplast® had the highest peel strength values, followed by Leukosilk® which also had a hypoallergenic formula, Micropore® with a hypoallergenic composition, and Askina Silk®.

During initial peel testing investigations, Mepore® tapes transferred almost all of their adhesive resin onto the steel plate substrate which is not a preferable characteristic for an adhesive; as well, the tape fabric deformed during the testing process. Material elongation interfered with data collection from the material being in tension rather than transferring the tension to the peeling front. For this reason, the alternative testing method previously mentioned

was created which significantly reduced material elongation (see Figure 8 in the Experimental section).

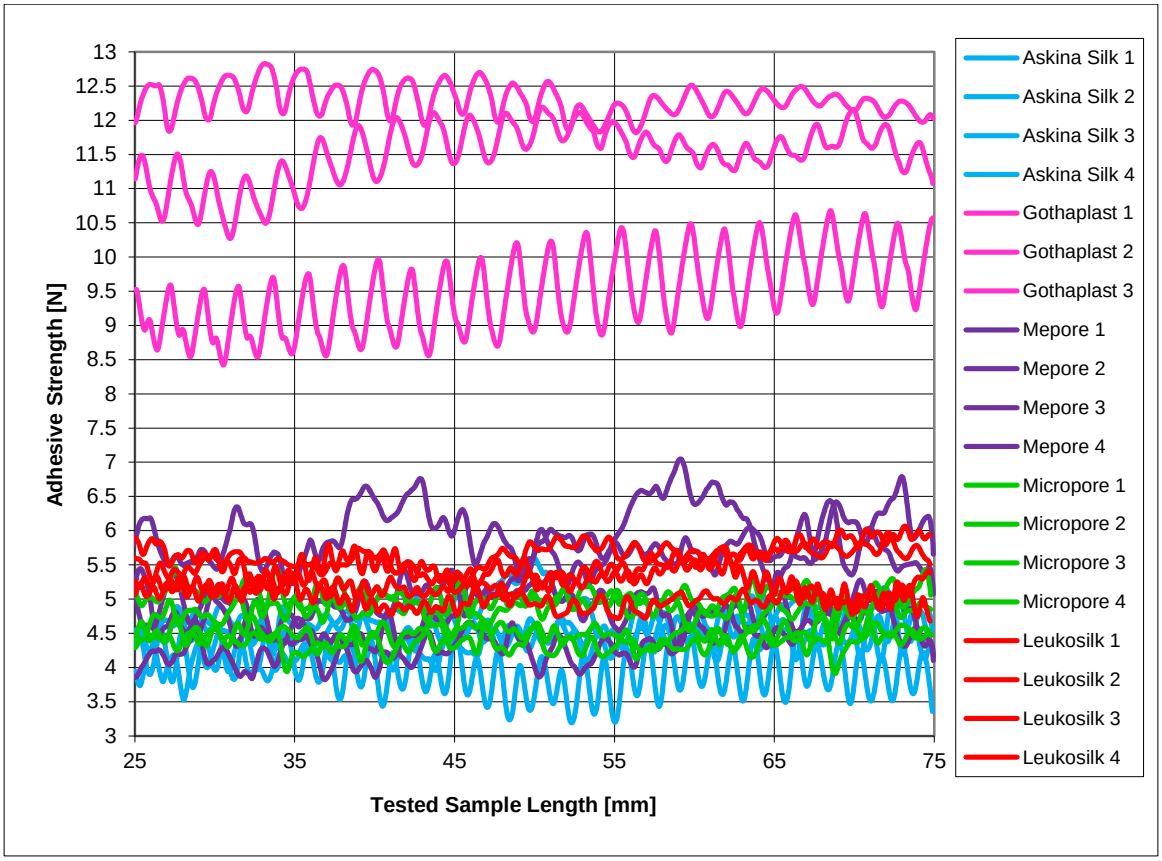

Figure 9 Peel test data from commercial acrylate bandages

Sinusoidal data were obtained as a result of tear propagation horizontally along the peel front. As the tear propagates across the peel front, it creates a stress concentration which spikes the peel strength values; as the peeling front is relocated to the next adhered area, the adhesive peel strength values decrease. Mepore® samples did not exhibit this behavior but rather form quite variable and inconsistent data patterns. This is most likely the result of some adhesive stretching prior to delamination from the carrier material. Adhesive delamination occurs when the bandage's peel strength from the substrate is higher than the carrier material's peel strength from the adhesive. This can also occur if an adhesive is not pressure sensitive; in this case, the

adhesive does not have enough elasticity to de-wet or be removed from a substrate without some adhesive delamination.

4.1.2 Tack testing of commercial bandages and adhesives

Tack testing results of the commercial bandages ranged from 0.2 – 0.5 N, as summarized in Table 4. Askina Silk® and Leukosilk® showed the highest tension values which means that both had the highest tack or ability to quickly flow and wet a substrate surface. Comparing the commercial bandages' tack values with their peel test data, it is obvious that there was no correlation between peel resistance and adhesive tack. This can be observed from Gothaplast and Micropore samples which had similar tack tension values but very different peel resistance ranges. An example of an ideal bandage adhesive was Leukosilk®; Leukosilk has an adequately high tack without being too tacky, and its peel resistance was not too large which reduces pain upon adhesive removal.

Table 4 Tack testing tension results of commercial acrylate bandages

Sample Id	Tension (N)	Standard Deviation
Askina Silk®	0.5	0.05
Gothaplast®	0.3	0.02
Mepore®	0.2	0.01
Micropore®	0.2	0.01
Leukosilk®	0.5	0.01

The lack of correlation between peel and tack tests occurs because the tests target different polymer properties. Since tack is a measure of the adhesive's instantaneous surface wetting capabilities without an applied force, tack is directly related to the polymer's surface tension and specific adhesion. Decreased surface tension permits surface pore permeation which forms mechanical adhesion through an interlocking connection at the adhesive and porous surface interface. [53] As well, specific adhesion is the formation of secondary forces (i.e. hydrogen

bonds, dipole-dipole interactions, and van der Waals forces) between the two interfaces. [53] Figure 10 is a schematic representation of mechanical adhesion from interlocking connections and specific adhesion. On the other hand, peel resistance is strongly related to polymer viscoelasticity. Peel resistance is a measure of a tacky adhesive's bonding strength to a substrate after a predetermined force is applied. The applied force is dissipated to some extent by polymer flow and the remaining energy is stored within the polymer's molecular bonds until its release upon laminate debonding. Therefore, peel test results are related to the polymer's viscoelastic nature, and tack is directly related to the polymer's surface tension and specific adhesion.

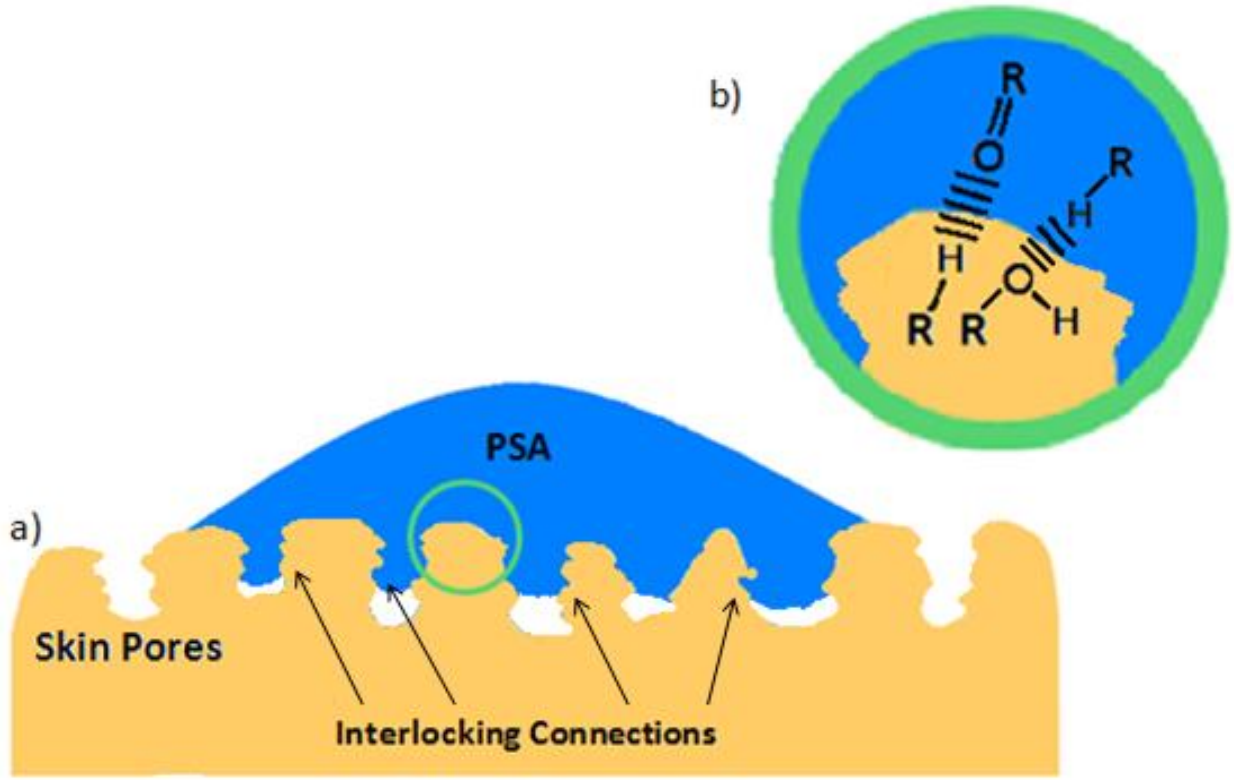

Figure 10 Schematic of PSA wetting skin. Mechanical adhesion (a) could originate at the interfaces from interlocking connections between the pores and adhesive. Specific adhesion (b) is shown in the form of hydrogen bonds between the PSA and skin.

Overall, peel and tack testing of commercial bandages showed that the characteristics of currently utilized adhesives varied to a considerable extent. One of the goals of this project was to develop a bandage adhesive with a novel foam morphology that would have superior properties in regard to the tack and peel attributes of commercial bandages with adhesive slab geometries. Furthermore, this project aimed to develop a foam adhesive with drug delivering capabilities, such as for delivering anesthetics, without losing the adhesive's rheological characteristics.

4.2 Synthesis of alternative adhesive morphology

For initial studies, polymerization experiments were conducted based on a patent formulation [55] with modifications for the adhesive to form a stable foam. Since the copolymer structure was unknown, reactivity ratios were calculated and a possible theoretical structure was proposed. As monomer ratios, initiators, solvents, and other additives were varied, the products were characterized by their viscosity, tack, and peel properties. Finally, an attempt was made to incorporate a drug (benzocaine) into the adhesives; UV-Vis testing was utilized to observe whether the drug release could be determined.

4.2.1 Adhesive composition

An adhesive monomer mixture (A0_S1) based on AI1_P was prepared without initiator which, as expected, did not polymerize under the reaction conditions. Evaporation of A0_S1 product left no residue which suggested that polymer product formation did not occur with the acetate and acrylate monomers alone; this was expected because vinyl ester monomers are categorized only as free-radical polymerizing monomers [53]. Likewise, for HEA monomer

(A0_S2), no polymer product formation occurred indicating that the hydroxyl functional group on the monomer does not participate in ionic polymerization during the reaction.

Polymer formation for AI1_P occurred, indicating that free-radical polymerization had happened. The polymer gel formed was tacky and elastically responded to different manual pressure applications. The FT-IR spectra of the polymer product is provided in Figure 11 together with A0_P (control reaction) and AI1_S3 (modified version of patent). As can be seen in the FT-IR spectra, the carbon-carbon double bonds are present at 1620-1680 cm^{-1} for sample A0_S which did not polymerize. However, these are not present for samples AI1_P and AI1_S3, indicating that polymer formation was achieved. Due to the very high viscosity of the AI1_P gel, the polymer could not be cast into a film, so modifications to this formulation had to be developed.

Modifications were made to the initiator and alcohol concentration to find a formulation which would result in lower product viscosity. Decreasing the initiator amount by 30% (AI1_S1) resulted in a high viscosity liquid with limited tack. Increasing the isopropanol amount by 100% from AI_P (AI1_S2) resulted in a tacky gel which did not show a significant viscosity decrease from AI1_P. Therefore, a 300% increase (AI1_S3) in isopropanol based on the patented formula was used which created a tacky, less viscous liquid, that could be spread into a film. Reducing the initiator content by 30% from AI1_S3 (AI1_S4) produced an almost nonviscous, tacky liquid. Tack and viscosity measurements for AI1_P and AI1_S3 are discussed in chapter 4.4. Since sample AI1_S3 was used as a model formulation for future experiments, this sample was characterized further with ^{1}H-NMR, GPC, DSC, and TGA.

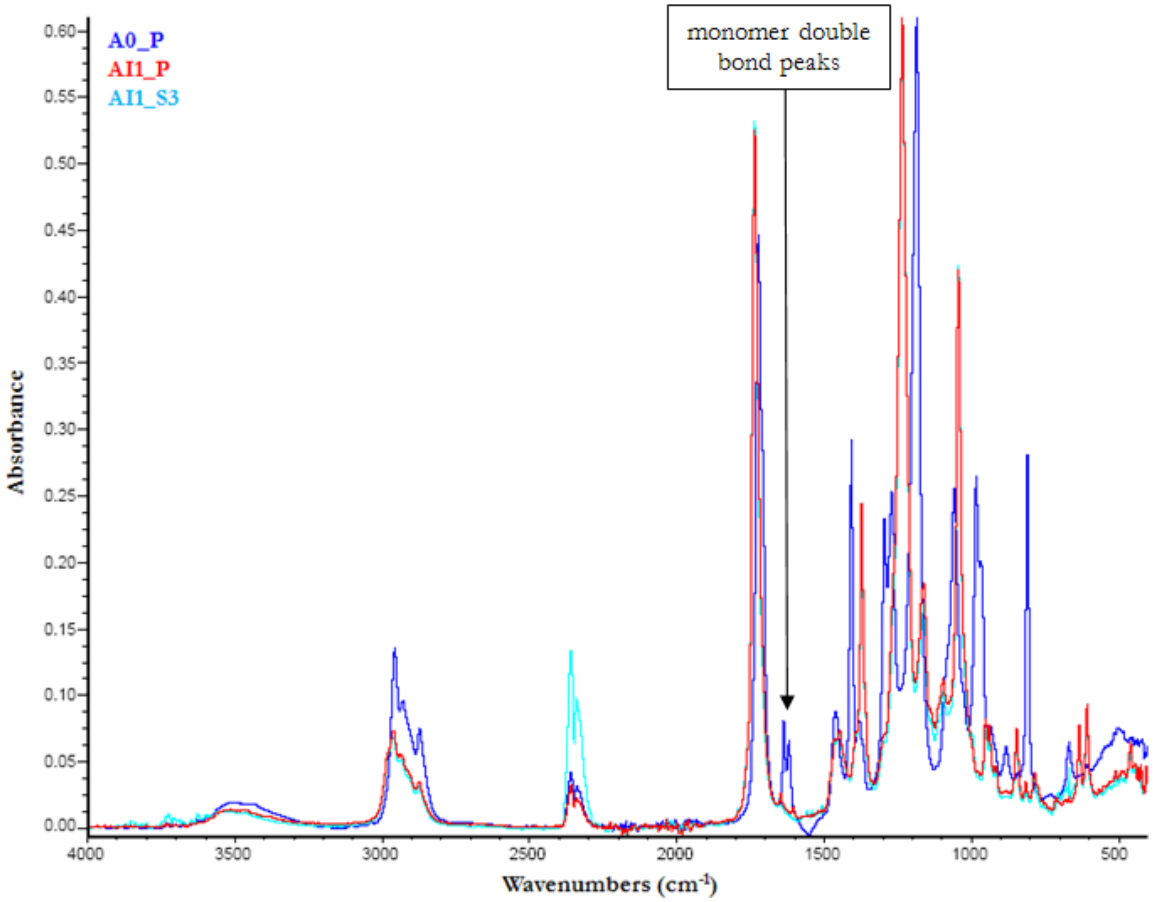

Figure 11 FT-IR spectra of A0_P, AI1_P, and AI1_S3 products

4.2.2 Further characterization of the model formulation, AI1_S3

To determine whether the adhesive was hydrophilic or hydrophobic, water's contact angle on the adhesive was observed. Figure 12 showed that the contact angle is less than 90°, indicating that the surface is hydrophilic. The actual contact angle was measured as approximately 60°.

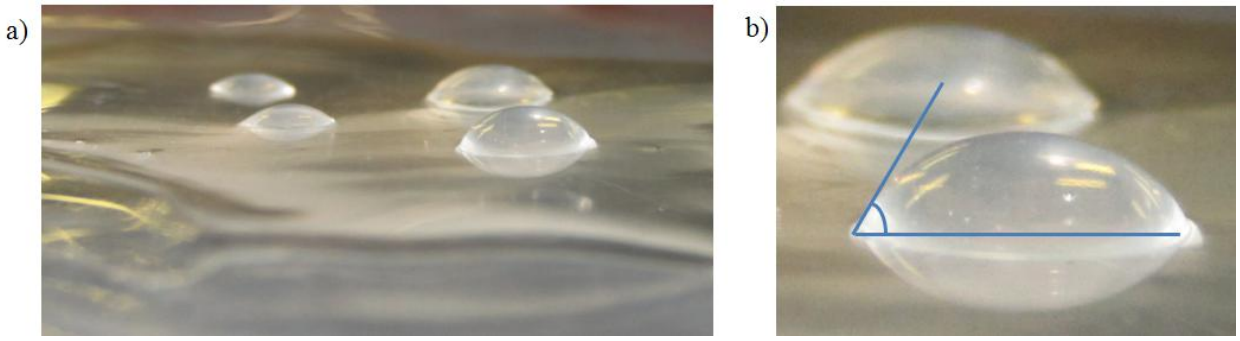

Figure 12 Water on the surface of AI1_S3 (a); contact angle of water on AI1_S3 (b)

AI1_S3 was found to dissolve in chloroform; this indicated that the polymer has a solubility parameter similar to that of chloroform which has a total solubility parameter of 18.7 $MPa^{1/2}$. [53] Since the polymer could dissolve in chloroform, deuterated chloroform was used for conducting ^{1}H-NMR. ^{1}H-NMR of the sample (Figure 13) shows that IOA, HEA, and VA monomers polymerized during the reaction. Monomer ^{1}H-NMR was conducted in deuterated chloroform for comparison and confirmed that resonance bands for monomer double bonds occurred between 4.5 and 6.5 ppm. The ^{1}H-NMR spectrum of IOA monomer indicated double bonds with bands at 6.4, 6.1, and 5.8 ppm. Peaks at 5.5, 5.8, and 6.1 ppm are indicative of double bonds in HEA monomer. VA monomer exhibits bands at 7.3, 4.9, and 4.6 ppm. There was a slight shoulder at 4.9 ppm in the polymer's ^{1}H-NMR spectrum which might be irrelevant to the chemical structure due to ^{1}H-NMR sensitivity. This is supported by the fact that only VA monomer presents a band at this ppm range which is due to the double bond in its monomer structure; however, there was no supporting peak at 4.6 ppm, and the only other peak at 7.3 ppm was the chloroform reference peak.

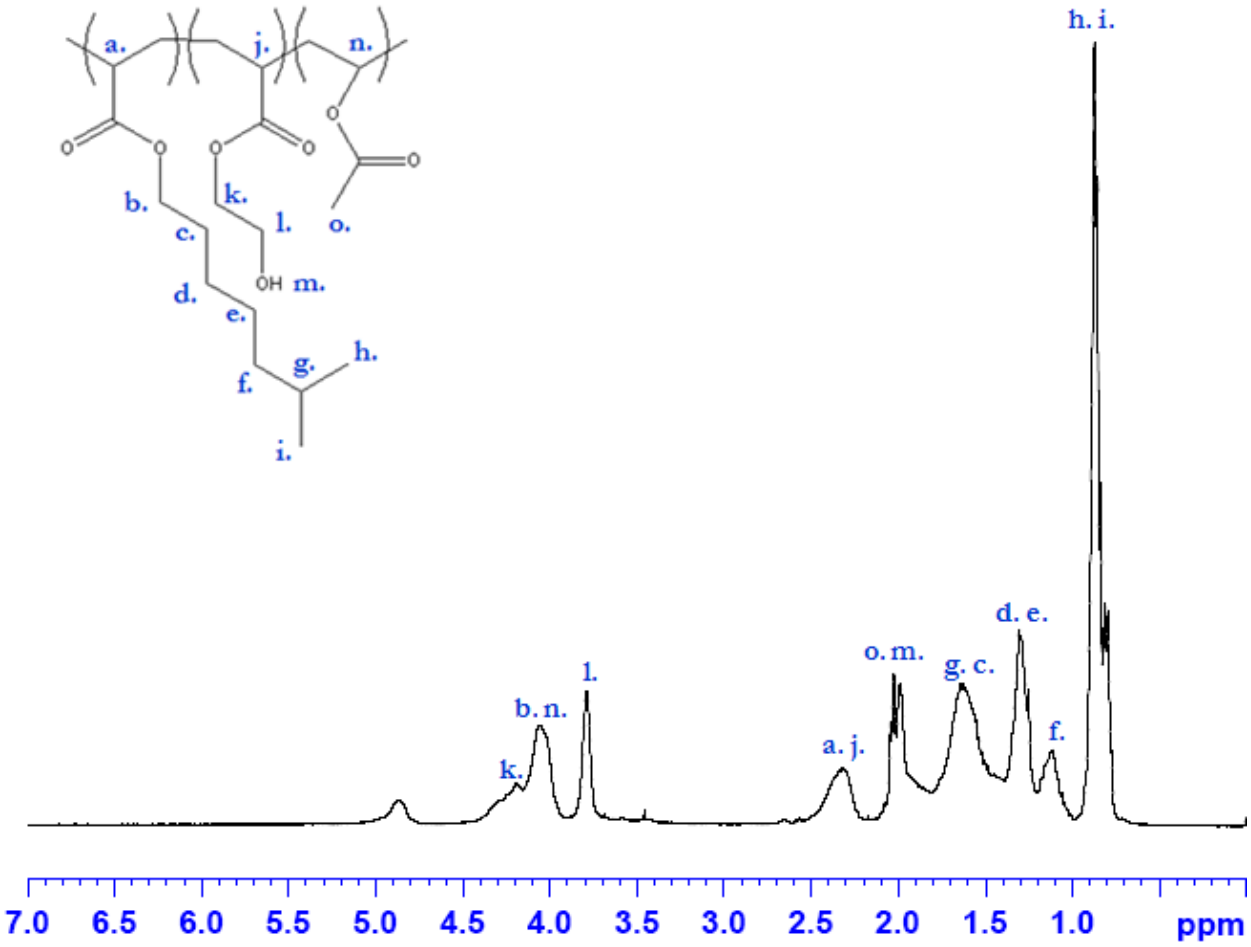

Figure 13 H-NMR of IOA-HEA-VA polymer in deuterated chloroform

GPC analysis of the AI1_S3 adhesive revealed high MW, as expected for addition polymerization. The adhesive polymer was found to have a number-average MW (M_n) of 401,412 Daltons, a weight-average MW (M_w) of 781,260 Daltons, and a z-average MW (M_z) of 3.729 E^6 Daltons. The polydispersity index (M_w/M_n) of the polymer was 1.946 indicating that the product polymer was not a monodisperse system and consisted of polymers or oligomers with a range of molecular weights.

Thermal analysis of AI1_S3 reactants using the DSC and TGA revealed that the adhesive was a thermoset. In Figure 14, there are no reversible transitions suggesting that the polymer has a very low glass transition. DSC analysis of the polymer up to 300°C showed no melting point

transition either. As shown in Figure 15, sample decomposition seemed to begin at approximately 300°C and continued to about 465°C.

From the lack of melting point prior to decomposition, it can be inferred that the polymer is amorphous; as well, due to the randomness of the monomer solutions, the polymer is assumed to have an atactic conformation. Since the polymer only had one glass transition temperature at about -40°C, it was suggested that a true copolymer has been formed. However, further analysis from the reactivity ratio study was needed for confirming this theory.

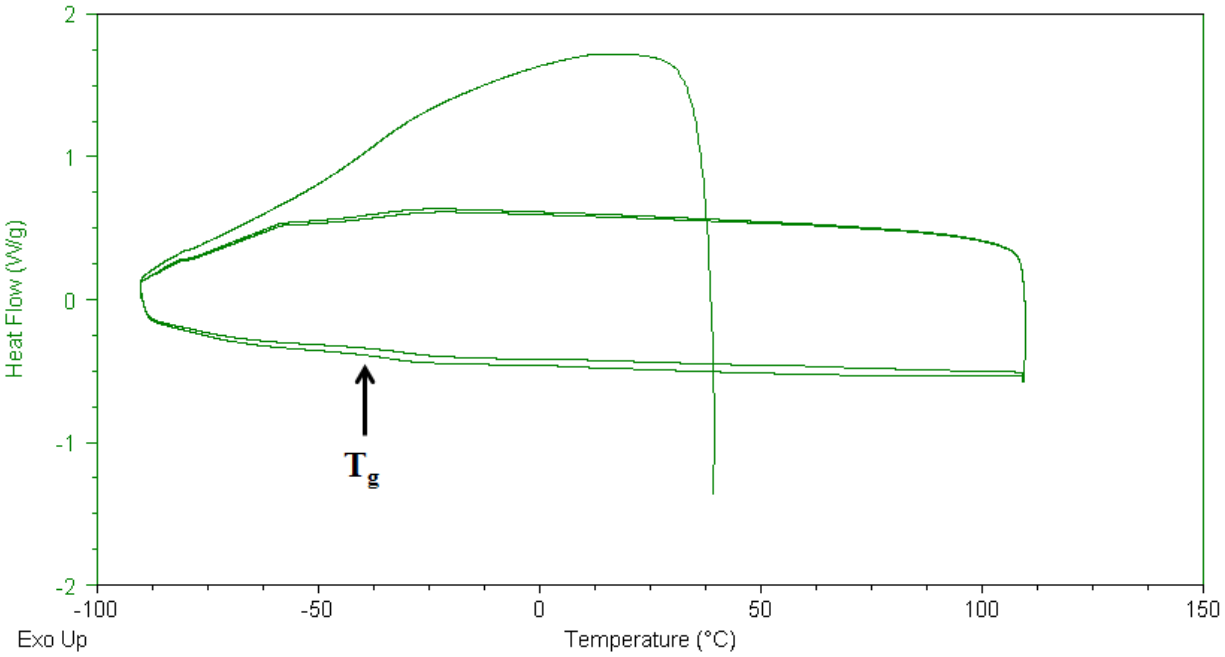

Figure 14 DSC graph of AI1_S3 polymer

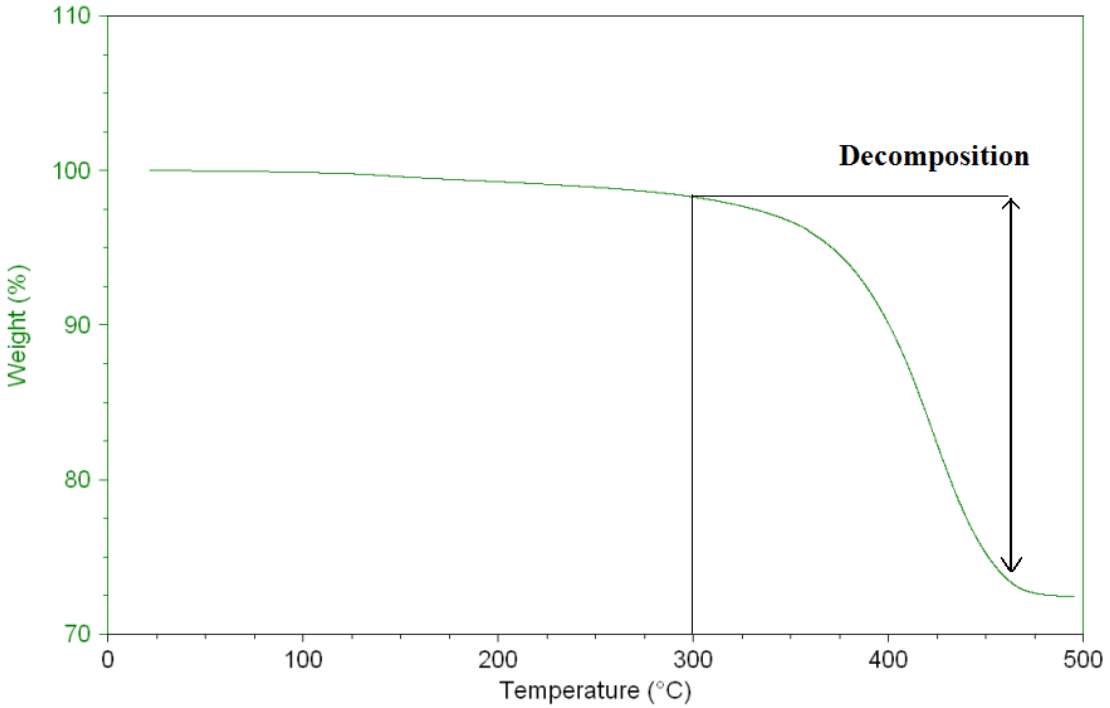

Figure 15 TGA graph of sample AI1_S3

4.3 Reactivity ratio studies on AI1_S3

Since the original formulation for these adhesives, including AI1_S3 was based on proprietary information, an attempt was made to elucidate their potential chemical structure using the reactivity ratios of each of the monomer combinations. Reactant combinations shown in Table 5 were used to calculate the theoretical chemical structure, followed by FT-IR spectra analysis for comparison. Control samples (AI1_RR1 and AI1_RR2) were included in the reactivity ratio studies since free-radical polymerization would not occur without the monomers present.

4.3.1 Characterizing the adhesive copolymer structure using reactivity ratios

In order to determine the type of copolymerization occurring during this polymerization reaction, the reactivity ratios for each of the monomer pairs must be found or properly estimated.

Reactivity ratios of this three monomer system are listed below in the form r_{ij} where k_{ij} is the rate constant of the propagation step. The subscript *i* identifies a particular monomer species with a radical that is located at the end of a propagating chain. Subscript *j* identifies the monomer that will react with species *i* on the propagating chain. [56, 57]

$$r_{12} = \frac{k_{11}}{k_{12}} \qquad r_{13} = \frac{k_{11}}{k_{13}} \qquad r_{21} = \frac{k_{22}}{k_{21}} \qquad r_{23} = \frac{k_{22}}{k_{23}} \qquad r_{31} = \frac{k_{33}}{k_{31}} \qquad r_{32} = \frac{k_{33}}{k_{32}}$$

All propagation rate constants, k_{ij}, can be found using the Q-e scheme proposed by Alfrey and Price [58] (Eq. 1)

$$k_{ij} = P_i Q_j e^{-e_i e_j} \qquad \textbf{(Eq. 1)}$$

where P_i is a radical characteristic of species *i*, Q_j is the mean reactivity of monomer species *j*, e_i is the characteristic charge constant that is proportional to the actual monomer charge of species *i*, and e_j is the proportional charge constant for the double bond in the monomer of species *j*. From this equation, the following equations were constructed

$$r_{12} = \frac{k_{11}}{k_{12}} = \frac{Q_1}{Q_2} e^{-e_1(e_1 - e_2)} \qquad r_{13} = \frac{k_{11}}{k_{13}} = \frac{Q_1}{Q_3} e^{-e_1(e_1 - e_3)} \qquad r_{21} = \frac{k_{22}}{k_{21}} = \frac{Q_2}{Q_1} e^{-e_2(e_2 - e_1)}$$

$$r_{23} = \frac{k_{22}}{k_{23}} = \frac{Q_2}{Q_3} e^{-e_2(e_2 - e_3)} \qquad r_{31} = \frac{k_{33}}{k_{31}} = \frac{Q_3}{Q_1} e^{-e_3(e_3 - e_1)} \qquad r_{32} = \frac{k_{33}}{k_{32}} = \frac{Q_3}{Q_2} e^{-e_3(e_3 - e_2)}$$

The values for the mean reactivity, *Q*, and proportional charge constants, *e*, of IOA, HEA, and VA monomers can be obtained from literature [59-61]. Monomer *Q* and *e* values are accompanied with copolymer reactivity ratios listed in Table 5. Table 6 compares reactivity ratios to determine the theoretical copolymer structures.

Table 5 Monomer *Q* and *e* values [59-61] and the reactivity ratios of the monomer combinations

#	Monomer	*Q*	*E*	Resulting Reactivity Ratios					
1	IOA	0.63	2.01	r_{12} =	0.055	r_{21} =	2.88	r_{31} =	0.003
2	HEA	0.75	0.65	r_{13} =	0.073	r_{23} =	10.7	r_{32} =	0.009
3	VA	0.026	-0.88						

Table 6 Theoretical copolymer structure based on reactivity ratios

Reactivity Ratio Comparison	Theoretical Copolymer Formation
$r_{31} = r_{13} \approx 0$ and $r_{21,}\ r_{23} >> 1$	Alternating VA & IOA
$r_{21} > r_{12}$	Predominantly HEA homopolymer in IOA presence
$r_{23} >> r_{32}$	HEA homopolymer in VA presence

Hypotheses on the theoretical copolymer formation are supported by the monomer reactivity ratio comparisons, as detailed in Table 6. VA and IOA have reactivity ratios that are both approximately zero indicating that copolymer formation will be alternating because both are less likely to homopolymerize in the presence of one another. Since IOA and VA have low reactivity ratios with HEA and since HEA reactivity ratios (r_{21} and r_{23}) are larger than one, the HEA monomer has a tendency to self-propagate rather than copolymerize with IOA and VA. As a result, HEA homopolymer blocks will be present in the polymer system. However, since HEA has a lower reactivity ratio with IOA than with VA, HEA can potentially react with some IOA in the early stages of polymerization, although IOA will more preferentially react with VA. Additionally, if HEA copolymerized with IOA and VA, HEA homopolymer blocks will more likely be attached to IOA than VA in the polymer structure. From the information provided by the theoretical analysis, it can be inferred that the actual polymer structure is probably a tercopolymer or a blend of HEA homopolymer with the IOA-VA copolymer.

4.3.2 Reaction combinations from reactivity ratio studies

Based on the theoretical results, some assumptions can be made about the copolymer system. These theoretical results have been paired with FT-IR analysis of the experimental studies to provide a more accurate hypothesis on the polymer system. Comparison of FT-IR absorbance intensity and band widths revealed changing polymer compositions between samples. Viscosity and tack measurements were conducted; the results are documented in chapter 4.4. Since the weight ratios were maintained constant, direct comparison of viscosity between some of the formulations was not discussed as BP weight percentages changed in order to maintain constant monomer weight ratios.

Experiments for these studies were classified into two groups. Experiments AI1_RR1 to AI1_RR15 were conducted as solvent polymerizations with EA. Bulk polymerization without EA solvent and IPA were carried out in experiments AI1_RR16 to AI1_RR20. Table 7 details the reaction times and visual products observed from each experiment.

Within the solvent polymerization group, there were two control experiments (AI1_RR1 and AI1_RR2) and three subcategories of experiments. Reactions AI1_RR3 to AI1_RR5 were to determine whether homopolymerization occurs in EA solution; AI1_RR6 to AI1_RR9 were reactions with varying monomer combinations in EA solution. Experiments AI1_RR10 to AI1_RR15 were reactions which include IPA to see if chain terminating specificity occurred, where AI1_RR10 to AI1_RR12 contain single monomers and AI1_RR13 to AI1_RR15 contain monomer combinations.

Bulk polymerization was conducted to determine the solvent's influence on polymer product. Reactions AI1_RR16 to AI1_RR18 were for homopolymerization and had an increased weight ratio that was constant for each monomer. AI1_RR19 contained all monomers, and AI1_RR20

was an IOA homopolymerization with a decreased weight ratio from AI1_RR16 to observe product changes.

Table 7 Reaction times and qualitative observations of the reactivity ratio study products

Sample ID	Reaction time (h)	Color and clarity of liquid solution	Color and clarity of gel or foam
AI1_RR1	7	Transparent, tan	None
AI1_RR2	7	Transparent, tan	None
AI1_RR3	7	Transparent	None
AI1_RR4	7	Transparent	Transparent gel
AI1_RR5	7	Transparent, tan	None
AI1_RR6	7	None	Translucent gel
AI1_RR7	7	None	Translucent gel
AI1_RR8	7	Transparent	Opaque, white gel
AI1_RR9	7	None	Transparent gel
AI1_RR10	7	Transparent, tan	None
AI1_RR11	7	Opaque, white	Transparent gel
AI1_RR12	7	Transparent	None
AI1_RR13	7	Transparent, tan	None
AI1_RR14	7	Transparent	None
AI1_RR15	7	Transparent	Transparent gel
AI1_RR16	1.3*	None	Opaque, white foam
AI1_RR17	7	Translucent, white	Transparent gel
AI1_RR18	2.5*	None	Transparent gel
AI1_RR19	1*	None	Opaque, white foam
AI1_RR20	1*	None	Opaque, white foam

* Reaction completed before 7 h

4.3.2.1 Solvent polymerization in reactivity ratio studies

Control experiments AI1_RR1 and AI1_RR2, as expected, did not polymerize in the presence of the BP initiator. Homopolymerization experiments with VA (AI1_RR3), HEA (AI1_RR4), and IOA (AI1_RR5) produced only homopolymer product for HEA and IOA. Solvent evaporation of AI1_RR3 did not leave any polymer product. FT-IR analysis of AI1_RR3 solution and the dried products from AI1_RR4 and AI1_RR5 are shown in Figure 15. Stacked FT-IR spectra of all samples AI1_RR3 to AI1_RR20 can be found in Appendix A.

FT-IR spectra showed distinct differences between the compounds. The peak between 1620-1680 cm^{-1} shows that the VA monomer in AI1_RR3 still had carbon-carbon double bonds; whereas, AI1_RR4 and AI1_RR5 had both homopolymerized. AI1_RR3 and AI1_RR4 had the same weight ratios in solution; however, the results implied that HEA reacted with itself rather than with VA, probably due to the hydroxyl group. HEA from AI1_RR4 exhibited a very broad band for the O – H stretching from 3100-3650 cm^{-1}; this broad band accounted for the hydroxyl group's stretch along with hydrogen bonds formed between the hydroxyl group's hydrogen and another oxygen. C – H stretching from the compounds was indicated by the bands in the 2800-3000 cm^{-1} range. The lower range end from around 2880-2950 cm^{-1} accounts for hydrogen bonded to sp^3 carbons. Hydrogen attached to a sp^2 carbon from a double bond has spectral bands at higher wavenumbers from 2950-3075 cm^{-1}. As shown in the FT-IR spectra, AI1_RR5 had the highest C – H absorption, as this polymer contains IOA which has far more C – H bonds than both of the compounds containing HEA and VA. The ester bonds from AI1_RR3-AI1_RR5 can be observed as the ketone and ether stretching. Ketone stretching occurs at 1700-1750cm^{-1}. Ether stretching in acetate generates one peak between 1200-1280cm^{-1}, whereas, acrylate produces a peak at 1120-1220cm^{-1} and wider band at 1200-1330cm^{-1}. Comparing the acrylate C – O stretches for AI1_RR4 and AI1_RR5, there was a noticeably larger acrylate composition for HEA than IOA indicating that HEA probably homopolymerized better than IOA did.

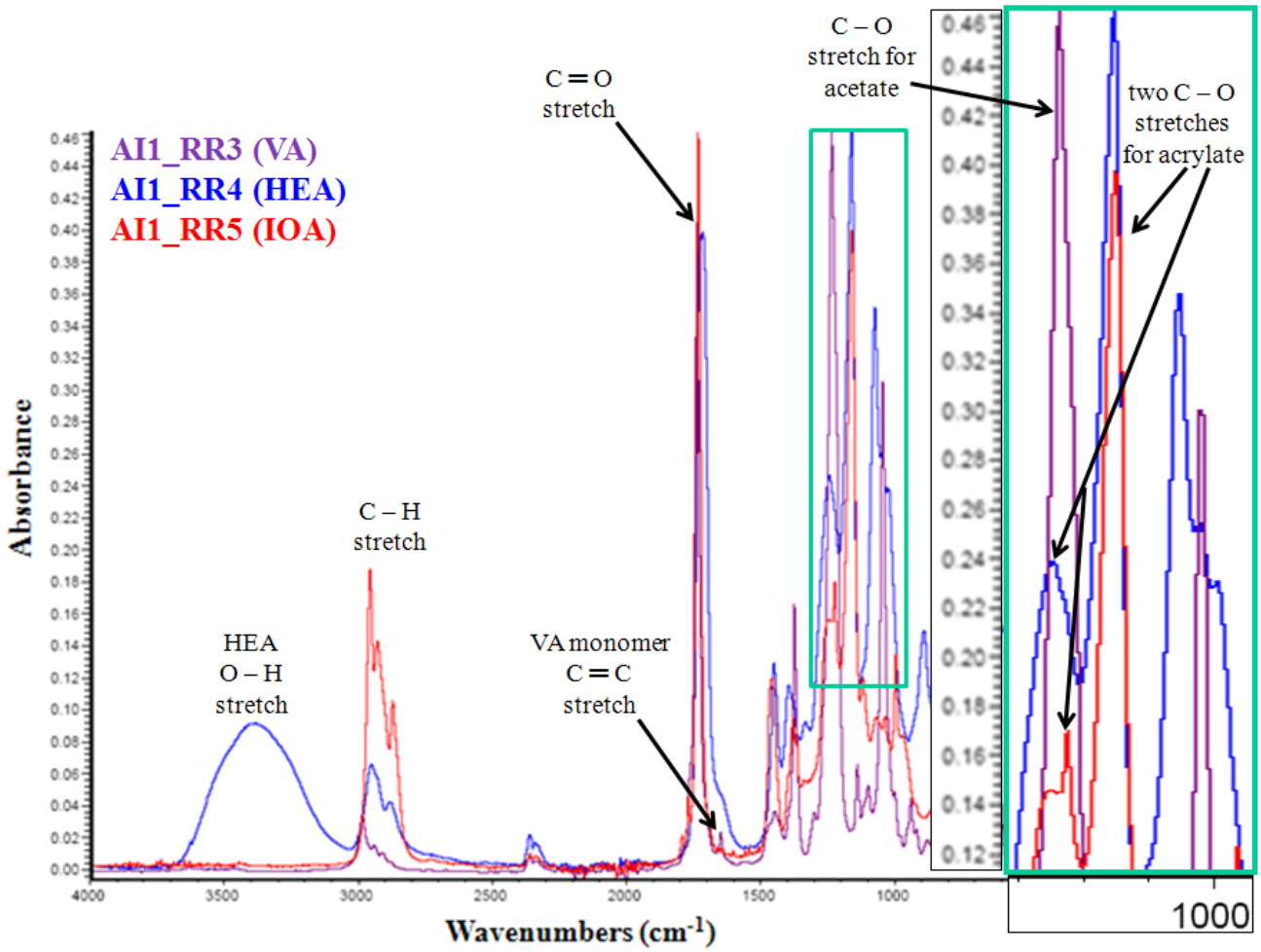

Figure 16 FT-IR spectra of homopolymerization experiments AI1_RR3 to AI1_RR5

FT-IR spectra from Figure 15 were utilized to help identify polymer composition trends of the remaining samples from the reactivity ratio study. Identification of the ketone and hydroxyl groups was accomplished by using the FT-IR functional group region. Further FT-IR analysis of the fingerprint region enabled ether linkage discrimination between acrylates and acetates which was useful since IOA and VA have similar FT-IR spectra.

Samples AI1_RR6 to AI1_RR9 of mixed monomers which were solution polymerized, produced FT-IR spectra shown in Figure 17. Comparison of the absorption spectra indicated that the highest HEA composition (based on highest O – H absorption) was from AI1_RR8; the IOA compositions all practically had the same amount of IOA. The highest acrylate composition, as

expected, was from AI1_RR7, followed closely by AI1_RR9 and AI1_RR6, and the lowest from AI1_RR8. Acetate composition was highest for AI1_RR8, followed by AI1_RR9, and then AI1_RR6. FT-IR of AI1_RR8 suggests that HEA in fact did copolymerize with VA regardless. HEA and VA solution copolymerization was confirmed since AI1_RR3 revealed that VA could not homopolymerize under these conditions. AI1_RR8 probably had the highest VA content in the polymer structure since the HEA to VA weight ratio was 1:1.

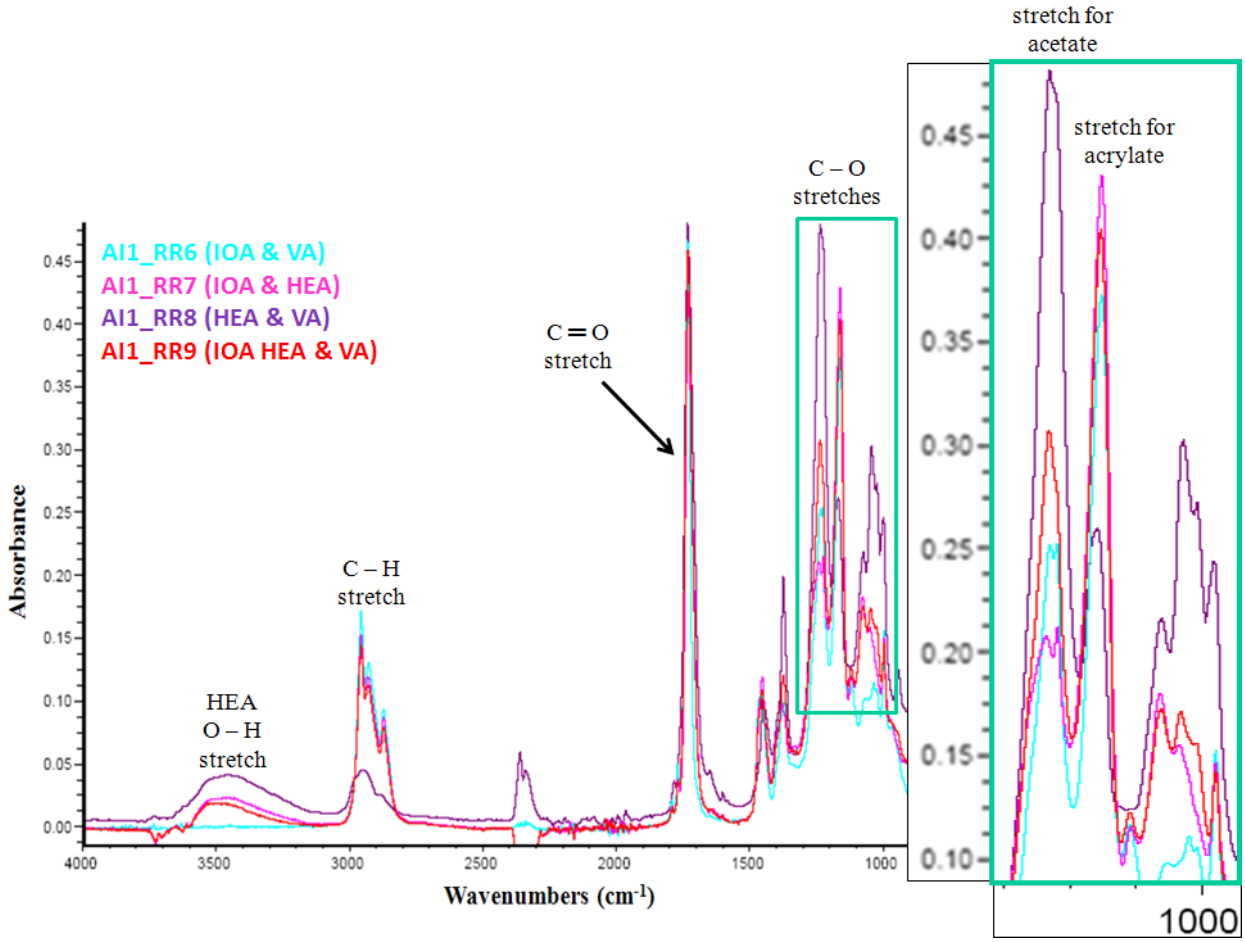

Figure 17 FT-IR spectra for AI1_RR6-AI1_RR9 dried product

Experiments with solutions of only one monomer in the presence of IPA, a known radical chain transfer agent, were also conducted. FT-IR spectra from the dried products can be found in Figure 18. After solvent evaporation, experiment AI1_RR12 which contained the VA monomer

formed no product. Acrylate C – O stretches for AI1_RR10 were less intense than those from AI1_RR11, indicating IPA could have affected IOA polymer formation more than HEA. IOA could have a lower reactivity rate in IPA than HEA did. Results from viscosity measurements (chapter 4.4) indicated that AI1_RR11 had a slightly higher viscosity than AI1_RR10 which could support this theory.

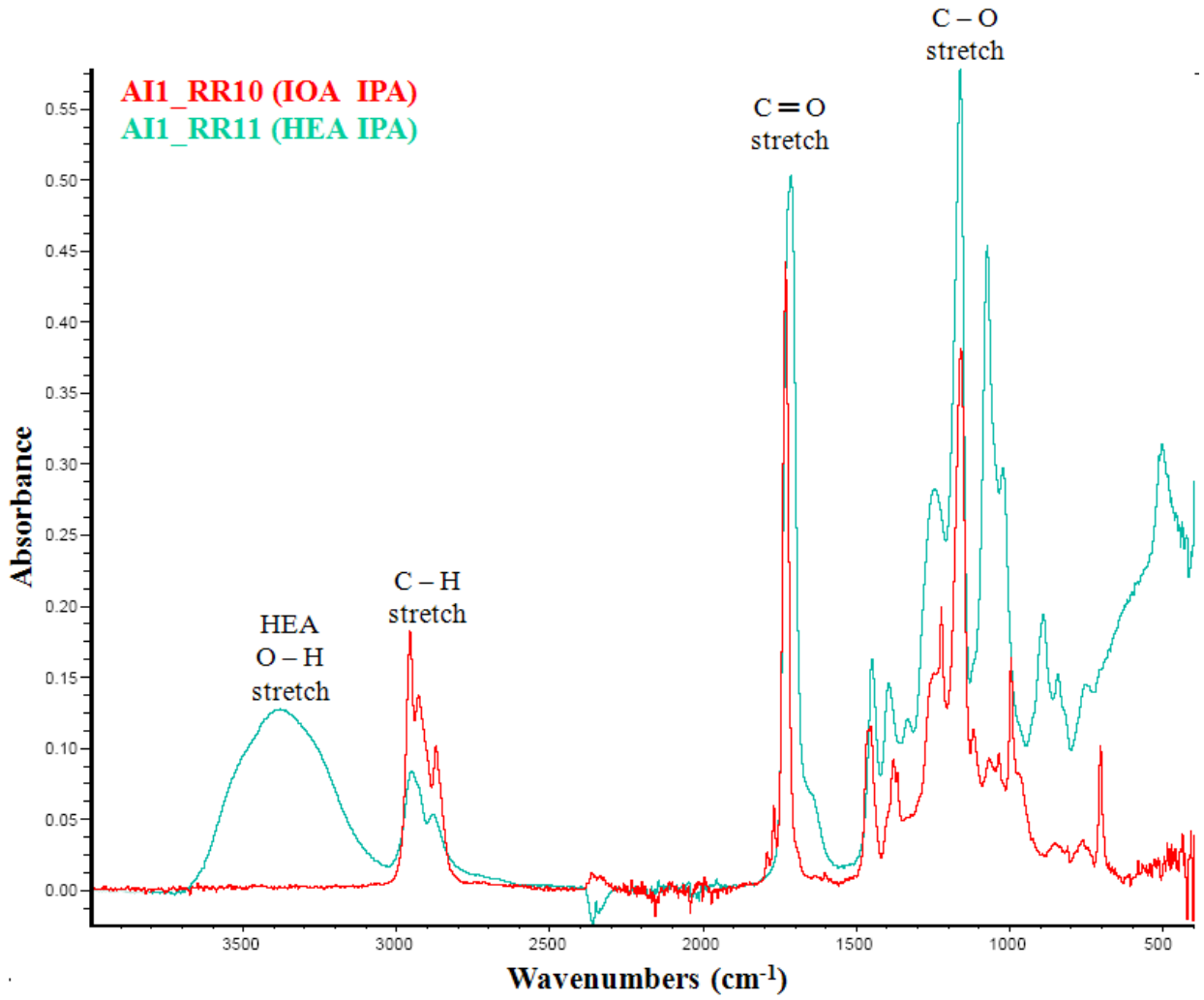

Figure 18 FT-IR spectra from dried products from AI1_RR10 and AI1_RR11

Figure 19 shows FT-IR spectra from monomer combinations with IPA. Some IPA O-H stretches in AI1_RR13 and AI1_RR14 can be seen up-field of the more pronounced HEA O-H stretches. Based on the absorbance from Figure 19, IPA had notably lowered the acetate C – O

stretch intensity in AI1_RR14 and AI1_RR15. Respectively, this indicated that IPA addition resulted in higher HEA and IOA polymer content rather than VA. Upon comparison of the acrylate C – O stretch, there was a noticeable change in the acrylate C – O peaks intensities suggesting that IPA decreased IOA polymerization more than HEA, as can be seen by comparing absorbance intensities from AI1_RR4 and AI1_RR5 (without IPA) from Figure 16 as well as AI1_RR10 and AI1_RR11 (with IPA) from Figure 18. The shape and intensity of the IOA band (AI1_RR5) in Figure 19 has changed from its previously shown absorption band (Figure 16).

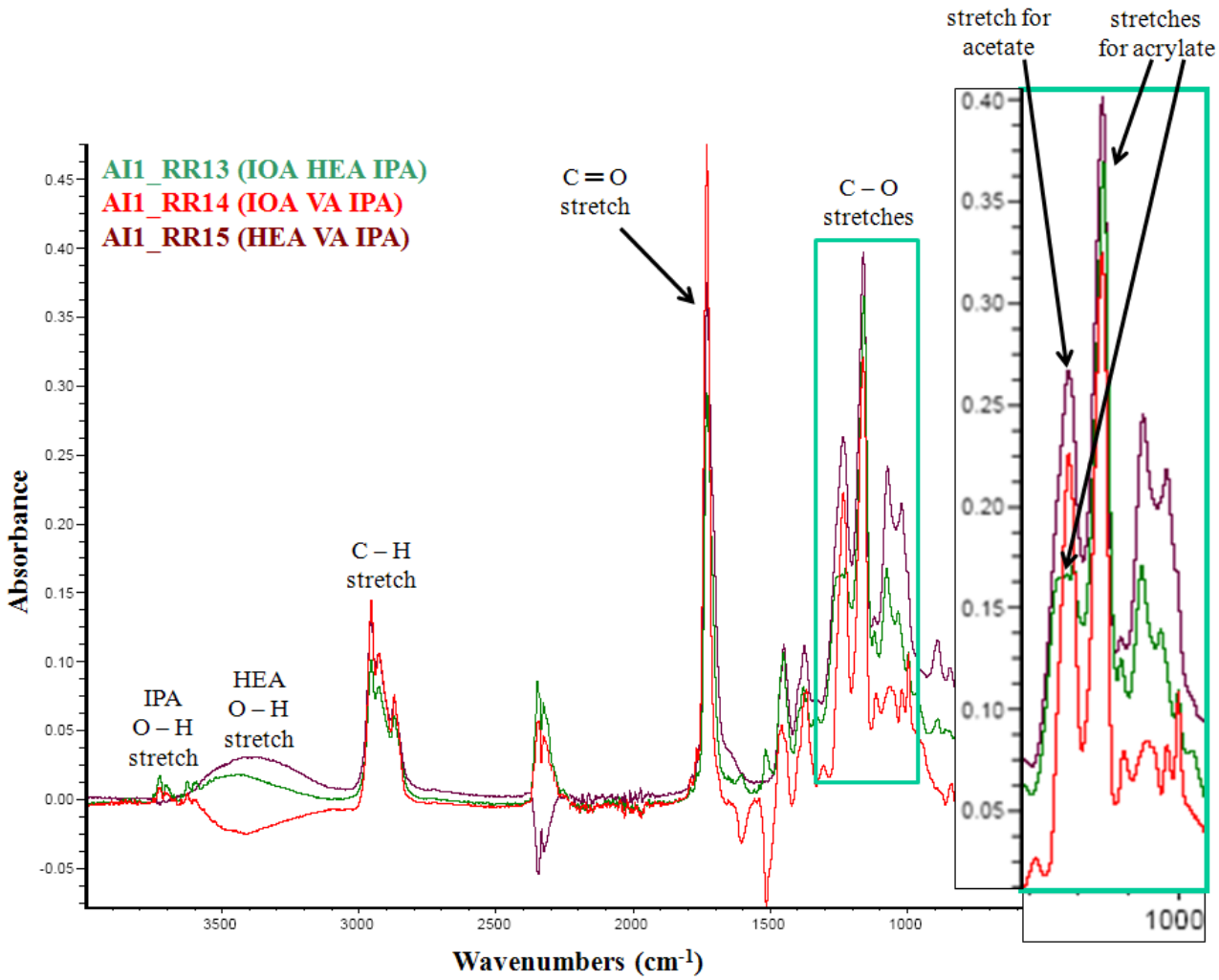

Figure 19 FT-IR spectra from dried products of AI1_RR13-AI1_RR15

4.3.2.2 Bulk polymerization in reactivity ratio studies

As shown in Table 6, bulk polymerization decreased the reaction times necessary for polymerization since the EA solvent was removed. The resulting difference in reaction times indicated that the solution diluted the monomer solution to the extent of lowering the MW because solvent addition decreased the probability that a radical species would encounter a monomer to react with.

Bulk polymerization was conducted for homo-monomer solutions, as well as, a monomer mixture based on AI1_S3. The same weight of BP initiator was used in all formulations; however, the monomer volume was significantly increased for samples AI1_RR16 to AI1_RR18. Weight ratios for AI1_RR19 and the IOA homo-monomer solution, AI1_RR20, were based on AI1_S3. Without the presence of the solvent and IPA, polymerization of all the monomers was possible. AI1_RR17 (HEA) produced the strongest acrylate bands followed by the monomer mixture AI1_RR19 and the IOA foams (AI1_RR16 and AI1_RR20). AI1_RR19 exhibited both acetate and acrylate character. AI1_RR19 had a distinct hybrid peak similar to the acetate C – O peak but less intense and slightly wider; this was also accompanied by the second C – O acrylate peak. The high absorbance peak of AI1_RR17 (HEA) was possibly due to its higher sample density; this sample was not a foam.

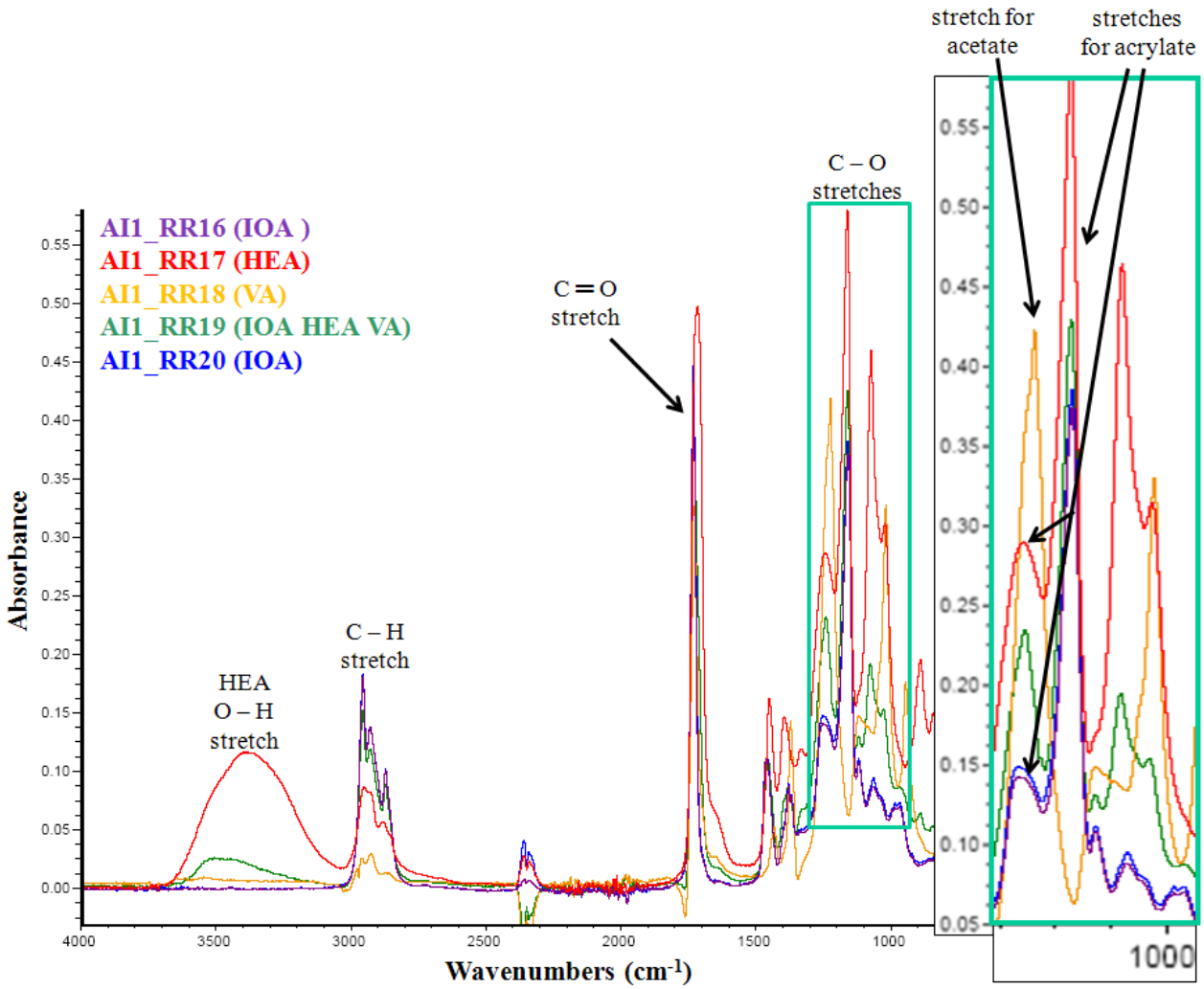

Figure 20 FT-IR spectrum from dried product of AI1_RR16-AI1_RR20

IOA foams (AI1_RR16, AI1_RR19, and AI1_RR20) produced translucent, high viscosity polymer gel solutions prior to violent exothermic reactions which produced foam formation. Based on the sheer volume of bubbles in the foam, the foam probably resulted from remaining IOA monomer evaporation in the form of a white gas out of the foams.

4.3.2.3 Reactivity ratio studies separated by monomer type

FT-IR spectra of IOA, HEA, and VA adhesives separately are presented in the following figures. Solution polymerized and bulk polymerized IOA adhesives were compared using FT-IR

absorbance in Figures 21 and 22, respectively. Comparison of HEA and VA sample FT-IR spectra are shown in Figures 23 and 24, correspondingly.

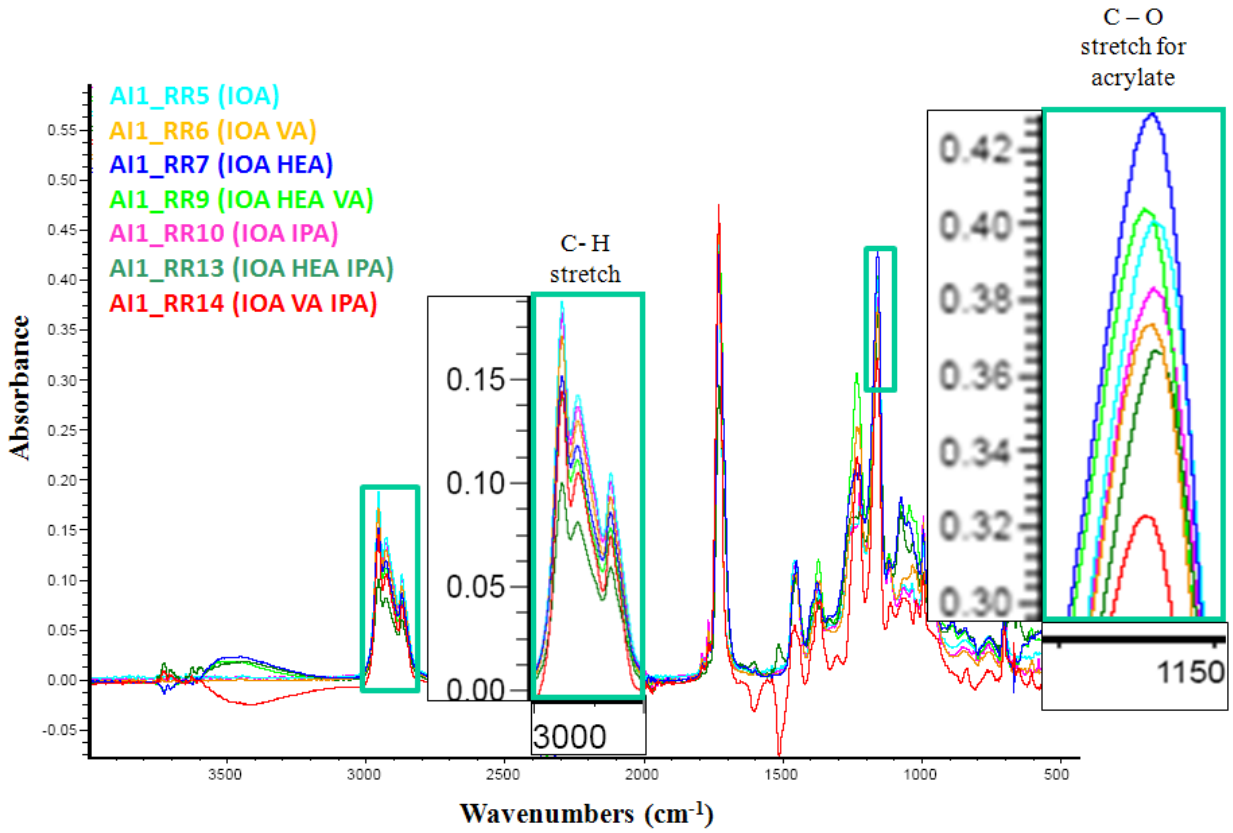

Figure 21 FT-IR spectra of IOA solution polymerized products from reactivity ratio studies

Absorptions from the 1175-1150 cm^{-1} acrylate C – O stretch region were analyzed from both IOA solution and bulk polymerized products (Figures 21 and 22, respectively). Sample AI1_RR7 had the highest acrylate character of the solution polymerized samples as it only contained both acrylate monomers (HEA and IOA). VA presence in solution polymerized samples AI1_RR6, AI1_RR9, and AI1_RR14, verified from the characteristic acetate C – O stretch, displayed decreased acetate C – O absorbance. This indicated that VA formed bonds with IOA (see AI1_RR6). Apparently, VA became integrated into the polymer structure in AI1_RR6, AI1_RR9, and AI1_RR14. Additionally, IPA significantly decreased acrylate

character as seen from comparing samples AI1_RR5, AI1_RR6, and AI1_RR7 with samples AI1_RR10, AI1_RR14, and AI1_RR13, correspondingly. In these samples, IPA notably decreased both acetate and acrylate C – O stretch intensities, indicating their acetate and acrylate content decreased with IPA addition. This could be expected since IPA is a chain transfer agent.

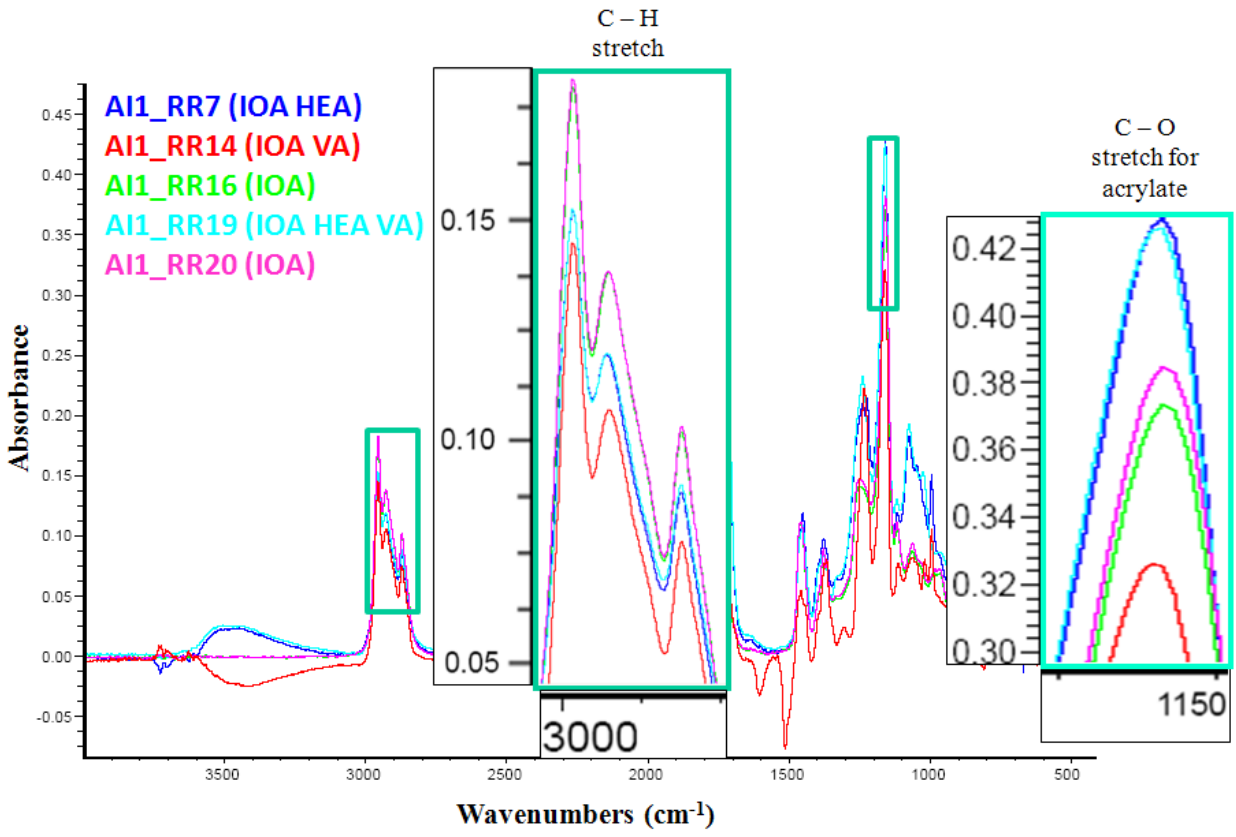

Figure 22 FT-IR spectra of IOA bulk polymerized products and two reference peaks (AI1_RR7 and AI1_RR14).

Reference peaks in Figure 22 were used to demarcate the highest (AI1_RR7) and the lowest (AI1_RR14) acrylate absorbance from the solution polymerized products for comparison. A slight VA C – O stretch from 1225-1260 cm^{-1} and minimal decrease in the acrylate stretch implied that VA made up only a small percentage of the bulk copolymerized structure. From the C – H stretch region, samples AI1_RR16 and AI1_RR20 had the highest IOA content as their C

– H stretch absorbance was the highest. Close behind were samples AI1_RR7 and AI1_RR19, followed by sample AI_RR14. As well, sample AI1_RR16 showed a slightly lower absorbance than AI1_RR20 which could be related to the sample density, as both samples have the same refraction index. AI1_RR20 produced slightly more dense IOA foam with smaller foam cell diameters as seen from the micrographs in chapter 4.5. AI1_RR16 produced a foam with 0.90 g/cm^3, and AI1_RR20 produced a less dense foam with 0.66 g/cm^3, which indicates that AI1_RR20 had a higher content of gas-filled foam cells than AI1_RR16 since both formulas have the same monomer composition.

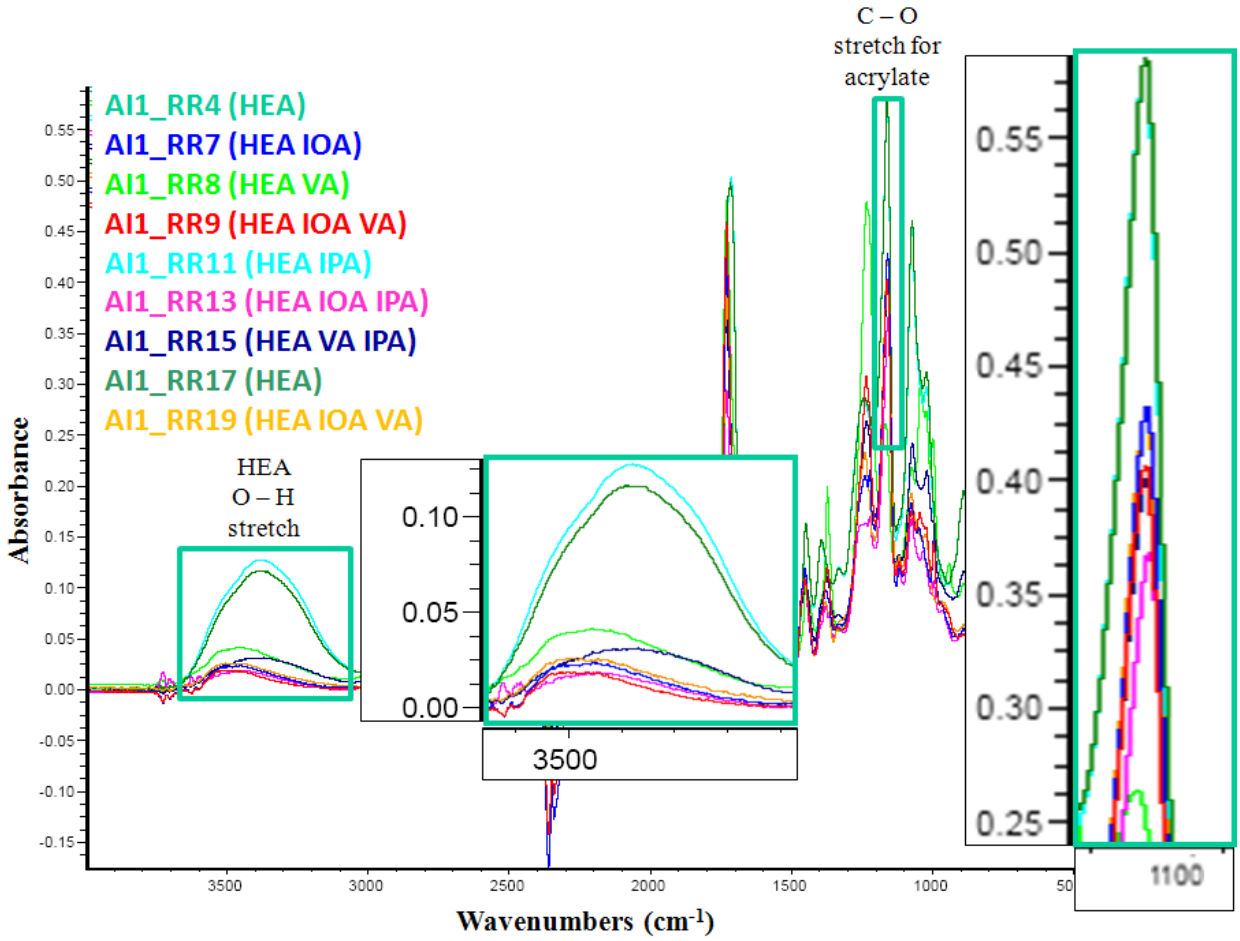

Figure 23 FT-IR spectra of all HEA samples from the reactivity ratio studies

HEA comparison in Figure 23 showed that a more intense O – H stretch and C – O acrylate stretch occurred for AI1_RR4 and AI1_RR11 than for the other samples. This suggested that HEA homopolymer was not formed in the mixed monomer solutions. Interestingly, IPA addition did not significantly decrease HEA polymer production (AI1_RR11) as it did with IOA (AI1_RR10), even despite IOA's higher monomer to IPA ratio. This inferred that IPA chain transfer selectivity could occur during polymerization. Spectra of AI1_RR7 and AI1_RR9 suggested that a small amount of VA could have been integrated into the polymer structure. A slight decrease in intensity and a small acrylate C – O peak from 1200-1300cm^{-1} pointed towards the presence of VA in the structure of AI1_RR9. Based on the O – H stretch, HEA composed more of the copolymerized structure with VA (AI1_RR8) than with IOA (AI1_RR7); this result was the opposite of what the theoretical reactivity ratio analysis projected. In fact, none of the mixed HEA samples showed FT-IR spectra with exclusive, 100% HEA homopolymer characteristics, indicating that HEA either copolymerized with both IOA and VA or that it formed a polymer blend.

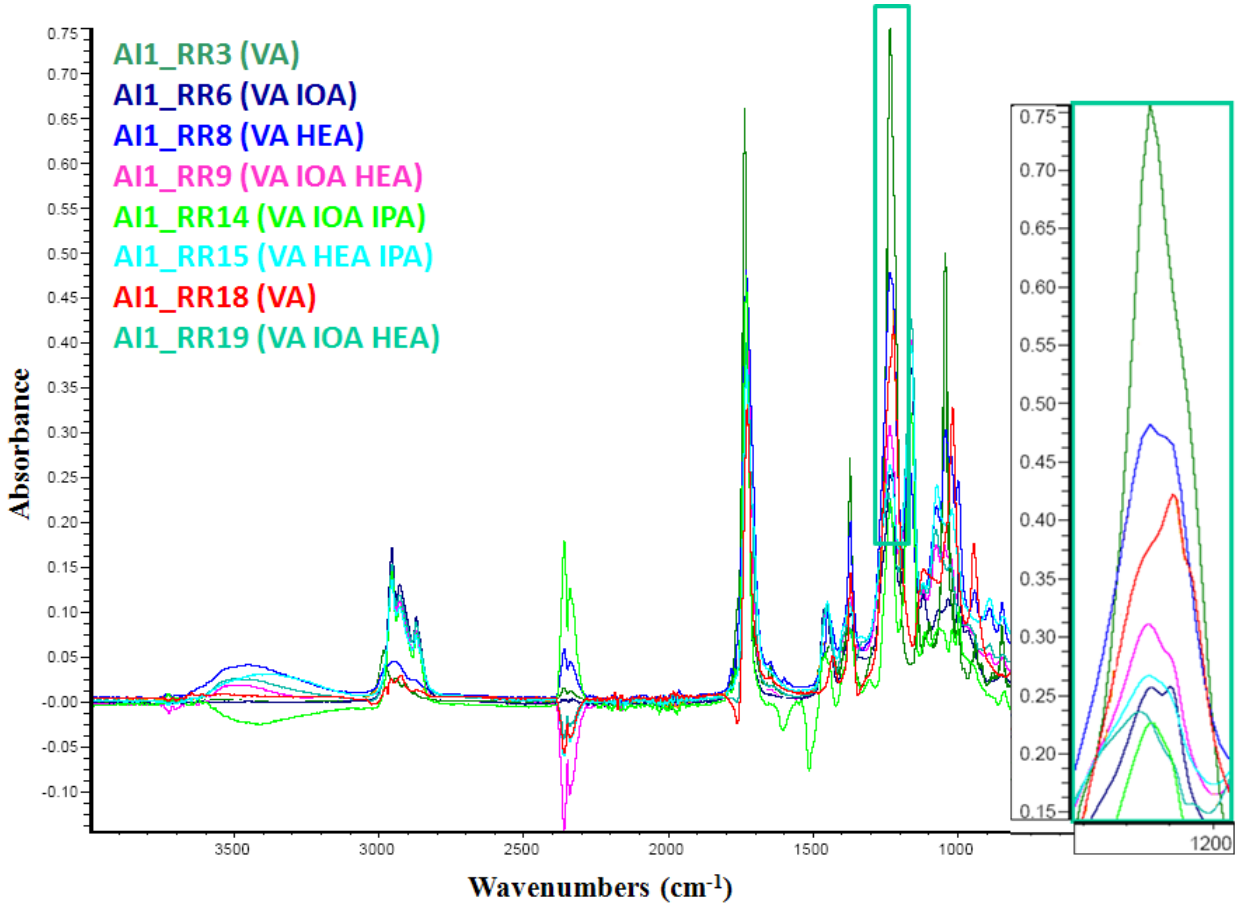

Figure 24 FT-IR spectra of VA samples from reactivity ratio studies

Acetate content varied for all samples shown in Figure 24 (highest in AI1_RR3, the unpolymerized acetate solution). From Figure 24, AI1_RR6 appeared to have higher acetate absorption than AI1_RR18 (VA). However, the band shown for AI1_RR6 actually represented both the acrylate and acetate character of this sample. IPA addition to VA samples resulted in decreased VA polymerization; this was supported by the C – O absorption decrease between AI1_RR8 and AI1_RR15, as well as between AI1_RR6 and AI1_RR14. As previously noted, IPA affected IOA homopolymer formation in AI1_RR10 more than it affected HEA homopolymerization in AI1_RR11. Nevertheless, IPA addition to the HEA-VA solution (AI1_RR8 and AI1_RR15) affected absorbance intensity and band width more than IPA affected the IOA-VA solution (AI1_RR6 and AI1_RR14). This result did not seem to be related to the

monomer reactivity ratios but rather was possibly attributed to IPA acting as a stronger diluent for the HEA-VA system. As a side note, the HEA-VA solution had a 1:1 monomer volume ratio; whereas, the IOA-VA solution had a more diluted VA concentration with a 3.2:1 monomer volume ratio, so IPA addition did not drastically affect VA concentration in the latter solution.

4.3.3 Hypothesis on adhesive copolymer structures

Comparison of FT-IR spectra and visual observations from Table 6 allowed polymer structural analysis to be conducted for the system. Experimentation supporting the reactivity ratio studies proved that VA, unlike HEA, was not capable of homopolymerization in solution at low concentration under these reaction conditions. However, FT-IR analysis of VA polymers confirmed that solution polymerization of VA with both HEA and IOA did occur to some extent, even in the presence of IPA. FT-IR analysis of HEA solvent polymerized samples indicated that polymer formation not only of HEA but also of VA and IOA occurred. FT-IR analysis confirmed that both IOA-VA and HEA-VA polymerization occurred from solution polymerizations. However, since IOA could homopolymerize, further proof was required to confirm that IOA and HEA were not homopolymerizing in solution to form a blend. Comparing visual observation of transparent HEA (AI1_RR4) and IOA (AI1_RR5) homopolymers with a homogenous, translucent HEA-IOA gel (AI1_RR7) showed that the HEA-IOA polymer system's light refraction notably changed. A change in refraction occurs when two media meet that have different refractive indexes. Since both homopolymers are transparent, this change in refraction suggests that a block copolymer of the monomers had formed rather than a miscible blend, as the miscible blend of the two would more than likely be transparent similar to the homopolymers.

Bulk polymerized samples of IOA (AI1_RR16 and AI1_RR20), HEA (AI1_RR17), and VA (AI1_RR18), respectively, homopolymerized to form a white opaque foam, a white translucent

liquid, and a transparent gel. However, upon their combined polymerization in AI1_RR19, they produced a homogenous white opaque foam which FT-IR analysis pointed to IOA, HEA, and VA polymers within the sample. As the polymer appeared homogenous and all three monomers were proven with FTIR to be present in the polymer system, the polymer more than likely is a tercopolymer of IOA, HEA, and VA with segregated blocks causing the opacity.

As a final measure, DSC of the bulk polymerized homopolymer was conducted and compared with AI1_S3. As well, a dissolution test was conducted in chloroform since the polymer was soluble in this solvent. The dissolution test proved that if the polymer system was a blend, it was not an immiscible blend because all of the homopolymers dissolved. DSC analysis Figure 25 of the bulk polymerized homopolymers revealed that poly(HEA) had a T_g of approximately 2°C; VA had a T_g of about 0°C, and IOA showed a T_g around -75°C. Because the AI1_S3 specimen showed only one T_g at -40°C, which was below both poly(VA) and poly(HEA) T_g values but higher than the poly(IOA) T_g. This suggested that a tercopolymer of IOA, HEA, and VA had formed. Comparison of the copolymer T_g with the calculated Flory-Fox equation T_g, found a theoretical copolymer T_g of -52°C, which was close to the observed T_g.

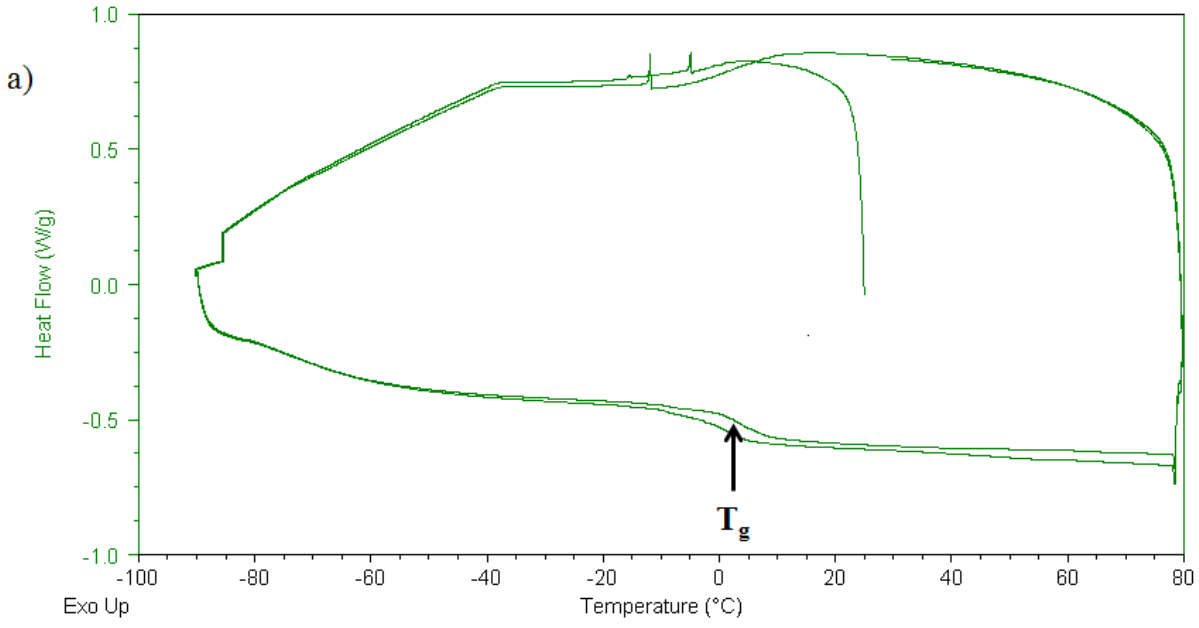

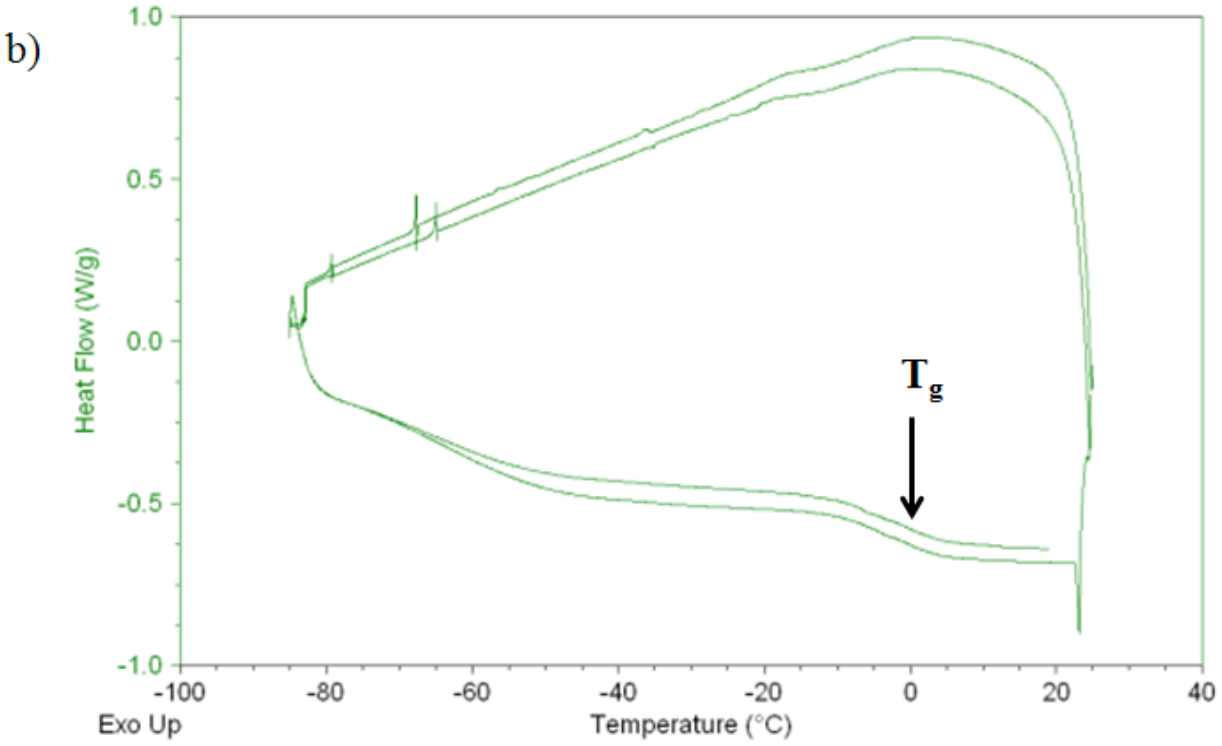

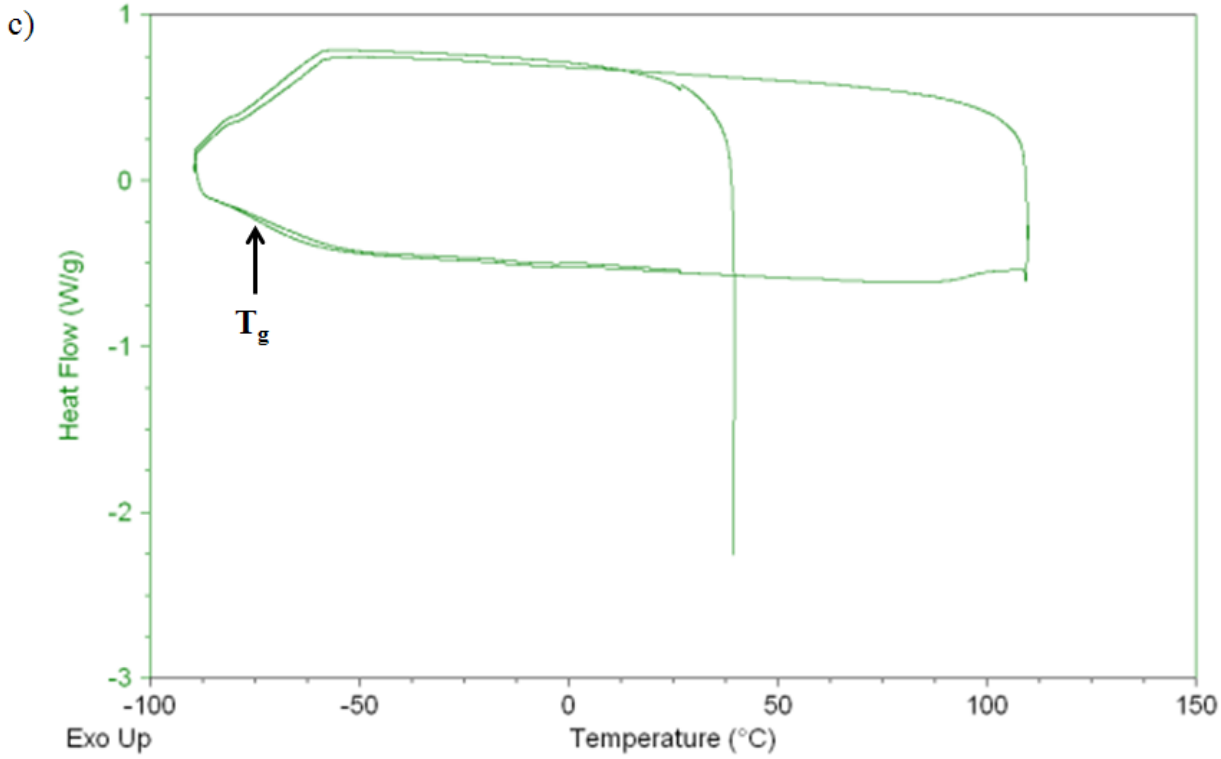

Figure 25 DSC runs of high viscosity liquids: poly(HEA) (a); poly(VA) (b); poly(IOA) (c)

Based on the reactivity ratios, FT-IR analysis, miscibility study, and DSC analysis, it is likely that a tercopolymer of IOA, HEA, and VA formed in the adhesives based on the AI1_S3 formula. FT-IR analysis and the solution weight ratio 3.2:1:1 of IOA:HEA:VA suggest that the polymer should predominantly be composed of IOA and HEA acrylate monomers as VA was more sensitive to IPA addition. Since IOA and HEA are capable of homopolymerizing in solution conditions, IOA and HEA could both be grafted onto the polymer backbone to form side chains. Since VA was incapable of homopolymerizing at a low IPA:BP ratio (in solution) but did homopolymerize at a higher IPA:BP ratio (from bulk polymerization), it is probable that VA only alternately polymerizes with IOA as theoretically predicted. Since VA is at a low concentration in the adhesive solutions and since it has low reactivity ratios, VA will most likely not form homopolymer blocks when copolymerizing.

4.4 Tack and viscosity of adhesives

Tack and viscosity of adhesives are important for considering their instantaneous adhesive properties and their cohesiveness or resistance to applied shear stress. These properties can be affected by additives and polymerization methods. The polymers with tack values of 0.2 or higher were considered acceptable for bandage use. Higher tack is preferred for creating better mechanical interactions with the skin. Adhesives with the lowest standard deviations were considered more preferable. For the viscosity measurements, only the maximum viscosity was taken because some samples exceeded the machine's load cell at very low shear rates and some samples were pushed out of the viscometer at different points during the experimentation.

Tack, as previously mentioned, increases with increasing MW_e (Figure 26). It can also increase from using monomers with longer projections. For example, IOA has a longer aliphatic

chain than both VA and HEA. As a result, poly(IOA) should have a higher tack value than both poly(HEA) and poly(VA). This could explain why AI1_RR16 (poly(IOA)) had a tack value and neither poly(HEA) nor poly(VA) did. The addition of IPA (AI1_S2, AI1_S3, and AI1_BE_RT1-AI1_BE_RT3) did result in increased tack values from AI1_P due to the creation of more branched chains.

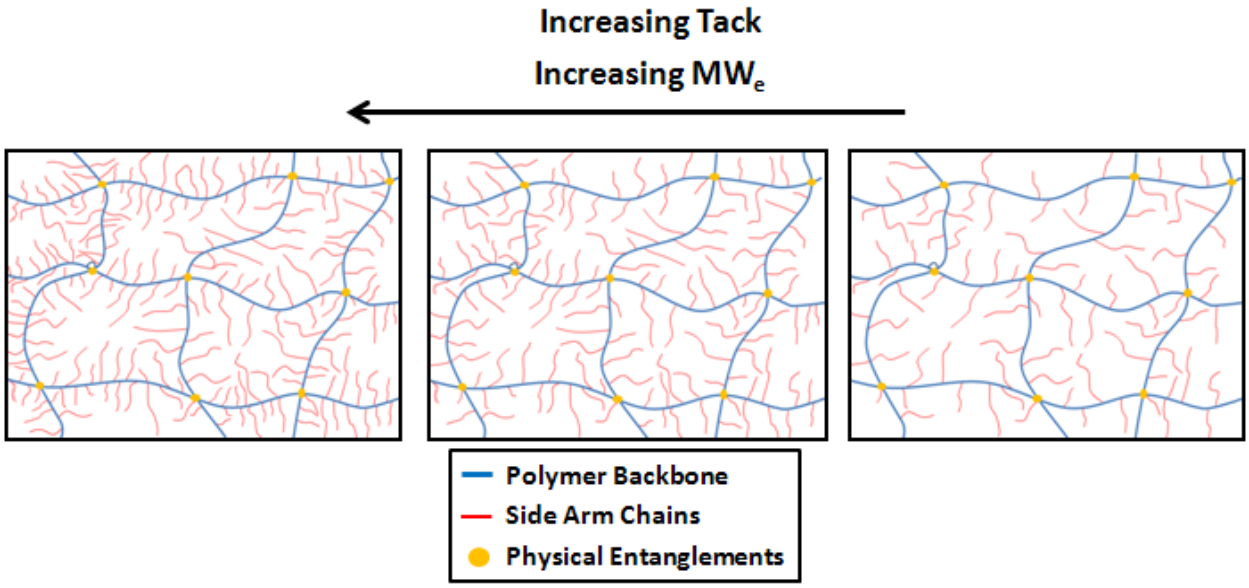

Figure 26 Relationship between tack and MW_e

As can be seen from Table 8, solution polymerizations (AI1_RR1 to AI1_RR15) had dramatically reduced viscosity from bulk polymerizations (AI1_RR16 to AI1_RR20). This is most likely a result of the reduced probability that a macroradical chain will propagate with another monomer. As solution polymerization occurs in the later stages of polymerization, it is more likely for the macroradical to terminate with itself or another formed chain than to continue propagating.

Isopropyl alcohol acts as a chain transfer agent as can be inferred from comparing the viscosity values of sample AI1_S2, AI1_S3, and AI1_BE_RT1 to AI1_RT3. As IPA concentration increases, viscosity decreases. From the Mark-Houwink-Sakurada relationship, it

is proven that viscosity is proportional to MW. As a result, it can be inferred that IPA produced lower molecular weight polymer and oligomer chains. For viscosity comparison, see AI1_D1 to AI1_D4 which show increased viscosities from methanol addition because methanol is not a chain transfer agent.

No direct relationship between tack and viscosity can be made, since both low viscosity polymers and high viscosity polymers can have lower MW polymer chains or side chains present to produce tack. This can be observed from the variety of tack values found at each different viscosity range (low and high) which suggests that no correlation exists.

Table 8 Tack and viscosity measurements of polymer samples without drug loading

Sample Id	Tack Tension (N)	Standard Deviation	Viscosity (Pa•s)
AI1_P	0.5	0.08	34,230
AI1_S1	0.5	0.04	40,190
AI1_S2	2.2	0.26	27,890
AI1_S3	5.8	0.41	24,970
AI1_S4	0.8	0.28	11,510
AI1_RR4	0.6	0.06	*
AI1_RR5	0.2	0.08	589.4
AI1_RR6	0.2	0.02	8,732
AI1_RR7	0.2	0.06	15,090
AI1_RR8	0.7	0.05	66,660
AI1_RR9	0.1	0.02	20,320
AI1_RR10	1.1	0.35	367.6
AI1_RR11	none	none	*
AI1_RR13	1.3	0.31	13,620
AI1_RR14	2.4	0.93	58,520
AI1_RR15	0.6	0.01	818.7
AI1_RR16	0.1	0.02	107,200
AI1_RR17	none	none	*

AI1_RR18	none	none	*
AI1_RR19	0.6	0.04	102,300
AI1_RR20	0.2	0.04	100,000
AI1_D1	**	**	110,900
AI1_D2	**	**	196,100
AI1_D3	**	**	14,670
AI1_D4	**	**	39,040
AI1_BE_RT1	0.9	0.17	20,440
AI1_BE_RT2	2.8	1.78	12,220
AI1_BE_RT3	1.4	0.35	16,340

* Very high viscosity liquids and solid samples could not be viscosity tested.

** Samples were tacky but too cohesive to tack test.

4.5 Adhesive foams

Adhesive foams were created by high speed mixing, adding blowing agents, freeze drying, heating, and IOA bulk polymerization. Foam methods were selected as appropriate for commercial use if the resulting foams showed acceptable porosity and stability. These experiments noted the significance of adhesive viscosity on foam formation, since adhesive liquids with too low (AI1_S4) or too high of a viscosity (AI1_S2) were not suitable for foam formation. Figure 27 provides a comparison of the foam morphology obtained by the five methods.

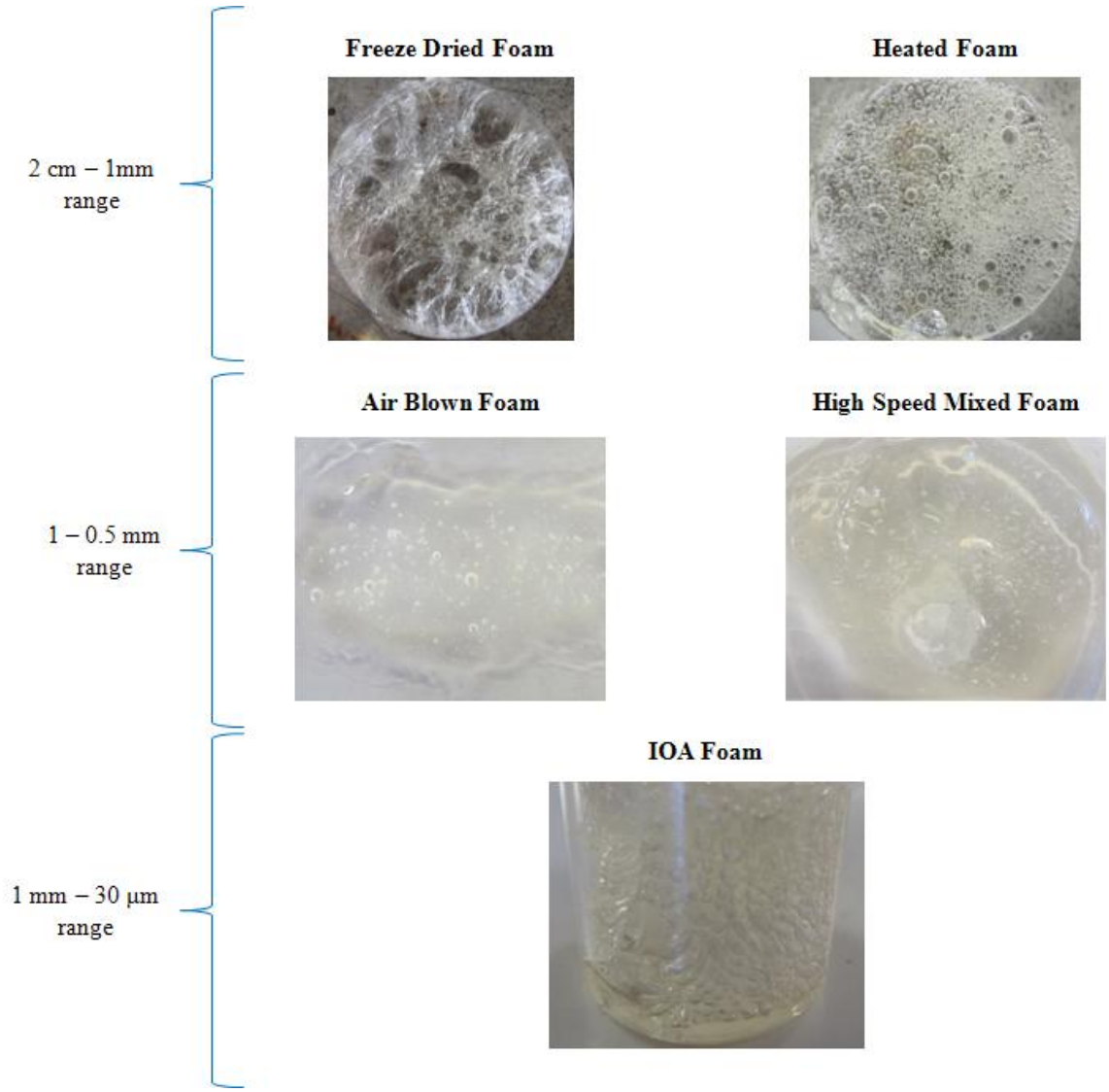

Figure 27 Foam cell size comparison

High speed mixed foams only maintained a stable closed-cell foam structure for 24 h. Their formation was strongly dependent on the mixing speed. Foam formation occurred at 3000 rpm after 1 min; whereas, no foam was formed at 2800 rpm from 1 to 3 min. After increasing mixing time to 2 min at 3000 rpm, the foam became denser. Mixing at 3200 rpm for 1 min caused the foam to collapse. In comparison, air-blown foam was more stable but still only lasted for approximately 2 weeks. Since foams made by either of the two methods could not be preserved

for a long duration, neither method was further investigated with additives for extending shelf life.

Freeze drying the adhesives produced more stable foams which lasted 1 month without additives and 3 months with surfactant addition. Open-cell foams were produced with freeze drying, as the decreased pressure and temperatures triggered rapid solvent evaporation from phase change (see Figure 28); rapid evaporation caused large bubble formation which collapsed and resulted in irregular, open-cell foam structure. Two Teflon® coated glass slides were used to control foam height but produced poor cell content in the foam's core from restricted solvent evaporation.

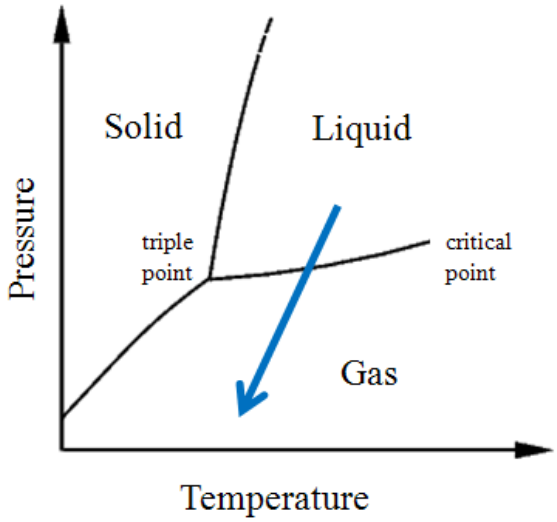

Figure 28 Phase diagram (adapted from [62]) showing liquid to gas phase change due to low pressure and temperature

Since surfactants reduce contact angles and may stabilize bubbles, two surfactant additives (Figure 29), isopropyl tetradecanoate and sodium dodecylbenzene sulfonate, were used to stabilize the freeze dried foam structure. Surfactant addition produced more regular foam cells with smaller cell diameters and reduced foam height. This regularity was attributed to the

surfactant lowering surface tension at the liquid-gas interface; this reduction in surface tension allowed more local bubble formation rather than forming larger bubbles with more surface area. Isopropyl tetradecanoate, a common skin wetting agent with an acidic pH [63], decreased foam stability to 1 week with only a 0.25% weight ratio. Sodium dodecylbenzenesulfonate is an anionic surfactant used in Alconox® detergent with a basic pH. [64] Foam stability varied as Alconox® surfactant was added in 0.25%, 1%, and 3% weight ratios. Foams with 3% Alconox diminished foam shelf life to 10 days; whereas the 1% ratio raised it to 3 weeks. Furthermore, 0.25% Alconox addition resulted in increased shelf life of up to 3 months. These results suggested that a small range of surfactant concentrations can significantly impact foam stability.

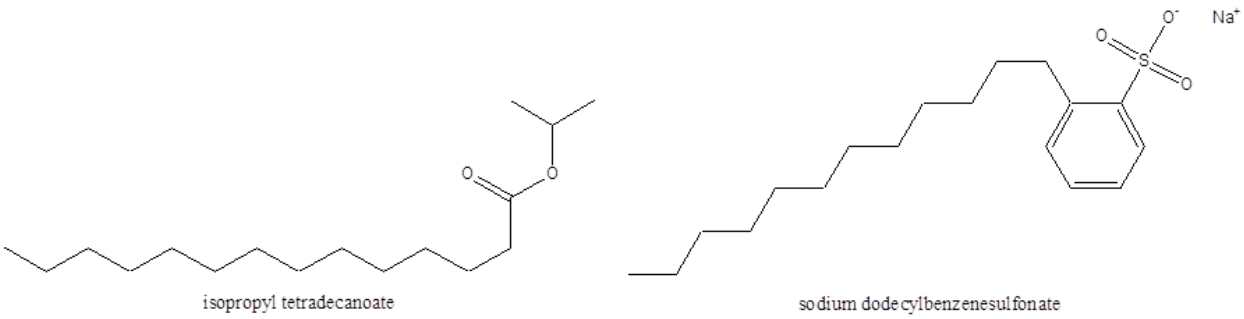

Figure 29 Surfactant additives for foam stabilization

Based on these results, adhesive foam stability could be impacted by surfactant pH and ionic charge, since these factors affect intermolecular secondary forces, which in turn can impact the rheological stability of viscous liquids. A balance of secondary forces between the surfactant and the adhesive is attributed to attaining foam stability. [65] Since the polymer is a polar liquid, there are pH-dependent electrostatic repulsions between polar groups in the surfactant and the liquid adhesive, or similarly, attractive forces from hydrogen bonding and van der Waals interactions. Since isopropyl tetradecanoate is a nonionic surfactant, its polar ester group probably was not well balanced by the hydrocarbon chains' weaker attractive forces which resulted in decreased foam stability. It is possible that dodecylbenzenesulfonate's anionic charge

and basic pH allowed it to more readily dissociate and bond with protons in the polymer structure. If this occurred, the additional bonding capability would increase attractive forces between the surfactant and adhesive which could have attributed to increased foam stability at very low concentrations.

Heating produced adhesive foams with excellent stability. Foams from heating had more regular foam cells, cell diameters, and foam height than freeze dried samples. As well, they were stable for more than 4 months without any noticeable changes in foam structure.

Bulk polymerization of IOA foams (AI1_RR16, AI1_RR19, and AI1_RR20) created closed-cell foams with bubbles in the millimeter to micrometer range. Foam cell size was significantly enlarged by increasing the BP:IOA ratio between AI1_RR16 and AI1_RR20. Colloidal foam was almost achieved by increasing this ratio (AI1_RR20), as the thickness between bubbles was less than 30 μm. The micrograph of each sample is shown in Figure 30 since the foams could not easily be visually differentiated as closed-cell or open-cell. As shown in the figure, these are closed-cell foams. Larger ellipsoidal bubbles were formed in AI1_RR20 which further supported the hypothesis that the density decrease from AI1_RR16 and AI1_RR20 was a result of a larger bubble volume in AI1_RR20 foam.

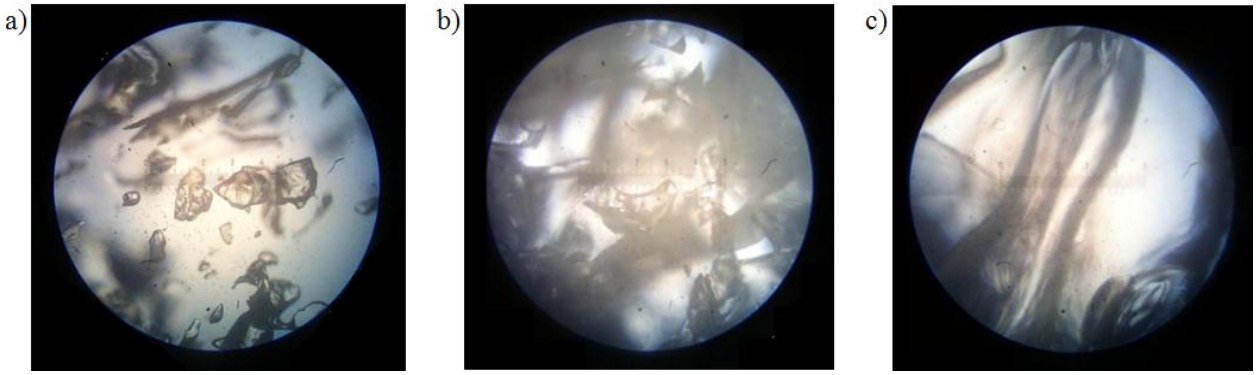

Figure 30 Micrographs of bulk polymerized foams a) AI1_RR16, b) AI1_RR19, and c) AI1_RR20 at 10X magnification showing closed cell foam formation occurred

From foam adhesive studies, only foam formation from heating and bulk polymerization of IOA based samples produced successful products with reasonable cell content, regular foam height, and superior shelf life. As a result, these methods were further investigated for drug loading (refer to section 4.6.1).

4.6 Incorporation of a drug for pain relief in adhesives

Benzocaine is reported as soluble in methanol [66]; however, the adhesive formulation contained isopropanol instead. Prior to drug loading, benzocaine solubility tests (BM1, BI1, BIM1-BIM3) were conducted on isopropanol and methanol mixtures. Benzocaine was only soluble in methanol (BM1) and in methanol-isopropanol mixture (BIM1 and BIM2).

As a result, methanol was substituted for isopropanol in AI1_D1 to determine whether it could act as a molecular weight limiting agent and simultaneously as a dispersing agent for benzocaine in the adhesive solution. The methanol content was increased to an excess of 40% in AI1_D2. Since neither of these modifications lowered the viscosity (see Table 8), two adhesive solutions with isopropanol and methanol mixtures were tried (AI1_D3 and AI1_D4). AI1_D4 maintained a lower viscosity and was suitable for further experimentation in benzocaine loading studies.

4.6.1 Adhesive with incorporated drug

Sample AI1_D4_BC1 was prepared with benzocaine incorporated into the alcohol mixture prior to mixing in the solution. AI1_D4_BC1 reacted to form a product of bright crimson red color with a distinctly lower viscosity than AI1_S3 and AI1_D4 samples. To further investigate whether benzocaine could be included into the adhesive under these circumstances or whether it underwent an unwanted reaction, each chemical was individually tested with initiator and then

without initiator. All samples (AI1_D4_BC1 to AI1_D4_BC6) formed brilliant red products, regardless of the N_2 purge or heat. It was found that benzocaine did not react with the monomers but with benzoyl peroxide to cause a color change, as is supported by the reported [34] color change which indicated radical decomposition of benzocaine. Only one red, translucent, sticky, adhesive from HEA (AI1_BC4) with a relatively high viscosity could be produced under these conditions; the remaining samples were red, transparent solutions. It is possible that the alcohol group on HEA enabled polymerization in the presence of BP and benzocaine and prevented the complete decomposition of benzocaine. The alcohol of HEA could have made the monomer slightly more electronegative than the VA and IOA which enabled it to better compete with benzocaine for radical addition. Based on these experiments, methanol was discontinued for use in the adhesive solution because the monomers dissolved benzocaine and because methanol did not prevent color change or contribute to the polymer's decreased viscosity.

As a consequence, the experimental conditions were changed to avoid low adhesive viscosity and benzocaine reaction/decomposition. Benzocaine added to AI1_S3 after 7 h of polymerization produced a similar viscosity to AI1_S3 without benzocaine loading; however, color change still occurred. With increasing reaction time up to 12 h prior to benzocaine addition, the color shade and intensity changed from dark crimson red to orange; however, storing the adhesive at room temperature caused further benzocaine decomposition as indicated by further color change to dark crimson red after 1 month of observation. Benzocaine addition to polymers prevented further viscosity increase which indicated that benzocaine decomposition with BP probably terminated the polymerization reaction. Benzocaine addition to AI1_RR20 inhibited foam formation; foam was only created if the temperature was increased to 80°C. At this point, the foam nucleated in an area without decomposed benzocaine (as indicated by the

white foam color), and then foam spread out from the core. However, foam formation with AI1_RR20 was inhibited in areas where the benzocaine was decomposed; instead, a red liquid of reduced viscosity was formed. Since benzocaine could not be added before foam was formed for AI1_RR16, AI1_RR19, and AI1_RR20, these foams could not be used as a matrix for benzocaine release. However, these foams were successful examples of adhesive foams which could be implemented in bandages to replace the separate adhesive medium and foam carrier.

4.6.2 Radical termination prior to benzocaine loading

Based on the experiments reported in the previous section, it was assumed that radicals contained in the adhesive during preparation had the capacity to decompose benzocaine. Therefore, an effort was made to terminate those radicals. Initially water, ethanol, and oxygen were used as radical inhibitors, but none of those methods could successfully prevent the decomposition of benzocaine. As a result, several chain transfer agents (isopropyl alcohol, chloroform, TMIO, TEMPOH, and ascorbic acid) were employed. These reagents are capable of terminating a growing chain by donating a hydrogen and possibly producing a less reactive radical. In order to dissolve the TMIO, TEMPOH, and ascorbic acid in the adhesive solution, lower viscosity adhesives were created (AI1_BE_RT1 to AI1_BE_RT3). Only AI1_BE_RT3 was capable of foam formation as the other two were not viscous enough; of the prospective chain transfer agents, only ascorbic acid might have been able to prevent radical decomposition of benzocaine since no color change occurred.

4.6.3 Benzocaine release trial from loaded adhesive

Benzocaine has reported ultraviolet (UV) spectrum maxima (in methanol) at 220 nm and 292 nm, respectively.[66] Figure 31 (a) shows results from UV-Vis spectroscopy of the 40% PPG/PBS solution, skin medium solution, which suspended heated foams from AI1_BE_RT3

adhesives: a control, an ascorbic acid loaded specimen, and an ascorbic acid and benzocaine loaded sample. Figure 31 (b) shows the UV-Vis absorbance of the skin medium as the benzocaine and ascorbic acid are released over a 15 min time period. For the drug release trial, the different foam adhesives were suspened in the skin medium solution and high speed mixed at 500 rpm as described in an accelerated drug release study trial [33] to determine whether benzocaine and ascorbic acid could both be released from the adhesive into the skin medium solution.

The UV-Vis spectrum of the control adhesive sample indicated with three UV-Vis wavelength ranges that a small amount of polymer or oligomer was being released; in descending order, the peak maxima approximately occurred at 205 nm, 235 nm and 275nm. Ascorbic acid loaded adhesives showed a slight spectral shift from 235 nm to 240 nm and increased UV-Vis absorbance at 201 nm and 240 nm which suggest that ascorbic acid was being released as well. Benzocaine and ascorbic acid loaded adhesives showed increased intensity and a UV-Vis band shift to the 290 nm region; as well, there was increased band intensity at approximately 240 nm. This suggests that both ascorbic acid and benzocaine are being released with time from the adhesive.

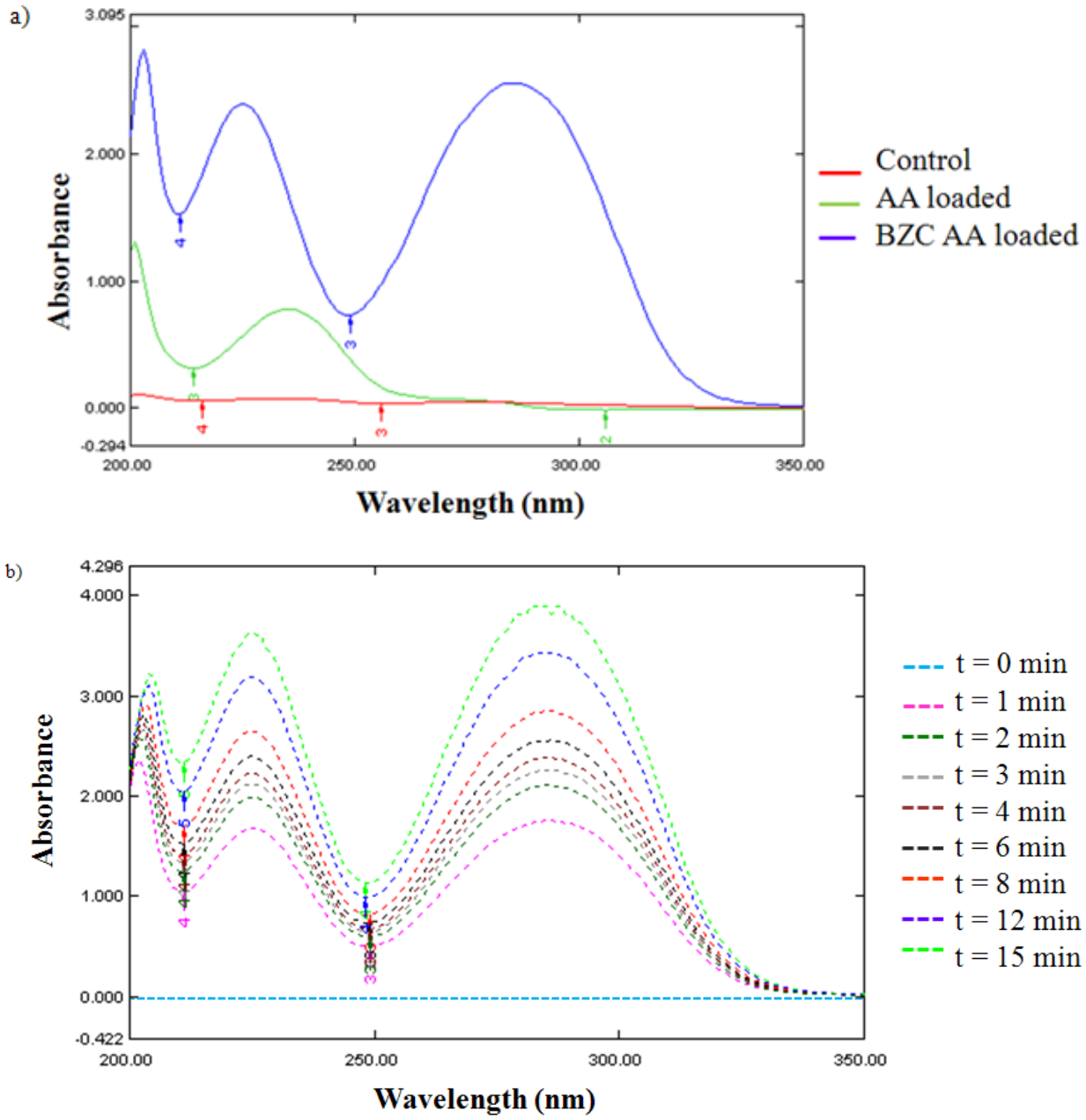

Figure 31 a) AI1_BC_RT3 UV-Vis spectra in 40% PPG/PBS after 8 min at 500 rpm of: control, ascorbic acid (AA) loaded, and ascorbic acid and benzocaine (BZC AA) loaded; b) UV-Vis absorbance spectra of the benzocaine and ascorbic AA loaded adhesive (BZC AA) from 0 min to 15 min after high speed mixing

4.7 Adhesive pressure sensitivity and peel test comparison

A pressure sensitivity comparison between AI1_S3 samples (with surfactant, without surfactant, with a decomposed drug) and the benzocaine and ascorbic acid loaded AI1_BE_RT3 foam was made. Table 9 shows the resulting adhesive debonding forces after a force was applied. As can be seen from these data and from Figure 32, all adhesive samples showed pressure sensitive bonding capabilities to some degree. Obviously, increased amounts of surfactant in AI1_S3 from 0% to 3% did reduce the pressure sensitivity; however, these samples also produced less variable debonding data as indicated by the standard deviations. For reasons of comparison, a decomposed benzocaine sample (AI1_S3) was also included which predictably showed poor pressure sensitivity. However, the foam AI1_BE_RT3 sample with loaded ascorbic acid and benzocaine did not exhibit significantly reduced pressure sensitivity.

Table 9 Pressure sensitivity data from applied compressive forces of 0.1 - 20N; SD is standard deviation, BSC denotes benzocaine loaded adhesives, AA refers to ascorbic acid loaded adhesives, surf indicates Alconox surfactant addition, and decomp BZC refers to a sample with decomposed BZC in it.

	Adhesive Debonding Forces (N) from Applied Forces (N)											
Sample Id	**0.1N**	**SD**	**1N**	**SD**	**2N**	**SD**	**4N**	**SD**	**8N**	**SD**	**20N**	**SD**
AI1_S3	5.8	0.4	7.1	0.3	9.6	0.4	15.5	1.2	15.5	0.5	18.3	0.9
AI1_S3 (1% surf)	0.3	0.0	1.8	0.2	2.2	0.1	7.9	1.2	10.0	0.3	12.4	0.6
AI1_S3 (3% surf)	0.2	0.0	2.3	0.2	2.7	0.1	3.9	0.1	8.6	0.1	8.8	2.4
AI1_S3 (decomp BZC)	1.3	2.0	3.1	0.8	4.3	0.2	5.2	0.5	10.3	0.3	13.0	1.0
AI1_BE_RT3 (foam BZC AA)	0.5	0.3	5.2	0.6	7.2	0.5	11.0	0.4	13.8	0.3	18.0	0.9

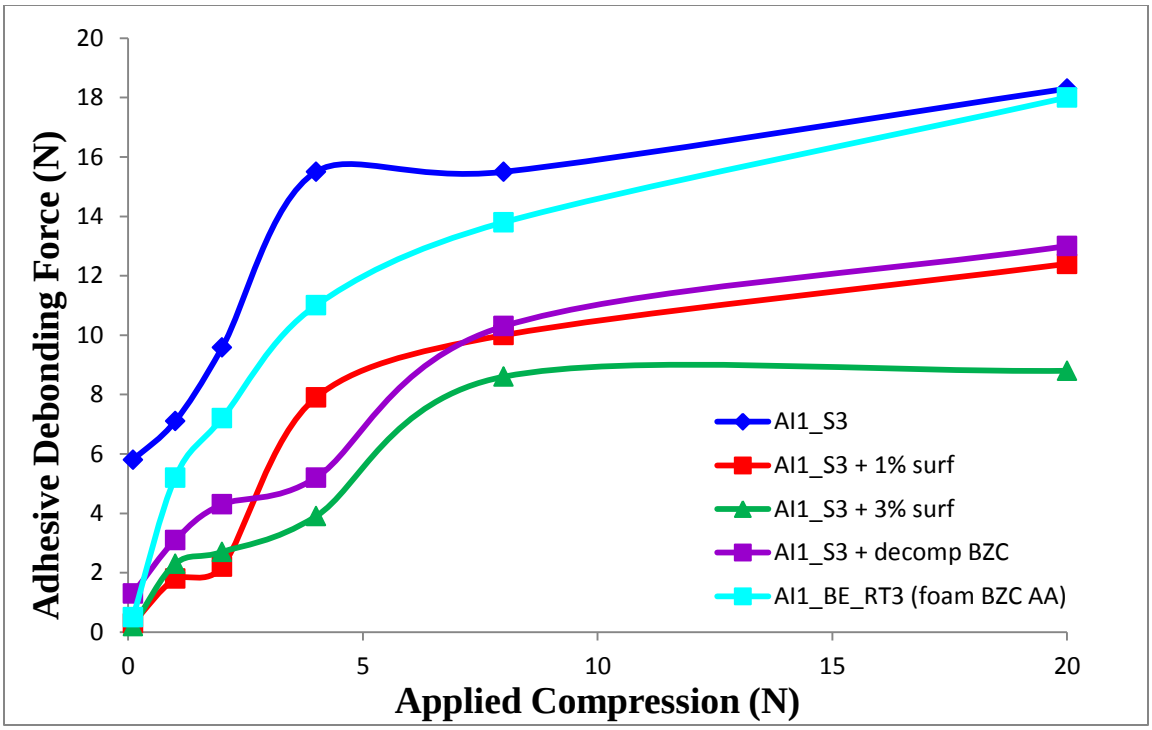

Figure 32 Adhesive pressure sensitivity

Finally, peel testing (Figure 33) of AI1_S3 with slab geometry and foam morphology from heating, as well as, AI1_BE_RT3 foam loaded with benzocaine and ascorbic acid was conducted for comparison with commercial bandage data. Peel test results indicate that AI1_S3 adhesive's peel resistance was rather high, though still within the range of the commercial polyacrylate adhesives (i.e. Gothaplast® bandages). However, the loaded sample AI1_BE_RT3 produced very high peel resistance due to extensive adhesive stretching prior to debonding; these values had a similar peel resistance range to natural rubber adhesives which tested between 19 and 22N. This increased peel resistance could be related to the lower cohesive nature of the drug loaded samples in comparison to unloaded specimen. A balance between cohesive and adhesive forces must exist for a PSA adhesive to properly bond to and debond from a surface without delaminating. [1] Based on the peel and pressure sensitivity studies, a small amount of surfactant additives could show improved cohesion of drug loaded foam samples.

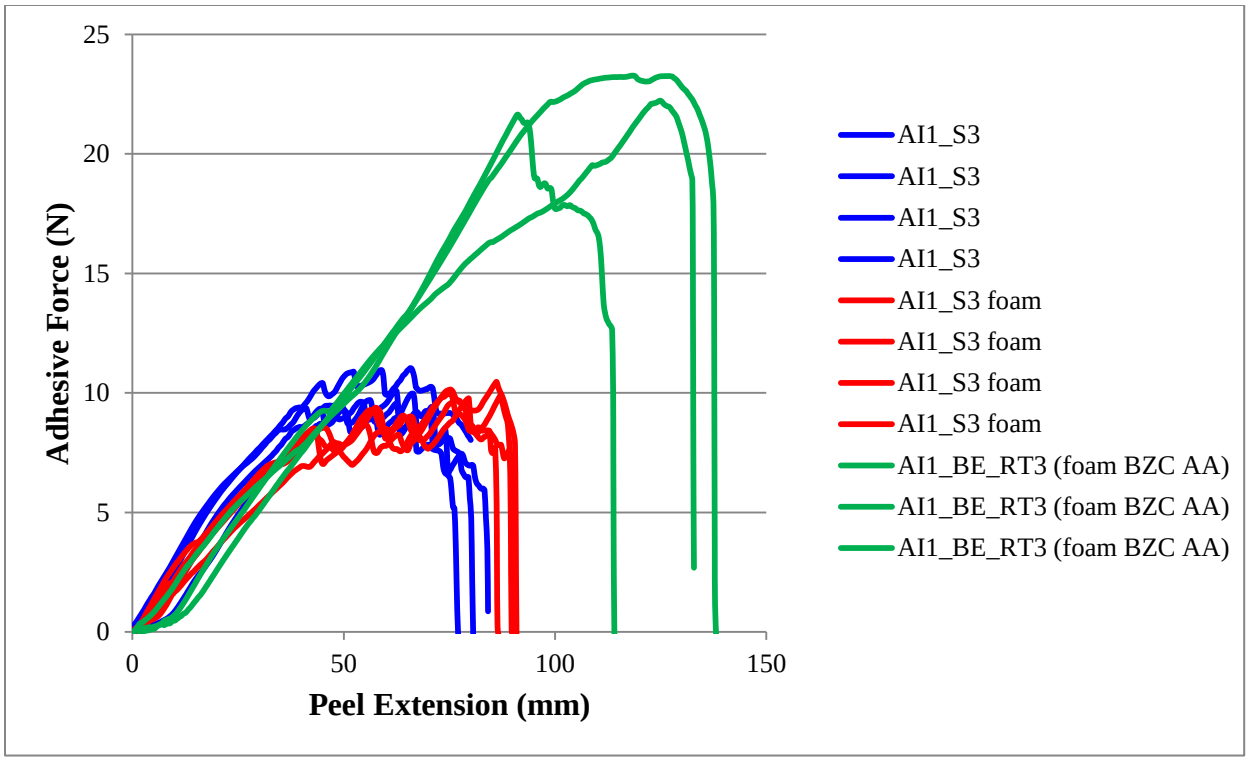

Figure 33 Peel test results of AI1_S3, AI1_S3 foam, and benzocaine and ascorbic acid loaded AI1_BE_RT3 foam

5 CONCLUSIONS

PSAs with foam morphology have not yet been reported for use in medical tapes. The goal of this project was two-fold: first, to create a successful PSA foam (with drug delivering capabilities) which could replace the separate adhesive and carrier mediums; secondly, to characterize the peel test results of commercial polyacrylate medical tapes as a standard for comparison, since these data have not yet been reported.

Characterization of polyacrylate tapes were found to have a wide range of peel resistance and variable tack values. Of these samples, Leukosilk had the highest tack without delamination and the lowest peel test values (around 3N) which was deemed as ideal for skin-friendly adhesives. As well, the data proved no correlation between tack and peel resistance, as these tests target different material properties. Tack is a result of the polymer's surface tension and specific adhesion, while peel resistance is related of the polymer's viscoelasticity.

A modified adhesive solution was created which could produce successful foam with a stable storage lives over 4 months. Characterization of the mixed adhesive system pointed to the possible formation of a tercopolymer of IOA, HEA, and VA. Foam formation was most successful by solvent evaporation from heating and the bulk polymerization of IOA based solutions. Adhesive viscosity was shown to affect foam formation.

In order to load the foams with benzocaine as a model drug, the polymer products had to be mixed with an antioxidant, radical terminator, ascorbic acid, since otherwise benzocaine seemed

to decompose. Foams made by bulk polymerization did not prove to be as useful as a matrix for drug release as modified adhesives from solution polymerization. Accelerated release studies were performed and UV-Vis spectra of the unloaded and loaded adhesives suggested that both ascorbic acid and benzocaine were released from the matrix. Further, peel resistance and pressure sensitivity testing suggested that the drug and ascorbic acid loaded adhesives could be considered a PSA, but that the adhesive was not sufficiently cohesive. It is suggested that a surfactant additive could probably improve its cohesive properties to create a product with a more acceptable peel resistance. Overall, this research pointed to two potentially successful methods to produce adhesive foams suitable for bandage PSAs. A PSA adhesive was created which might be utilized for drug delivery with minor modifications.

6 RECOMMENDATIONS FOR FUTURE WORK

Further work could be conducted on the freeze dried foams with nonpolar surfactants, as these additives could be compared with the foam storage life of adhesives with ionic and polar surfactants. Stability of foam made by heating could be investigated with the use of a compound such as ascorbic acid to see whether benzocaine decomposition could be prevented and shelf life improved. DMA analysis of all adhesive formulations could be conducted for MW comparison. A comparable system with a different primary PSA monomer other than IOA, such as 2-ethylhexyl acrylate, could be used. The longer substituent on the hexyl aliphatic chain could decrease the MW_c required for chain entanglements and, thus, provide a more cohesive adhesive structure.

REFERENCES

1. Benedek, I., ed. *Developments in Pressure-Sensitive Products*. 2nd ed. Buildup and Classification of Pressure Sensitive Products, ed. I. Benedek. 2006, CRC Press: Boca Raton. 6-9, 186-187,192-193.
2. Carlson, J.M. and S.R. Stoll, *Self-Adhering Friction Reducing Liner and Method of Use*. 2002, Tamarack Habilitation Technologies Inc.: US. p. 1-8.
3. Sun, R.L., *Breathable Non-Perforated Bandage*. 2003, Johnson & Johnson. p. 1-8.
4. Pexa, C., *Nose Bandage*. 1985.
5. Baschnagel, R.J., *Adhesive Bandage*. 2011. p. 1-19.
6. Schaar, C.H., *Adhesive Bandage with Foam Backing*. 1982, The Kendall Company: US. p. 1-4.
7. Tan, H.S. and W.R. Pfister, *Review: Pressure-sensitive adhesives for transdermal drug delivery systems.* Pharmaceutical Science & Technology Today, 1999. **2**(2): p. 60-69.
8. Ebnesajjad, S., ed. *Handbook of Adhesives and Surface Preparation: Technology and Manufacturing*. PDL Handbook Series, ed. S. Ebnesajjad. 2011, Elsevier Inc. 169-172.
9. Jeusette, M., et al., *Microscopic morphology of blends between a new "all-acrylate" radial block copolymer and a rosin ester resin for pressure sensitive adhesives.* European Polymer Journal, 2008. **44**(12): p. 3931-3940.
10. Webster, I., *Recent developments in pressure-sensitive adhesives for medical applications.* International Journal of Adhesion and Adhesives, 1996. **17**: p. 69-73.
11. Howe, D. (2002) *Anionic Products Boost NMS Application*. **Volume**,
12. Webster, I., *Recent Developments in pressure-sensitive adhesives for medical applications.* International Journal of Adhesion and Adhesives, 1997. **17**(1): p. 69-73.
13. Cantor, A.S. and D.J. Wirtanen, *Novel Acrylate Adhesive for Transdermal Drug Delivery.* Pharmaceutical Technology North America, 2002. **26**(1): p. 28-38.
14. Compeed. *How Compeed Beats Blisters!* 2011 [cited; Available from: http://www.beunstoppable.co.uk/education/.
15. Gerhardt, L.C., et al., *Influence of epidermal hydration on the friction of human skin against textiles.* Journal of the Royal Society Interface, 2008. **5**: p. 1317-1328.
16. Agache, P., ed. *Main skin biological and physical constants*. In Measuring the skin: non-invasive investigations, physiology, normal constants, ed. P. Agache and P. Humbert. 2004, Springer: Berlin, Germany. 727-757.
17. Cooney, D. Biomedical Engineering Principles: An Introduction to Fluid, Heat, and Mass Transport Processes, 1976. Marcel Dekker, p.1-244.
18. Saga, K., *Structure and Function of Human Sweat Glands Studied with Histochemistry and Cytochemistry.* Progress in Histochemistry and Cytochemistry, 2002. **37**(4): p. 323-386.
19. Verde, T., et al., *Sweat composition in exercise and in heat.* Journal of Applied Physiology, 1985. **53**(6): p. 1540-1545.
20. Morgan, R.M., M.J. Patterson, and M.A. Nimmo, *Acute effects of dehydration on sweat composition in men during prolonged exercise in the heat.* Acta Physiologica, 2004. **182**(1): p. 37-43.

21. Foster, K.G., *Relation Between the Colligative Properties and Chemical Composition of Sweat.* Journal of Physiology, 1961. **155**: p. 490-497.
22. Burry, J.S., et al., *Erroneous gender differences in axillary skin surface/sweat pH.* International Journal of Cosmetic Science, 2001. **23**(2): p. 99-107.
23. Patterson, M.J., S.D.R. Galloway, and M.A. Nimmo, *Variations in regional sweat composition in normal human males.* Experimental Physiology, 2000. **85**(6): p. 869-875.
24. Eberlein-Koenig, B., et al., *Skin Surface pH, Stratum Corneum Hydration, Trans-epidermal Water Loss and Skin Roughness Related to Atopic Eczema and Skin Dryness in a Population of Primary School Children.* Acta Dermato-Venereologica, 2000. **80**: p. 188-191.
25. Polliack, A.A. and S. Scheinberg, *A New Technology for Reducing Shear and Friction Forces on the Skin: Implications for Blister Care in the Wilderness Setting.* Wilderness and Environmental Medicine, 2006. **17**: p. 109-119.
26. Schaar, C.H., *Adhesive Bandage with Foam Backing*. 1982, The Kendall Company: US. p. 1-4.
27. Carlson, J.M. and S.R. Stoll, *Self-Adhering Friction Reducing Liner and Method of Use*. 2002, Tamarack Habilitation Technologies, Inc.: US. p. 1-8.
28. Wokovich, A.M., et al., *Review article: Transdermal drug delivery system (TDDS) adhesion as a critical safety, efficacy and quality attribute.* Europeal Journal of Pharmaceutics and Biopharmaceutics, 2006(64): p. 1-8.
29. Sugibayashi, K. and Y. Morimoto, *Polymers for transdermal drug delivery systems.* Journal of Controlled Release, 1994(29): p. 177-185.
30. Krogh, E. (2010) *The Octanol-Water Partition Constant: Kow*. **Volume**, 1-3
31. Ulness, D.J., *Physical Chemistry I and II*. 2006.
32. SPECTRUM. *Benzocaine MSDS*. 2003 [cited.
33. Sang-Chul, S., et al., *Preparation and evaluation of bioadhesive benzocaine gels for enhanced local anesthetic effects.* International Journal of Pharmaceutics, 2003. **260**(1): p. 77-81.
34. **Burkhart, C.** and **C. Burkhart**, ***Decreased efficacy of topical anesthetic creams in presence of benzoyl peroxide***. Dermatologic Surgery, 2005. **31**: p. **1479-80**.
35. Saeio, K., et al., *Factors Influencing Drug Dissolution Characteristic from Hydrophilic Polymer Matrix Tablet.* Scientia Phamaceutica, 2007(75): p. 147-163.
36. Shukla, M.K. and P.C. Mishra, *Electronic structures and spectra of two antioxidants: uric acis and asccorbic acid.* Journal of Molecular Structure, 1996. **377**: p. 247-259.
37. Buettner, G.R. and F.Q. Schafer, *Ascorbate (Vitamin C), its Antioxidant Chemistry*, in *Society For Free Radical Biology and Medicine*. 2001: Iowa City. p. 20.
38. Fakhraian, H., et al., *Preparation of pressure-sensitive adhesives for the production of sticky foam at ambient temperature.* International Journal of Adhesion and Adhesives, 2008. **29**(2): p. 111-113.
39. Kotzev, D. and V. Kotzev, *Novel uses of cyanoacrylate adhesives - polycyanoacrylate foams.* International Journal of Adhesion and Adhesives, 1992. **12**(3): p. 150-157.
40. Chino, Y. and D.C. Dunand, *Directionally freeze-cast titanium foam with aligned, elongated pores.* Acta Materialia, 2008. **56**(1): p. 105-113.
41. Deng, M., et al., *Preparation of nanoporous cellulose foams from cellulose-ionic liquid solutions.* Materials Letters, 2009. **63**(21): p. 1851-1854.
42. Thongprachan, N., et al., *Preparation of macroporous solid foam from multi-walled carbon nanotubes by freeze-drying technique.* Materials Chemistry and Physics, 2008. **112**(1): p. 262-269.
43. Vijayaraghavan, K., A. Nikolov, and D. Wasan, *Foam formation and mitigation in a three-phase gas-liquid-particulate system.* Advances in Colloid and Interface Science, 2006. **123-126**: p. 49-61.
44. Indrawati, L. and G. Narsimhan, *Characterization of protein stabilized foam formed in a continuous shear mixing apparatus.* Journal of Food Engineering, 2008. **88**(4): p. 456-465.

45. Tang, Z., et al., *Thermal degradation behavior of rigid polyurethane foams prepared with different fire retardant concentrations and blowing agents.* Polymer, 2002. **43**(24): p. 6471-6479.
46. Yang, D.H., B.Y. Hur, and S.R. Yang, *Study on fabrication and foaming mechanism of Mg foam using CaCO3 as blowing agent.* Journal of Alloys and Compounds, 2008. **461**(1-2): p. 221-227.
47. Tsivintzelis, I., E. Pavlidou, and C. Panaviotou, *Biodegradable polymer foams prepared with supercritical CO2-ethanol mixtures as blowing agents.* The Journal of Supercritical Fluids, 2007. **42**(2): p. 265-272.
48. Pugh, R.J., *Foaming, foam films, antifoaming and defoaming.* Advances in Colloid and Interface Science, 1996(64): p. 67-142.
49. Chen, Z.-L., Y.-L. Yan, and X.-B. Huang, *Stabilization of foams solely with polyoxyethylene-type nonionic surfactant.* Colloids and Surfaces A: Physiochemical and Engineering Aspects, 2008. **331**(3): p. 239-244.
50. Lacombe, R., ed. *Adhesion Measurement Methods Theory and Practice*. 2006, CRC Press.
51. Benedek, I., ed. *Pressure-Sensitive Adhesives and Applications*. 2 ed., Marcel Dekker, Inc.: New York. 1-2.
52. Stevens, M.P., ed. *Polymer Chemistry: an Introduction*. 3 ed. 1999, Oxford University Press: New York. 67-68.
53. Rodriguez, F., et al., eds. *Principles of Polymer Systems*. 5 ed. 2003, Taylor & Francis. 496.
54. Siepmann, J. and N.A. Peppas, *Review: Higuchi equation: Derivation, applications, use and misuse.* International Journal of Pharmaceutics, 2011: p. Article in Press.
55. Li, J., J.J. Masso, and S. Rendon, *Quantitative evaluation of adhesive properties and drug-adhesive interactions for transdermal drug delivery formulations using linear solvation energy relationships.* Journal of Controlled Release, 2002. **82**(1): p. 1-16.
56. Fried, J.R., ed. *Polymer Science and Technology, 2nd ed*. 2003, Prentice Hall PTR
57. Alfrey, T. and G. Goldfinger, *Copolymerization of Systems of Three and More Components*. Journal of Chemical Physics, 1944. **12**: p. 322.
58. Alfrey, T. and C.C. Price, Journal of Polymer Science, 1947. **2**: p. 101.
59. Li, X., et al., *Effect of Temperature on Copolymerization Parameters of Hydroxyethyl Acrylate and Methyl Methacrylate*
Chinese Journal of Polymer Science, 1998. **16**(1): p. 25-31.
60. Brandrup, J. and E.H. Immergut, eds. *Polymer handbook, 3rd ed*. 1989, Wiley: New York.
61. Brandrup, J., E.H. Immergut, and E.A. Grulke, eds. *Polymer Handbook*. 4 ed. 1999, John Wiley & Sons, Inc. 310.
62. Atkins, P. and J.d. Paula, eds. *Elements of Physical Chemistry*. 4 ed. 2007, Oxford.
63. Cardoso, V.M., et al., *Investigation of fatty acid esters to replace isopropyl myristate in the sterility test for ophthalmic ointments.* Journal of Pharmaceutical and Biomedical Analysis, 2006. **42**(5): p. 630-634.
64. Alconox. *Alconox MSDS*. 2009 [cited; Available from: http://www.alconox.com/downloads/pdf/msds_alconox_english_osha.pdf.
65. Angarska, J., C. Stubenrauch, and E. Manev, *Drainage of foam films stabilized with mixtures of non-ionic surfactants.* Colloids and Surfaces A: Physiochemical and Engineering Aspects, 2007. **309**(1-3): p. 189-197.
66. Ali, S.L., *Benzocaine*, in *Analytical Profiles of Drug Substances*. 1983. p. 73-104.

APPENDIX

FTIR spectra of reactivity ratio samples (AI1_RR3-AI1_RR20) listed as RR3- RR20

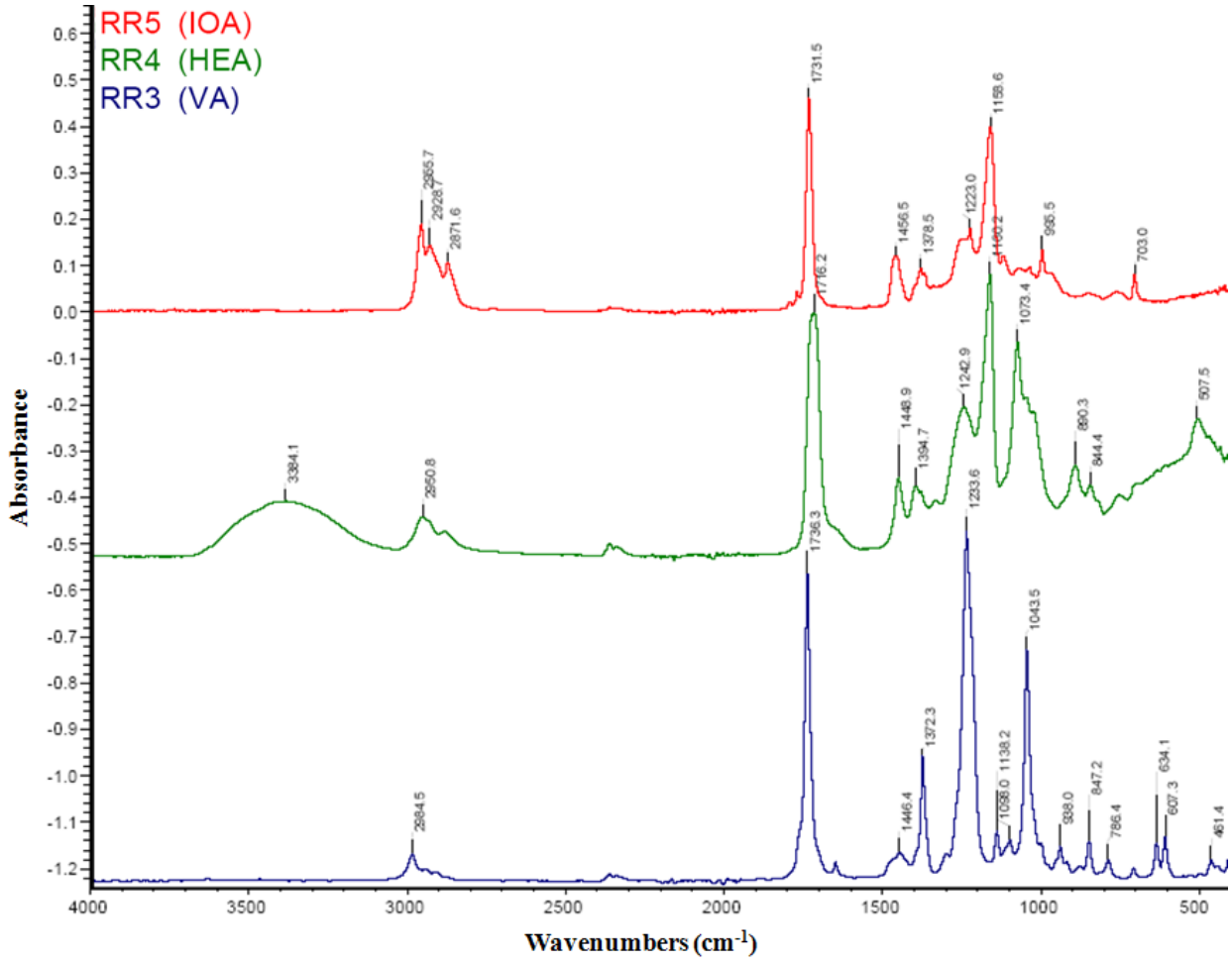

Figure 34 FTIR spectra of RR3 (AI1_RR3) to RR5 (AI1_RR5)

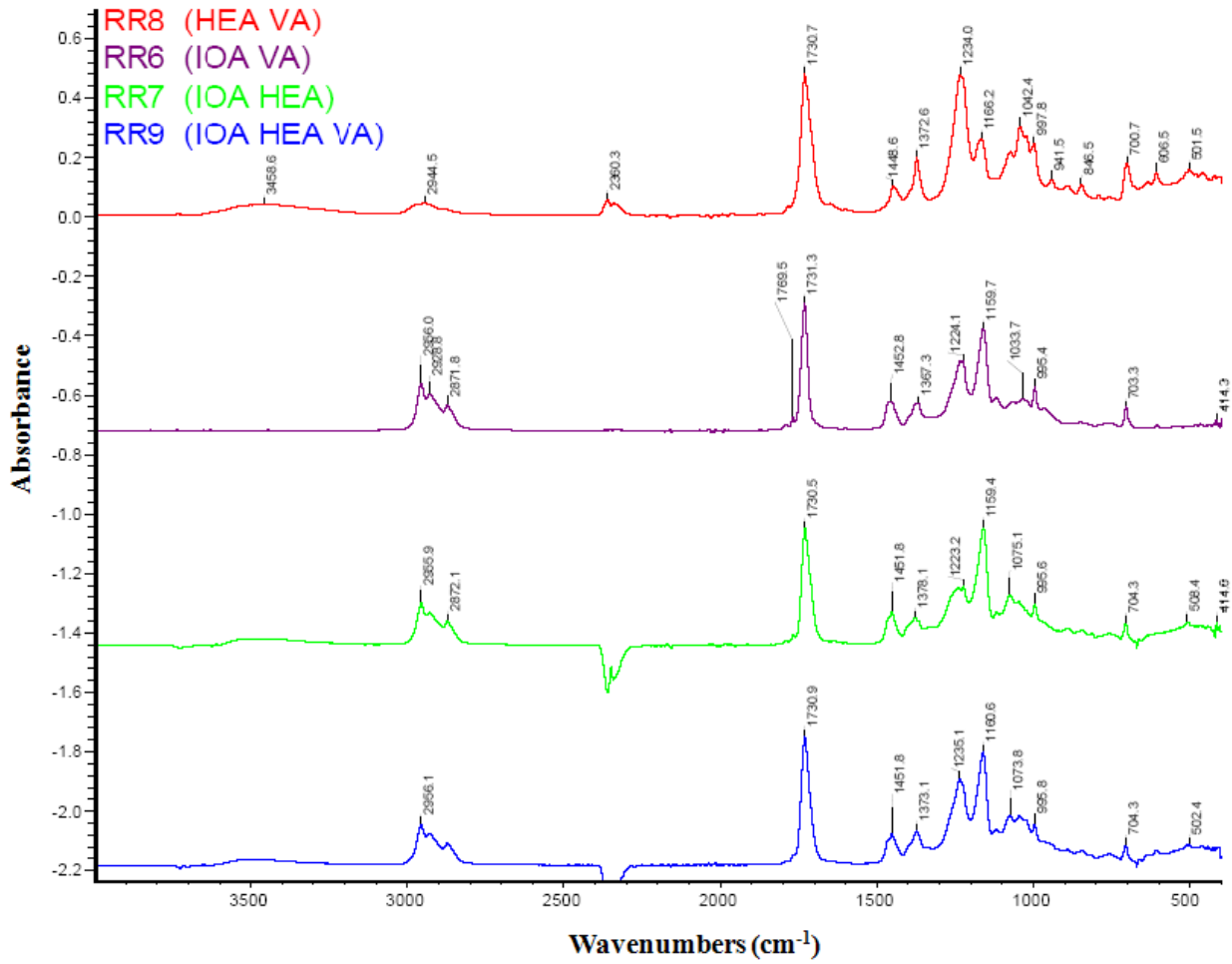

Figure 35 FTIR spectra of RR6 (AI1_RR6) to RR9 (AI1_RR9)

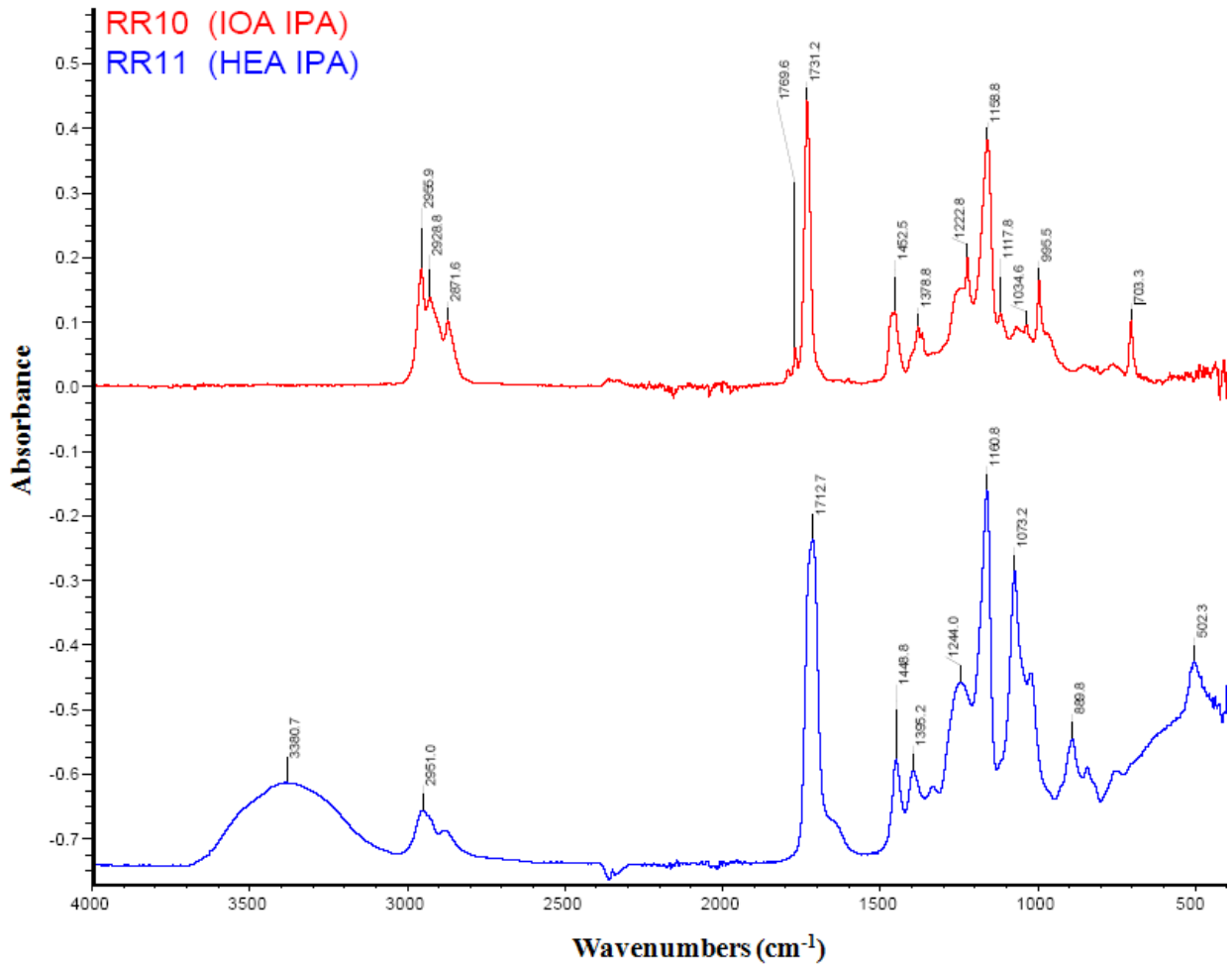

Figure 36 FTIR spectra of RR10 (AI1_RR10) to RR11 (AI1_RR11)

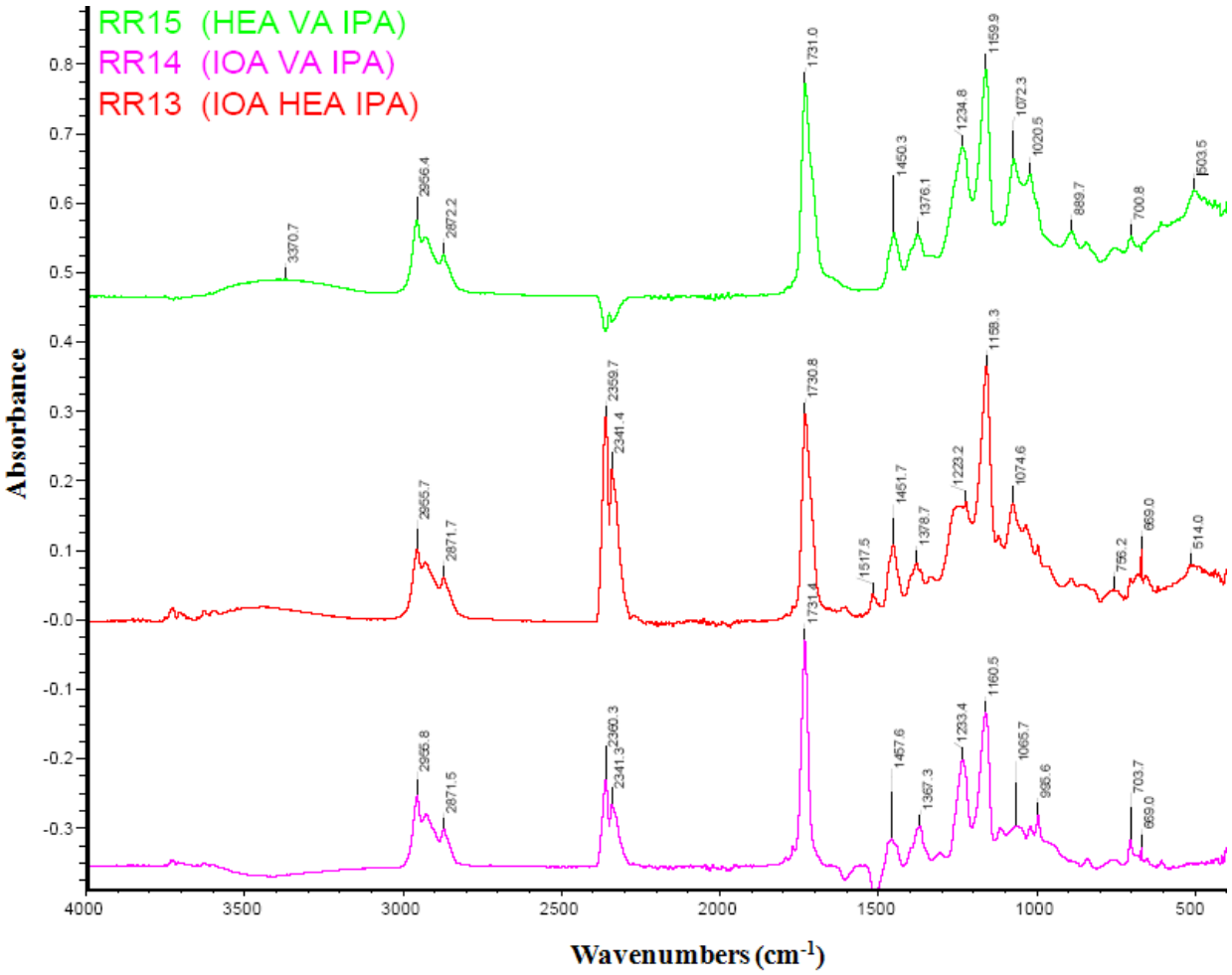

Figure 37 FTIR spectra of RR13 (AI1_RR13) to RR15 (AI1_RR15)

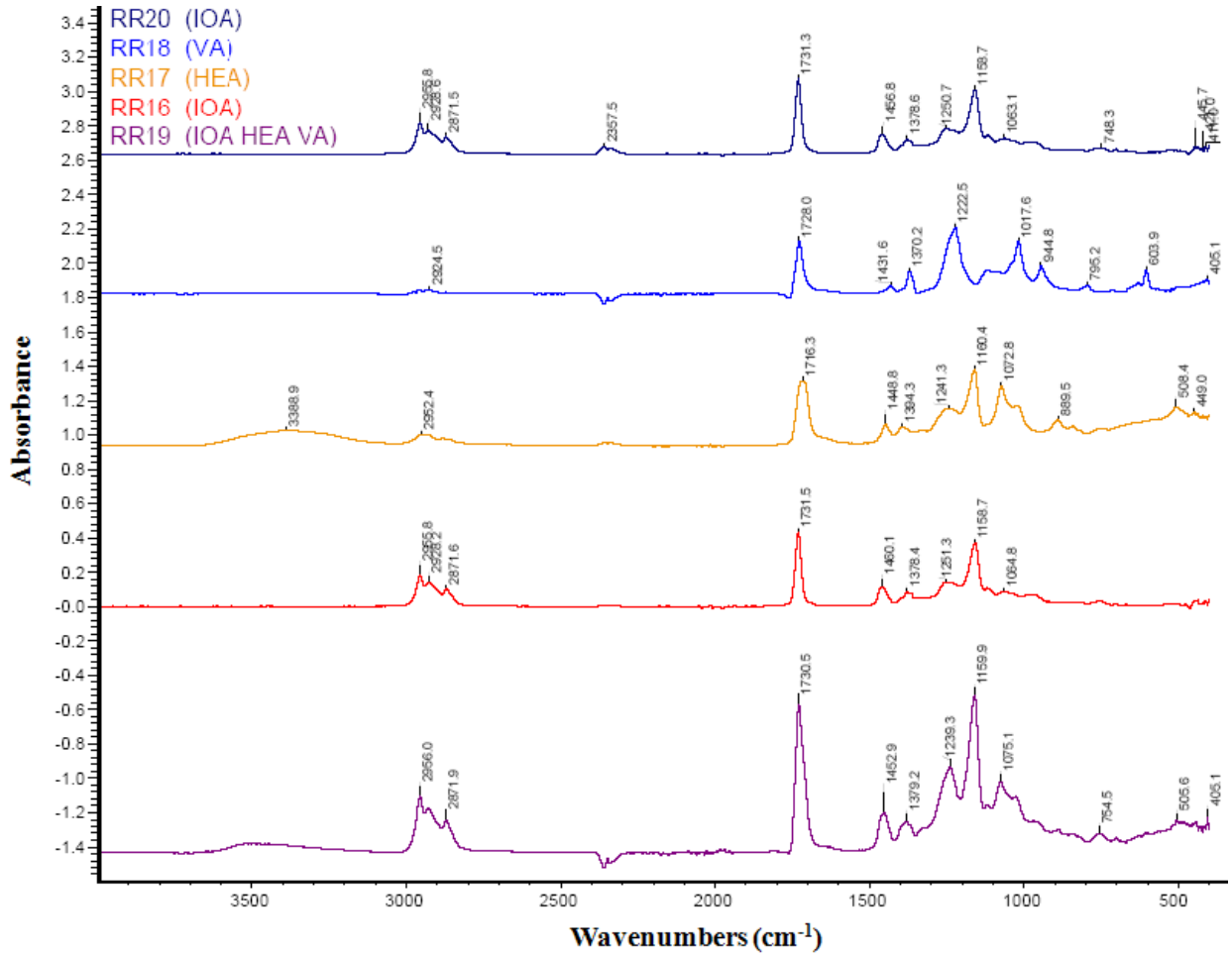

Figure 38 FTIR spectra of RR16 (AI1_RR16) to RR20 (AI1_RR20)